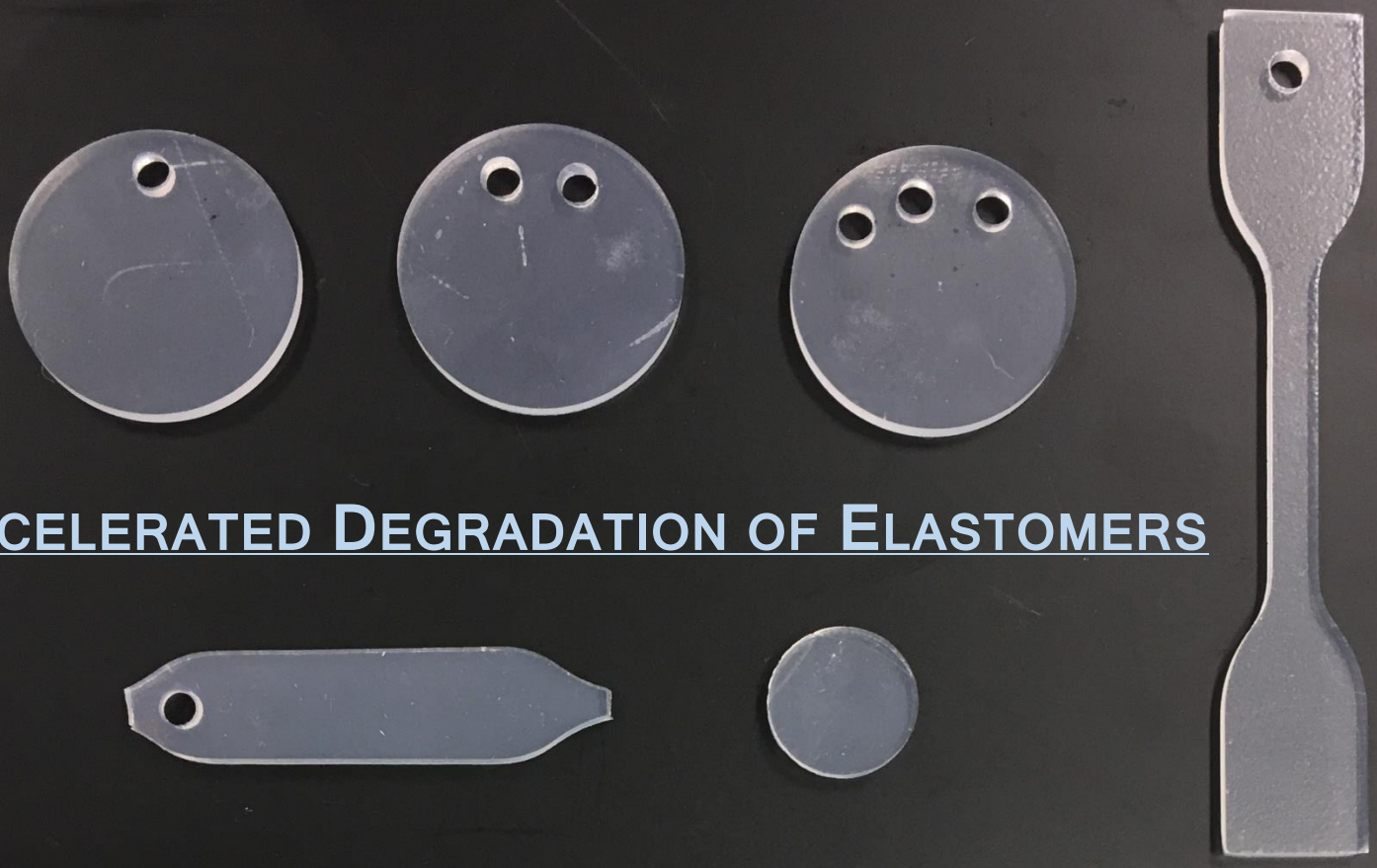

Accelerated Degradation of Elastomers

Effects of chemical degradation on mechanical properties and lifetime of LSR and TPV

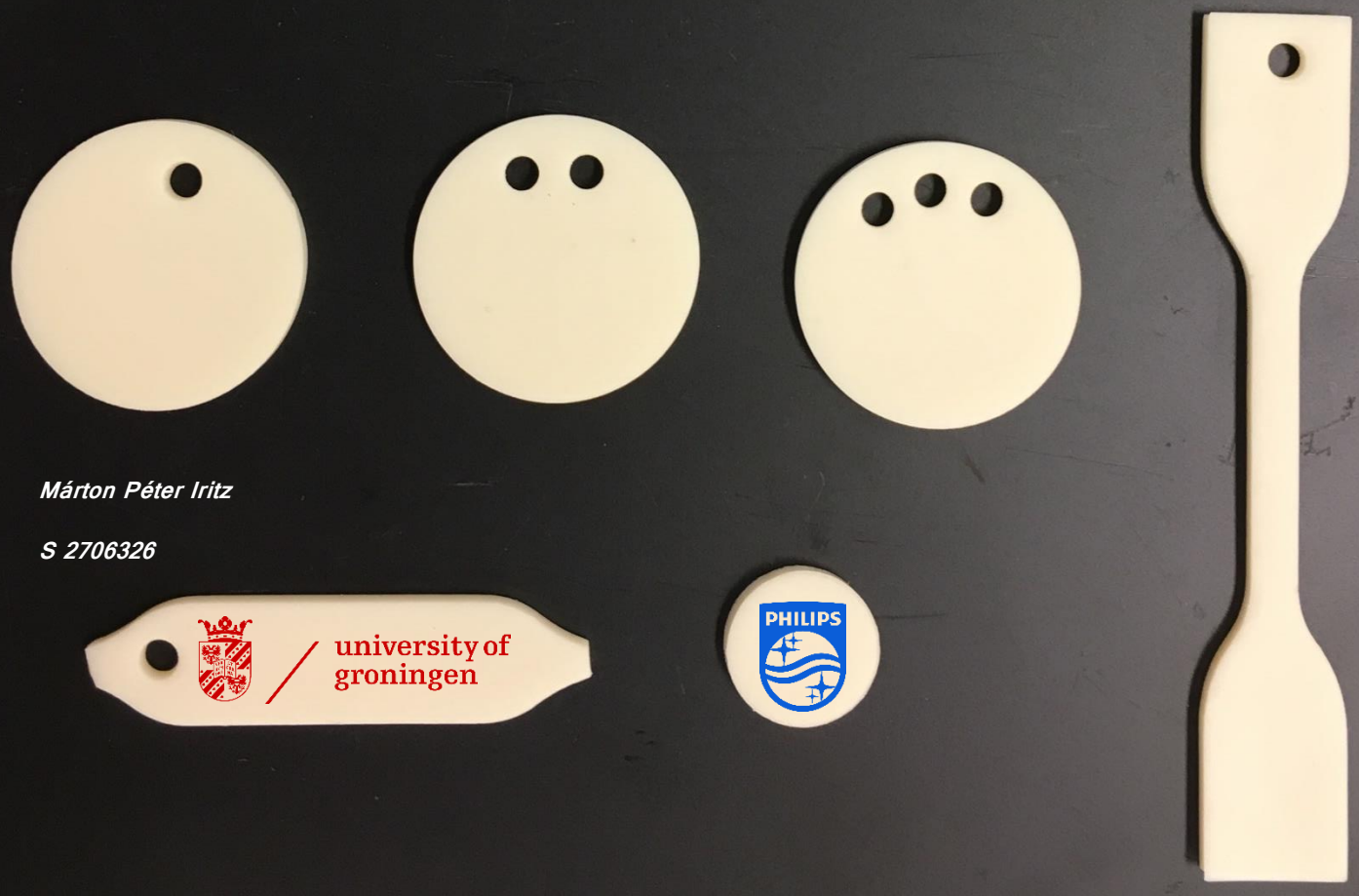

Márton Péter Iritz

S 2706326

university of groningen

PHILIPS

The cover shows the LSR and TPV specimens used to test the elastomers.

This thesis is dedicated to my parents, Ede and Ágnes.

Köszönöm!

Special thanks to Francesco Picchioni and Patrizio Raffa, my thesis supervisors from RuG; Sepas Setayesh for his inspiring enthusiasm about anything polymer related; Monique Velt for her guidance with laboratory equipment; Arjan Leussink for helping me gather data, and the many friendly faces at Philips Drachten. I would also like to thank Wouter J. J. Brouwer for his continuous emotional support outside my working hours.

ABSTRACT

Two different elastomers, a liquid silicone rubber from “COMPUNDER1” and a thermoplastic vulcanizate from “COMPOUNDER2”, were aged for 90 days at three temperatures (20, 40, 60 °C) in different surface disinfectants commonly used in healthcare. These disinfectants were sodium hypochlorite solution, isopropyl alcohol, DISINF1, containing peroxiacetic acid and DISINF2, containing a quaternary amine. The degradation of the two materials were followed by mechanical (weight change, hardness, compression set, stress-strain testing), analytical (FT-IR) and thermal measurements (TGA). The experiment aimed to point out the most significant effects of material degradation and to streamline the testing of elastomer ageing at Philips. Thermogravimetric analysis was used to assess the acceleration effect of these disinfectants on the useful lifetime of the materials. The ageing of the materials resulted in a two stage degradation, one controlled by chemical reactions and one reliant on mass transfer phenomena. It was shown that in the 90-day observation period, the mass transfer limitations prevail.

TABLE OF CONTENTS

TABLE OF FIGURES

TABLE OF EQUATIONS AND TABLES

ABBREVIATIONS

Natural rubber (polyisoprene)	NR
Parts per hundred weight of rubber	phr
Glass transition temperature	T_g
Cure site monomer	CSM
Koninklijke Philips N.V.	Philips
European Union	EU
United States' Food and Drug Administration	FDA
International Organization of Standardization	ISO
American Society of Testing and Materials	ASTM
Two-component (injection molding)	2K
European Economic Community	EEC
Healthcare-associated infection	HAI
Dry heat (sterilization method)	DH
Steam autoclave (sterilization method)	SA
Ethylene oxide (sterilization method)	EtO
Gamma irradiation (sterilization method)	GI
Electron-beam irradiation (sterilization method)	EI
Isopropyl alcohol	IPA
Quaternary amine	quat
Parts per million (0.0001%)	ppm
Polycarbonate-polybutylene terephthalate (blend)	PC/PBT
Ethylene-propylene rubber	EPM
Ethylene-propylene-diene rubber	EPDM
Thermoplastic vulcanizate	TPV
Polypropylene	PP
Styrene-ethylene/butylene-styrene triblock copolymer	SEBS
(Plasticized) poly(vinyl chloride)	(p)PVC
Liquid silicone rubber	LSR
Acrylonitrile butadiene rubber	NBR
Polyethylene	PE
Crosslink density	ρ_{CL}
Poly(dimethyl siloxane)	MQ
Vinyl methyl silicone	VMQ
Phenyl vinyl methyl silicone	PVMQ
Fluorinated vinyl methyl silicone	FVMQ
Room temperature vulcanizing silicone rubber	RTV
High temperature vulcanizing silicone rubber	HTV
Material safety data sheet	MSDS
Highly accelerated life test	HALT
Melting temperature	T_m
Williams-Landel-Ferry method (viscoelastic model)	WLF
High density polyethylene	HDPE
Polyether ether ketone	PEEK

INTRODUCTION

DESIGN CHALLENGE

Following global trends in healthcare and product development, Koninklijke Philips N.V. (*Philips*) launched its so called Philips 6.0 initiative. In this program, Philips describes their intention to improve the life of 3 billion people by 2025 through meaningful innovations with a focused attention in the healthcare sector while holding sustainability at the highest regard. As a direct consequence of their vision, the company is looking to broaden material knowledge and to replace non-recyclable plastics with more sustainable ones in their medical devices. Among various other plastics, rubbers have also been targeted.

Tackling the posed design challenge, the problem has to be divided into two parts that need to be inspected separately. Firstly, a better understanding of medical devices is needed. What are medical devices? What criteria is posed on the production and safety of these devices? What are the most severe degradation effects during the lifetime of a material used in such devices? How do we test the lifetime of such material in the most efficient and broadest way? Secondly, the material family of rubbers needs to be investigated. What are rubbers and where do they originate from? What are their physical and chemical characteristics? What subclasses are among them and what materials belong to rubbers? What could they be used for? What are the strengths and weaknesses of each representative of this group of plastics? In the following thesis, the author will attempt to answer these questions and draw conclusions on which materials are most suitable for further lifetime evaluation.

MEDICAL DEVICES

The fact that the material is used in medical devices, poses an interesting design goal from an engineering perspective. Philips expects that the rubber chosen conforms to medical requirements posed by the European Union (*EU*) and the US Food and Drug Administration (*FDA*) supported by *ISO* (International Organization of Standardization) and *ASTM* (American Society of Testing and Materials) test norms (Sastri, 2014). A material for medical application has to exhibit biocompatibility and stability against chemicals that are used for its decontamination.

In the EU, medical devices are regulated by the European Economic Commission (*EEC*). According to their definition in the Medical Device Directive, art. 1/2.a), a medical device is:

"any instrument, apparatus, appliance, software, material or other article, whether used alone or in combination, including the software intended by its manufacturer to be used specifically for diagnostic and/or therapeutic purposes and necessary for its proper application, intended by the manufacturer to be used for human beings for the purpose of:

- *diagnosis, prevention, monitoring, treatment or alleviation of disease*
- *diagnosis, monitoring, treatment, alleviation of or compensation for an injury or handicap,*
- *investigation, replacement or modification of the anatomy or of a physiological process,*
- *control of conception,*

and which does not achieve its principal intended action in or on the human body by pharmacological, immunological or metabolic means, but which may be assisted in its function by such means (EEC, 1993).”

As such, medical equipment is controlled by several regulations and has to fulfill numerous criteria before its market release. In the EU these standard is ISO 9001:2015, more specifically ISO 10993:2009 that examines the biocompatibility of medical grade materials; and ISO 13485:2016 which targets medical devices that satisfy the definition above.

Figure 1: The logo of the International Organization of Standardization (Source: Peerlyst)

Decontamination of medical devices

As a result, medical devices range from simple syringes to complicated permanent implants. They may differ in material of construction, shape and complexity but share one crucial point in their product life cycle. Decontamination is essential step for each of them before they enter any medical unit (Dettenkofer et al., 2005). Contaminated medical devices can result in healthcare-associated infections (*HAI*) that can potentially lead to death of patients (Klevens et al., 2007). Decontamination composes of three steps with decreasing efficiency of killing off microorganisms: sterilization, disinfection and cleaning. Single use items are exposed to these steps once in their product cycle. Reusable medical tools have to go through at least one of these processes after every use (NHS, 2017). As these methods aim to kill off microbiological contamination, sterilization generates harsh environments for the material to endure. Ultimately, this will result in change of the chemistry of the material, i.e. will degrade the material and shorten its estimated service time. Some materials may be suitable for one technique but cannot endure other cleaning methods. Understanding the decontamination methods and the chemicals associated with them brings us closer to correctly assessing the lifetime of rubber parts in medical devices.

Sterilization methods

Dry heat (*DH*) is the simplest sterilization technique. The material is heated to 160-170 °C for a few hours. Exposure to such heat for long period of time damages most elastomers permanently, loss of tensile strength and elongation are consequences of this technique (Sastri, 2014).

Better thermal sterilization technique is steam autoclave (*SA*), where the part undergoing sterilization is heated with saturated steam at around 120 °C for 10-60 minutes. Guidelines are laid down in ISO 17665-1:2006. Steam has better heat transfer than dry air, consequently it requires lower temperatures and shorter exposure times. SA does not suit moisture sensitive materials (Sastri, 2014).

One of the major advantages of ethylene oxide (*EtO*) sterilization is that the mechanism is chemical, not thermal as in previous cases. Thus thermal degradation of the material during sterilization is limited. Moisture sensitive materials can also be safely exposed to EtO. The way EtO sanitizes is thanks

to its reactive nature; it bounds to proteins and disrupts their structure. Reactivity often means toxicity, and it is the same case with EtO, therefore the reaction should be carried out in reduced pressure environments. Materials that absorb EtO are unfit for this sterilization technique or should be aerated before use. Regulations concerning EtO sterilization are outlined in ISO 11135-1:2007 (Sastri, 2014).

Irradiation sterilization relies on exposing the material to radiation that promotes the formation of radicals. These radicals attack microorganisms on the surface and in the bulk of the material. The formation of radicals can harm the irradiated part too. Without the presence of radical scavenging additives, the radicals formed can cause chain scission or crosslinking which change the material properties and lead to yellowing. In general, it can be said that aliphatic molecules are more prone to this kind of degradation than aromatic ones. ISO 11137-1:2012 describes in detail radiation sterilization techniques. Gamma irradiation (*GI*) is supplied from a cobalt-60 (Co_{60}) source and has a deeper penetration than electron-beam irradiation (*EI*) (Sastri, 2014). EI is produced by an electron beam and is the only sterilization method that can be carried out continuously (Sastri, 2014).

Disinfection methods

Disinfection of parts is important if the medical device is reused or needs to be sterilized again before use. It does not guarantee to kill all bacteria, germs and spores; for that any of the above-mentioned sterilization techniques should be used. However, it can help avoid contamination of patients in many cases. Most common disinfectants (antiseptics) to prevent HAIs are alcohols (e.g. ethyl and isopropyl alcohol), hypochlorites, iodophores (e.g. povidone-iodine), chlorhexidine, paracetic acid, quaternary ammonium compounds and aldehydes (e.g. glutaraldehyde) (NHS, 2017; Maki et al., 1991; Accini, 2012). These are capable of oxidizing or in other mean destroying the proteins of the microorganisms which lead to their death.

Figure 2: Clinell Universal Disinfectant wipes for surface disinfection (Source: Amazon.co.uk)

Cleaning

Cleaning is a prerequisite step before disinfection and sterilization. It usually consists of a lukewarm water bath with some sort of cleaning aid. This cleaning aid can be a detergent or an ultrasonic bath. Most hospitals use an automated system for this. Proper drying of the device is important before it proceeds to further decontamination steps (NHS, 2017).

In conclusion, resistance to chemically induced degradation is bottlenecked by the aforementioned decontamination methods. As discussed earlier, most frequent decontamination processes use oxidizing agents, chlorine containing solutions, alcohols, quaternary amines, and aldehydes. Although other degradation mechanisms can apply (wear and tear, UV, thermo-oxidative), the severity of chemical compatibility (swelling, dissolving) and hydrolytic and oxidative stability was chosen to be evaluated (Sastri, 2014).

Surface disinfectants used

To maximize the spectrum of the research, four inherently different disinfectants were chosen: isopropyl alcohol (*IPA*), the quaternary amine containing DISINF2, the peroxide containing DISINF1 and a low concentration solution of sodium hypochlorite (NaOCl). The first two are alcohol based solutions that are expected to cause mass transfer driven degradation and the second two are oxidizing agents that are likely to change polymer chemistry.

IPA, or 2-propanol is a colorless, ethanol smelling liquid that is miscible with water. It has disinfection properties although the exact mechanism is not understood. It is sold over the counter as a topological antiseptic in pharmacies as rubbing alcohol. It is used widely in cosmetics, the paint industry and perfumes (Pubchem, 2019).

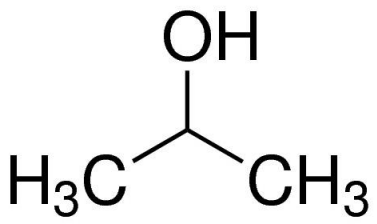

Figure 3: Isopropyl alcohol (Source: Pubchem)

NaOCl is the sodium salt of hypochlorous acid, HOCl. In solution it is a yellowish liquid, and contains several ions in equilibrium. Solutions of it is commonly referred to as bleach and is used as a cleaning and disinfecting solution (Dakin's solution) in many households and medical institutes. NaOCl is far more stable than HOCl, thus it is the preferred chemical to use in sterilization purposes. Degradation of hypochlorite ions is induced by temperature, light and trace minerals. Equations 2-5 show the solvation equilibria and the degradation mechanisms present therein (Sandin, Karlsson and Cornell, 2015; OxyChem, 2014).

$$NaOCl_l \rightleftarrows Na^+_{aq} + OCl^-_{aq} \quad (1)$$

$$OCl^-_{aq} + H_2O \rightleftarrows HOCl_{aq} + OH^-_{aq} \quad (2)$$

$$3\,OCl^- \rightarrow ClO_3^- + Cl^- \quad (3)$$

$$2\,OCl^- \rightarrow O_{2\,g} + 2\,Cl^- \quad (4)$$

Equations 1-4: (1) Solvation of NaOCl in water (2) Equilibrium of ions in solution; above pH 12 the equilibrium is shifted to favor the formation of OCl^-_{aq} (3) Temperature and concentration dependent decomposition of hypochlorite ions to chlorate and chlorine ions (4) Light catalyzed degradation of hypochlorite ions

DISINF2 is a quaternary amine (*quat*) containing, low alcohol disinfectant for non-porous surfaces. It offers sanitation against most bacteria, fungi and viruses even at short contact times. The active ingredients is 0.1-1% benzethonium chloride (N-Benzyl-N,N-dimethyl-2-{2-[4-(2,4,4-trimethylpentan-2-yl)phenoxy]ethoxy}ethanaminium chloride) in a 10-20% IPA and 1-5% 2-butoxyethan-1-ol solution with water. DISINF2 is the alkaline (pH 11-12.5) solution used in many other formulations such as wipes and sprays (DISINF2Supplier, 2019; DISINF2Supplier, 2001).

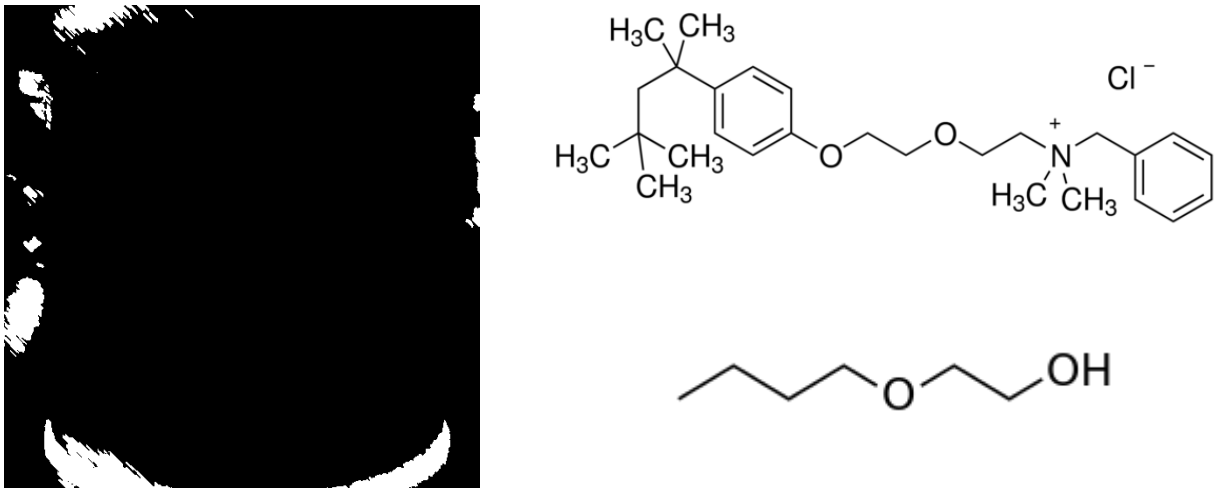

Figure 4: (l) Gallon bottle of DISINF2 supplied by DISINF2Supplier (r-t) Benzethonium chloride (r-b) 2-Butoxyethan-1-ol (Source: Pubchem)

DISINF1 is a powder that becomes, when dissolved in water, a pale green or yellow solution. 1% solution contains 600 *ppm* (parts per million) peracetic acid as active agent derived from sodium percabonate. Sodium percarbonate is an adduct of hydrogen peroxide and sodium carbonate (Pubchem, 2005). Citric acid makes up for the pleasant smell of the solution. Other stabilizers are added e.g. to prevent caking of the powder when stored for longer time, these include long chain alcohols. (DISINF1Supplier, 2019).

Figure 5: (l) 1.5 kg package of DISINF1 powder (r) Peracetic acid (Source: Pubchem)

HISTORY AND RELEVANCE OF RUBBER

First documentation of rubber dates back to the 11th century from the Mayan civilization. The Mayan Indians were known to play a game with a rubber ball but also used the material to coat their clothing to grant waterproof properties to textiles. They extracted the material from the bark of the *Hevea brasiliensis* by tapping the tree. Christopher Columbus described this ball game and the strange new material after arriving from his second voyage to the New World in 1496 and allegedly brought back some to Queen Isabella. Natural rubber (*NR*) did not find any commercial application because it was expensive, hard to process and its inability to keep its properties in a wide range of temperatures. When exposed to warm weather, the rubber became soft and sticky; in cold, it became hard and brittle. Even the extraction and transportation of the crude product, latex was difficult, e.g. Northern Mexican Indians traditionally chewed guayule rubber to coagulation. Obviously, this method could not be applied on an industrial scale. However, during the late 18th to early 19th century some rubber trade routes and the first rubber factory were created as some of its properties foreshadowed a great potential for rubber. (Hurley, 1981; Bhowmick and Stephens, 2001).

Figure 6: Collection of the latex in Thailand (Source: Seilnacht.com)

Charles Goodyear's discovery, however, changed the rubber industry significantly and allowed for this potential to be fulfilled. In 1839, he accidentally heated sulfur with NR, thus discovering vulcanization. This created sulfur crosslinks between the chains of rubber molecules and improved the mechanical and wearability properties of the material significantly. After his patented rubber products and Hancock's patent of solid rubber tires, the rubber industry and rubber production started blooming. After World War II, the concept of polymers consisting of small molecules started spreading and several synthetic rubbers appeared on the market. These new materials were engineered to fit certain applications. In turn, NR production was pushed back and gave space to superior materials (Hurley, 1981).

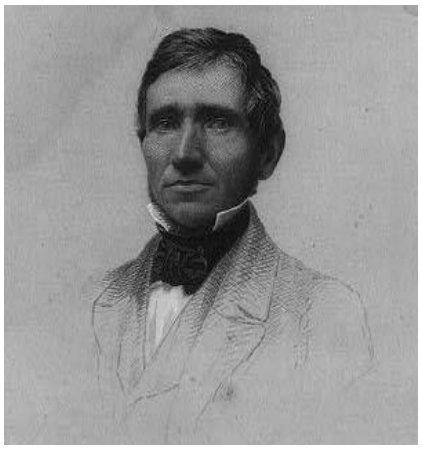

Figure 7: Charles Goodyear (1800-1860) (Source: Encyclopedia Britannica)

Currently, NR still makes up for 49% of global elastomer production. The majority of both production and consumption of synthetic and NR alike takes place in the Asia-Pacific region (Statista.com, 2018; CES, 2018).

CHEMISTRY OF RUBBERS

Rubbers are a subclass among polymers, which means that they are molecules bound by covalent bonding built up from repeating units of smaller chemicals. The more scientific term elastomer is used to describe them also, thus avoiding confusion between rubbers (a family of polymers) and NR (the most widely used elastomer). They are defined by their tendency to regain their original shape and form above their glass transition temperature (T_g) after a deforming force has stopped acting on the material. This recovery depends on the force applied on the rubber, the duration and rate that it has been applied. If either of these is high, the material is exposed to the risk of permanent distortion or rapture. The T_g is defined as the temperature range where the polymer chains' mobility is increasing, and in turn transfers the material from a rigid, glass-like phase (hence the name) to a softer, pliable rubbery state (Sperling, 2005).

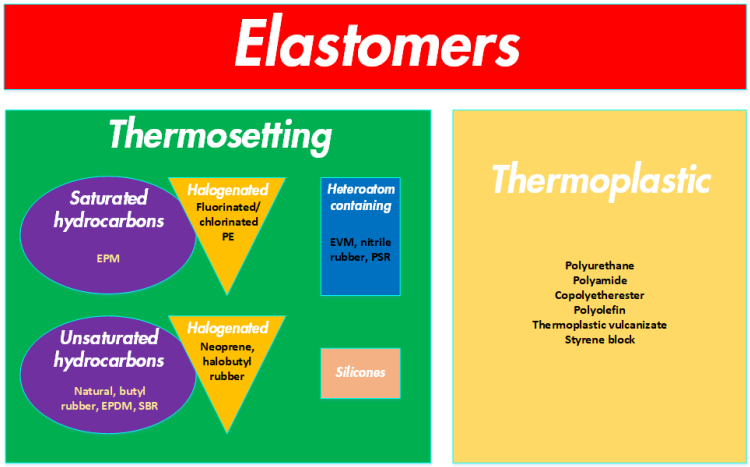

Figure 8: Diagram of classification of elastomers

The elastic property of theirs is something often undermined in applications. Rubbers appear in seals and gaskets, construction materials, most famously in tires of the automotive industry. Rubber products contain a variety of chemicals called fillers besides the polymers. Rubber composition is thus often presented as a “recipe”, where the amount of fillers is given in parts-per-hundred-rubber, i.e. *phr*. These fillers fulfill various functions and range from stabilizers, through plasticizers, to vulcanization agents. Fillers are also applied to reduce the price of the product and to optimize properties to fit the function and purpose of the rubber (Drobny, 2014).

Thermosetting vs thermoplastic: Rubber elasticity

Thermoplastic polymers are described as materials capable of softening when exposed to heat. Classical elastomers, on the other hand, are thermosets with chemical crosslinking, so exposure to heat leads to burning. Ergo, an elastomer is hard to recycle and form with heat unlike thermoplastics (Nash, 1979). Thus the advantages of a developing an elastic thermoplastic polymer is obvious.

The thermosetting elastomers are elastic due to their entropic resistance against stretching granted by the limitation on chain mobility that the crosslinking poses on the chains. When such a material is stretched, the number of chain conformations possible decreases resulting in a lower entropy state. This will lead to an increase in temperature in the material according to the inverse proportionality of these two variables in the Helmholtz free energy equation (Equation 5). As a direct conclusion, it can be said that the retractive force is entropic.

$$F \equiv U - TS, \tag{5}$$

Equation 5: Helmholtz free energy where F is the Helmholtz free energy in Joule, U is the internal energy in Joule, T is the absolute temperature in Kelvin and S is the entropy in J/K (Sperling, 2005)

A thermoplastic elastomer has no chemical crosslinks, which allows for good processability and recyclability. Leaving out the curing step to form crosslinks, leads to reduced production times which in turn saves money. The absence of curing calls for intermolecular interactions to take over the role of crosslinks. These interactions include ionic and hydrogen bonding, crystalline clusters or thermally unstable covalent bonds. These crosslinks are weaker than traditional curing techniques, therefore the main drawback of thermoplastic elastomers are reduced high temperature, oil and solvent resistance (Drobny, 2014; Sperling, 2005).

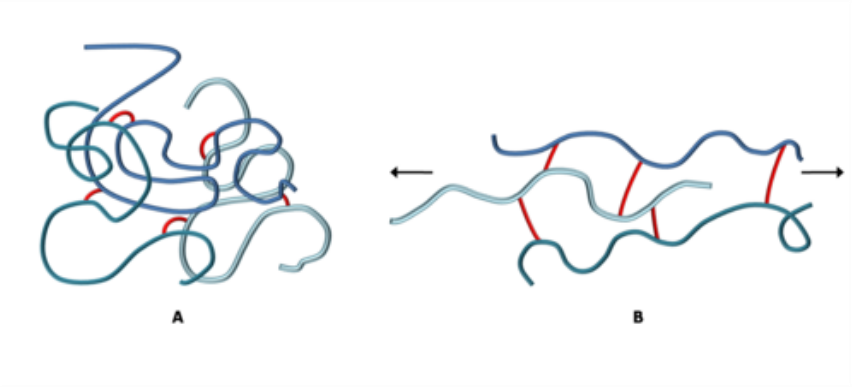

Figure 9: Effect of crosslinking on entropy in stretched materials; crosslinked elastomer in low entropy, stretched state (B) will regain its high entropy state naturally (A) (Source: Harvard.edu)

Crosslinking

As introduced earlier, crosslinking is a quintessential structural characteristic of thermosetting elastomers. Thermoplastic elastomers may not include permanent chemical linkages but physical crosslinking still contributes to their structure. Crosslinking is introduced in a vulcanization or curing step during or after the synthesis of the chains. The number of crosslinks are important characteristic of the material and is often represented by the molecular weight between crosslinks which can be translated into the number of monomeric units between neighboring crosslinks. Denser crosslink architecture leads to a harder rubber.

Chemical crosslinks are based on stable covalent segments bonding more than one chain together. Radical processes often catalyze their formation, such as a peroxide or radiation cure. These result in chain-chain crosslinks. For halogenated elastomers, a metal oxide such as ZnO or MgO can be used for an ionic fixation of the chlorine atoms. Sometimes an unsaturated cure site monomer (*CSM*) is introduced in the polymer chain, which will be susceptible to a chemical attack during curing. However, the most commonly used crosslinking technique is still sulfur vulcanization. In this method, the elastomer is heated in the presence of sulfur and the sulfur creates sulfide bridges between chains. An accelerator is often added to the mixture that helps to mediate this reaction and leads to a faster cure (Bhowmick et al., 2014).

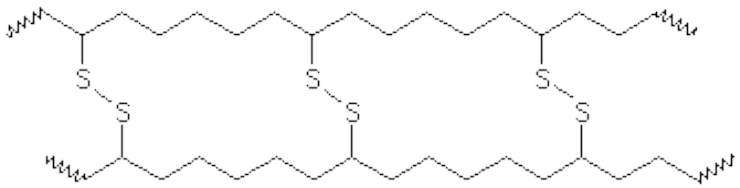

Figure 10: Sulfide crosslink representation (Source: CSUDH WWW Project for Chemistry)

In thermoplastic elastomers, there are no such covalent crosslinks. To aid processing of the material, the crosslinks are physical and are able to rearrange into new connections along the chain. The role of the crosslinks is taken over by ionic forces, van der Waals interactions of H-bonds (Drobny, 2014).

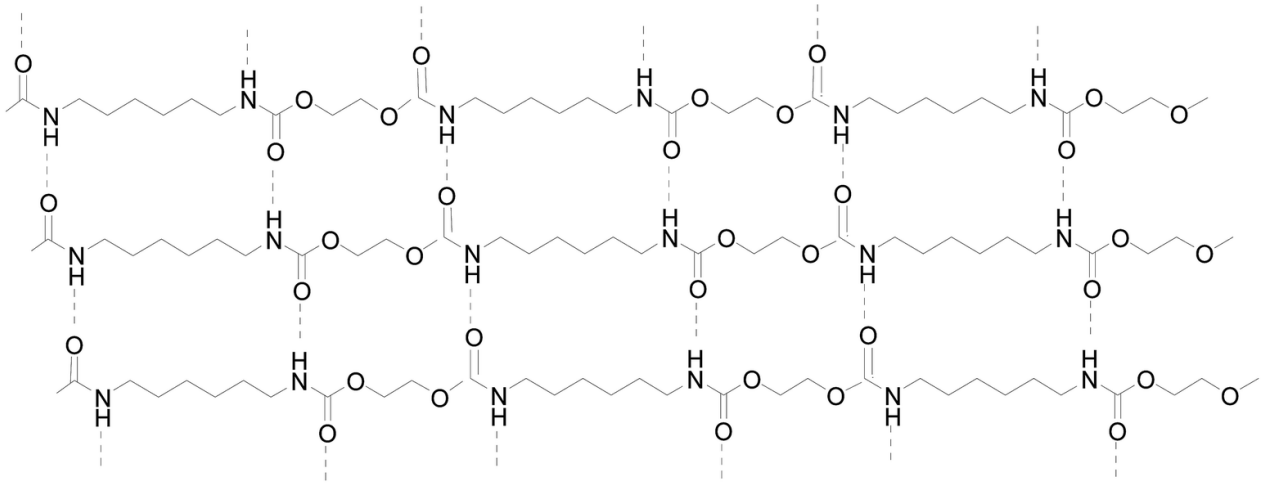

Figure 11: H-bonding in thermoplastic polyurethane rubber (Source: MSU Chemistry)

QUANTITATIVE ASSESSMENT OF DESIGN CRITERIA

Now that the two components of tackling the design challenge posed by Philips have been established, an assessment of the criteria that this poses on material selection can be executed. Table 1 collects some chemical, processability and biocompatibility requirements and assigns a numeric value to their importance. It also lists all (commercially relevant) elastomers and inspects them according to the preset criteria. Preliminary to this evaluation, a thorough literature research was conducted aiming to better understand the differences and properties of various elastomers. Due to the length of a detailed reasoning behind each value assigned in the table, only the selected materials will be introduced in this thesis. Said preliminary examination will be provided in a separate document.

Ethylene-propylene rubber (*EPM*) and ethylene-propylene-diene rubber (*EPDM*) stand out by only being limited in injection moldability. Thermoplastic vulcanizates (*TPV*) utilize these polymers in a poly(propylene) (*PP*) matrix. As a result, their performance is outstanding too. Silicone only degrades when exposed to concentrated H_2O_2, which is rare as most decontamination techniques use diluted solutions of peroxides if any. Styrene-ethylene/butylene-styrene triblock copolymer (*SEBS*) and plasticized poly(vinyl chloride) (*pPVC*) both show overall good properties, but the fact that they are prone to thermal degradation and their compression set is only optimal for softer grades, makes them only a secondary consideration for this application. As a direct conclusion of this analysis, TPVs and silicones will be further investigated in detail.

Name	Abbreviation	Injection moldable?	Oxidative degradation	Hydrolysis?	Thermolysis above 135 °C?	Compression set?	Medical grades?	Suitability	Rank
Importance (1-10)		**10**	**8**	**6**	**4**	**4**	**10**		
Relative importance (100%)		**0.24**	**0.19**	**0.14**	**0.10**	**0.10**	**0.24**		
UNSATURATED HYDROCARBONS									
Natural rubber (Polyisoprene)	NR	3	1	4	1	4	4	2.905	11
Polybutadiene	BR	4	1	4	1	4	0	2.190	19
Isobutylene isoprene (Butyl) rubber	IIR	3	1	4	1	4	4	2.905	11
Ethylene propylene diene rubber	EPDM	2	4	4	4	4	4	3.524	4
Polynorborene	PNR	3	1	4	4	3	0	2.143	21
Styrene butadiene rubber	SBR	3	1	4	1	4	0	1.952	24
HALOGENATED UNSATURATED HYDROCARBONS									
Polychloroprene	CR	3	1	4	1	4	0	1.952	24
Halobutyl rubber	C/BIIR	3	1	4	1	4	4	2.905	11
SATURATED HYDROCARBONS									
Ethylene propylene rubber	EPM	2	4	4	4	4	4	3.524	4
HALOGENATED SATURATED HYDROCARBONS									
Fluoroelastomer	FKM	3	2	4	4	3	0	2.333	18
Perfluorated elastomer	FFKM	0	4	4	4	2	4	2.857	14
Chlorinated polyethylene	CM	3	1	4	3	4	0	2.143	21
Chlorosulfonated polyethylene	CSM	0	4	4	1	4	0	1.810	26
OTHER HETEROATOM CONTAINING THERMOSETTING ELASTOMERS									
Ethylene vinyl acetate rubber	EVM	0	4	3	4	4	0	1.952	23
Nitrile rubber	NBR	3	3	3	1	4	0	2.190	19
Polysulfide rubber	PSR	0	1	1	1	4	0	0.810	28
Epichlorohydrin	CO	3	1	1	1	4	0	1.524	27
Silicone	(L)SR, VMQ	4	3	4	4	4	4	3.810	1
THERMOPLASTIC ELASTOMERS									
Polyolefin blends	TPO	4	4	4	3	1	0	2.667	15
Thermoplastic vulcanizate	TPV	4	3	4	4	3	4	3.714	2
Styrene-butadiene-styrene block copolymer	SBS	4	3	4	1	1	4	3.238	8
Styrene-isoprene-styrene block copolymer	SIS	4	3	4	1	3	4	3.429	7
Styrene-ethylene/butylene-styrene block copolymer	SEBS	4	4	4	1	3	4	3.619	3
Polyamide	TPA	4	1	1	1	1	4	2.429	16
Copolyetherester elastomers	TPC	4	3	1	4	1	4	3.095	9
Polyurethane, ester based	TPU-es	4	1	1	1	1	4	2.429	16
Polyurethane, ether based	TPU-et	4	1	3	2	3	4	3.000	10
Polyvinyl chloride, plasticized	PVC	4	4	4	1	2	4	3.524	4

Table 1: Preliminary design criteria assessment

THERMOPLASTIC VULCANIZATE

TPV is a mixture of chemicals, usually PP and EPM/EPDM but acrylonitrile butadiene rubber (*NBR*) and other α-olefinic, e.g. polyethylene (*PE*) enriched versions are favorable too. TPV was developed by Monsanto (now owned by ExxonMobile Chemical) when looking for alternative materials for injection moldable tire materials. It was first released to market under the name Santoprene in 1977 (Naskar et al., 2005; Whelan, 2013; TPE Magazine, 2017).

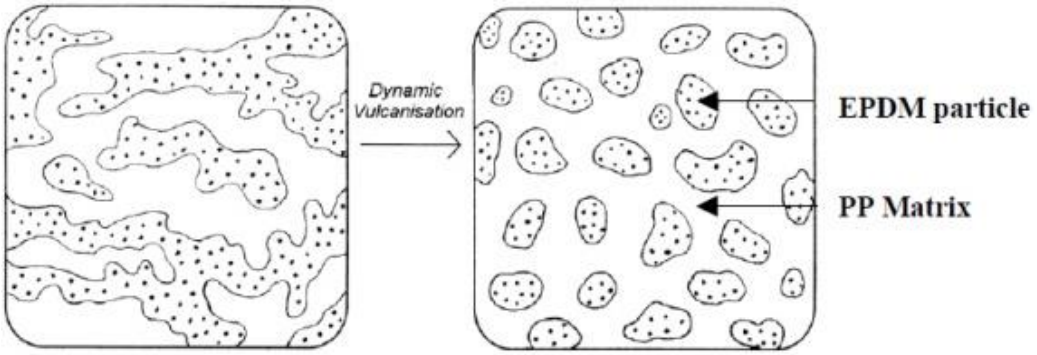

Figure 12: TPV microstructure before and after dynamic vulcanization with suspended micron sized EPDM particles in PP (Source: Elastron.com)

Synthesis and composition

What sets all formulations of TPVs apart from other elastomers, is the dynamic vulcanization process. This can be achieved by mixing either in a batch process using a mixer (Banbury or Brabender mixer) or continuously in an extruder. When mixed, the curing agent (usually a phenolic curative, but peroxide, sulfur cure is viable too) addition is limited to achieve a fully crosslinked product. Other methods include pulverizing the crosslinked rubber and then adding it to the matrix. The so-created, crosslinked EPDM particles are thus homogeneously dispersed in the PP continuous phase (Figure 12). As a result, TPVs are suitable for thermoplastic forming techniques despite the rubber molecules already being crosslinked.

Typical formulations of Santoprene TPVs consist of EPDM, PP, extender oil, stabilizers and other blend ingredients. The EPDM has 0.1-5% diene content, minimum crosslink density (ρ_{CL}) of $7*10^{-5}$ mol/mL and is at least 97% crosslinked. The rubber particles formed need to be smaller than 50 µm, preferably smaller than 5 µm. PP (or other high molecular weight α-olefin) needs to be crystalline, therefore, isotactic or syndiotactic PP is preferred. TPVs are capable of maintaining their thermoplastic processability and good tensile properties even with high oil contents. Noble formulations of TPVs can be described by Equation 6 (US 4,130,535, 1978; US 4,311,628, 1982).

$$\frac{W_{oil} + W_{EPDM}}{W_{PP}} \geq 0.33\ (or\ 0.5), \tag{6}$$

where W_X denotes the weight of X in the sample.

Equation 6: Thermoplastic elastomeric compositions of Santoprene (US 4,130,535, 1978)

Applications

TPVs appear in abundance on the market due to its colorability, stability and favorable mechanical properties. Several automotive and architectural applications are known and it is used for grips, grommets and seals as well (CES, 2018; TPE Magazine, 2017).

Figure 13: TPV grip on a Russian hunting knife (Source: Russianblades.com)

Degradation

TPVs are also prone to degradation but less than unsaturated hydrocarbons. Wear and UV resistance is one of the drawbacks for this material and leads to yellowing of the material. However, these vulnerabilities can be assessed with appropriate additives (Drobny, 2014; CES, 2018).

Chemical compatibility

Due to the almost fully saturated chains of TPV, chemically induced degradation happens only in some oils and fuels and chlorinated organic solvents. Initially its resistance to oil swelling was what set it apart from EPDM, and foreshadowed TPV's success to the developing engineers. It was determined that higher crosslinking density in the EPDM particles results in higher resistance to oils. (CES, 2018; US 4,130,535, 1978).

Property	Dimension	Value – TPV (PP+EP(D)M)
Glass transition temperature (T_g)	*°C*	-110 – -50
Elongation at break	*%*	340-660
Shore A hardness	-	35-100
Application temperature	*°C*	-65-140
Compression set at 100 °C	*%*	32-80
Tear strength	*kN/m*	12-92
Tensile strength	*MPa*	3-21
Young modulus	*MPa*	2-238
Sterilization	EtO, GI, EI *Medical grade available*	
Advantages	Processability, aesthetics, colorability, versatility	
Limitations	Weak to UV and wear	
Supplier	ExxonMobil Santoprene® Teknor Apex Uniprene® Elastron® V	

Table 2: General properties of thermoplastic vulcanizates

SILICONES

All silicones are differently modified chains of polyorganosiloxanes. The organosiloxane used most commonly is dimethyl siloxane and commercially available silicones are modified versions of this polymer, poly(dimethylsiloxane) (*MQ*). Modification happens by the replacement of some of the methyl groups of the chain, allowing for crosslinking to happen. Vinyl methyl silicone (*VMQ*), phenyl vinyl methyl silicone (*PVMQ*) and fluorinated vinyl methyl silicone (*FVMQ*) are all available on the market. The methyl groups on the surface of the chain are granting hydrophobicity to the chain. The polymer is characterized by low intermolecular interaction and highly flexible chains, which allow gas permeation to happen (CES, 2018).

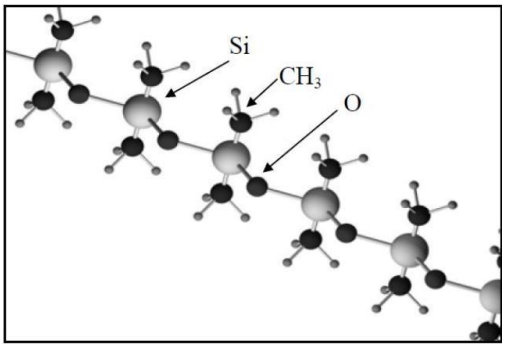

Figure 14: Silicone polymer chain (Source: Azo Materials)

Synthesis and processing

Silicone synthesis happens through a hydrolysis process of either chlorosilanes or acetoxy silanes. The former releases toxic HCl during synthesis, therefore the acetoxy silanes are used for medical grade silicone production (Bhowmick and Stephens, 2001).

Crosslinking of the polymers happens at the vinyl sites or by adding a trifunctional monomer to the synthesis mixture. Curing can be catalyzed by platina and tin containing compounds and organic peroxides. Processing also helps to distinguish between different types of silicones. Room temperature vulcanizing silicones (*RTV*) are soft elastomers. As the name would suggest, it cures and sets from liquid form without the application of heat. Can have one or two component systems, named RTV-1 and RTV-2 respectively. High temperature vulcanizing silicone rubber (*HTV*) on the other hand, produces gum like rubbers. LSR is supplied in two components (frequently in an injection molding process) which are mixed and are cured with heating it for a short time at a high temperatures. 2K molding is also possible if adhesion is good. Fillers of silicones differ from conventional organic rubbers; instead of carbon black, fumed silica is used (Bhowmick and Stephens, 2001; Whelan, 2013).

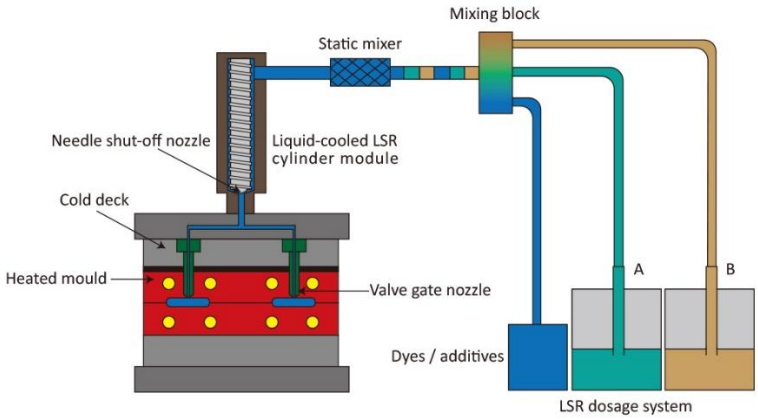

Figure 15: LSR injection molding process. Tank A would have the catalyst and B the inhibitor. (Source: JWT Rubber)

Applications

Silicones have a wide range of applications thanks to their appealing mechanical and chemical characteristics. They are inert and have low amount of extractables in them, making them suitable for biocompatible applications such as implants, sex toys and other medical devices. They appear in tubes, insulators, cushioning, seals and sealants. Due to their broad range of application temperature, they also appear in kitchens, in the form of baking sheets, mats and spatulas. It is also used in technology development due to its electric and dielectric properties. PVMQ has improved low temperature resistance, FVMQ is used for its improved chemical resistance (CES, 2018).

Figure 16: Silicone Foley 2-way catheter (Source: DiaMedical USA)

Degradation

Silicones are prone to mechanical damage through their low tear strength. UV and oxidation degradation are not affecting the material. Silicone is inherently flame resistant, and is self-extinguishing (CES, 2018).

Chemical compatibility

Silicones are regarded as chemically inert, but chlorinated organic solvents will cause swelling, and will eventually lead to the dissolution of the polymer. Concentrated acids also destroy the chain (Bhowmick and Stephens, 2001).

Property	Dimension	Value – VMQ
Glass transition temperature (T_g)	*°C*	-65
Elongation at break	*%*	270-600
Shore A hardness	-	5-85
Application temperature	*°C*	-60-250
Compression set at 100 °C	*%*	5-10
Tear strength	*kN/m*	10-40
Tensile strength	*MPa*	7-11.5
Young modulus	*MPa*	5-50
Sterilization	EtO, SA, DH *Medical grade available*	
Advantages	Wide range of application temperature, stability, weatherability, good electric properties, sealing capability, low density, breathability	
Limitations	Short shelf life, poor oil resistance, hydrolysis at high temperatures, expensive	
Supplier	Momentive™ ShinEtsu Silicones™ Tufel® (FVMQ) Baysilone® (silicone oil)	

Table 3: Vinyl silicone rubber properties (CES, 2018)

CES SELECTOR AND MSDS – VALUABLE TOOLS FOR MATERIAL COMPARISON

It can be concluded that TPVs and liquid silicone rubbers (*LSR*) are the ones most fitting the criteria previously set. Consequently, these materials are going to be the ones tested and investigated in detail for this application. Namely the following representatives of these material families:

1. COMPOUNDER1 LSR (LSR),
2. COMPOUNDER2 TPV (TPV).

GRANTA's CES Selector 2018 has proved to be a very valuable tool to understand and compare material characteristics. Below, two graphs will be presented that set TPV (red) and LSR (green) side by

side with other members of the elastomer family (blue). To help the reader navigate through this rather qualitative assessment of material properties, two more rubbers were market with color. Yellow denotes an unreinforced NR, and orange marks an SEBS rubber with Shore A hardness value of 65.

As it can be seen in Figures 17 and 18, both LSR and TPV are available in a wide range of hardness, density and elongation to best fit customer requirements. LSR tends to be available in softer grades than TPV, but TPV has a lower T_g that can be undermined in low temperature applications.

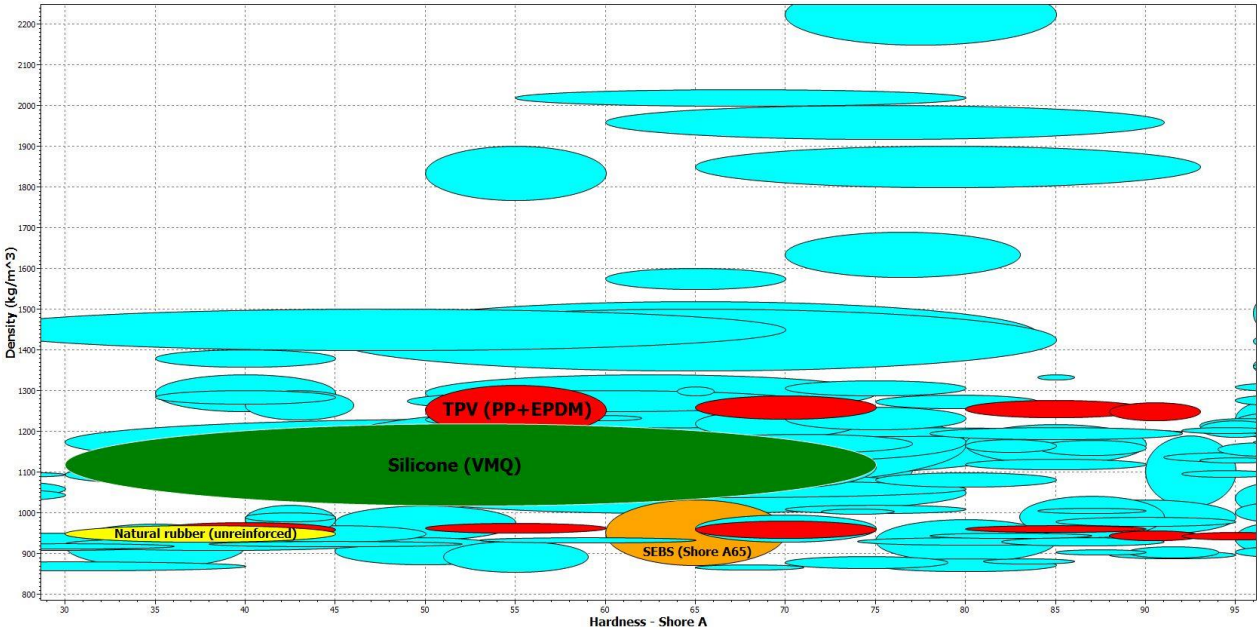

Figure 17: Hardness of commercial elastomers compared with their density in CES Selector 2018

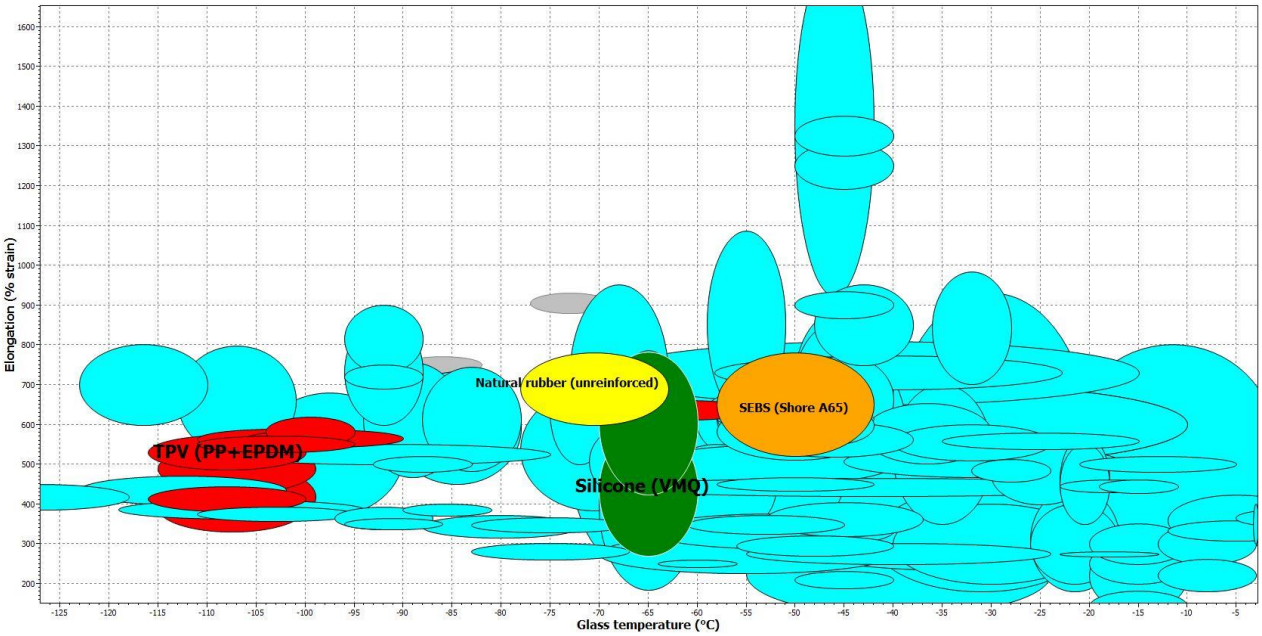

Figure 18: Glass transition temperature of commercial elastomers compared with their ultimate elongation in CES Selector 2018

Besides CES Selector, the material safety data sheets (*MSDS*) also provide with an opportunity to compare important plastic and elastomer properties. The two materials are quite different in many aspects. This does not conclude that one is better but shows that they may find suitable applications in different products. Also, the MSDS gives a baseline for unaged materials. However, it is good to keep in mind that these values, despite being confirmed by ISO or ASTM norms, are not representative of the very samples provided by their manufacturer (COMPOUNDER1, 2018; COMPOUNDER2, 2014).

Property	**Dimension**	**TPV**	**LSR**
Density	kg/m^3	970	1120
Processing temperature	*°C*	210	175
Glass transition temperature	*°C*	-60	N/A
Color	-	natural (colorable)	transparent (colorable)
Hardness	*Shore A*	69	38
Ultimate elongation	*%*	450	700

Table 4: Quantitative comparison of the two selected materials in numerous important physical and mechanical properties

LIFETIME ESTIMATION OF ELASTOMERS

Assessing lifetime of a rubber is a daunting task and depends on many factors. One product behaves differently when placed in the close proximity of a window or radiator than when it is placed further away from those. Several aspects cannot be accounted for as some depend on the user of said product. Not to mention that these products are expected to perform over several years. As a way of reducing the time of *in situ* testing, accelerated methods have been proposed that mimic long-term exposure to degradative forces. For example, increasing the temperature will increase the rate of degradation processes, etc. A test that aims to determine the lifetime of a polymer over a short period of time in an accelerated manner is called a Highly Accelerated Life Test (*HALT*).

Lifetime estimation is a difficult to assess problem for polymers and HALT methods are only capable of providing an approximate solution. Acceleration of the real-life degradation extrapolates poorly when the factor of acceleration is larger than 2-3. For a company this can be expensive to test due to the time consuming nature of HALT. For example for Philips, whose products are expected to perform without complications on the scale of several years. Therefore, efficiency and accuracy in estimation of service time is vital to material specialists. Current trends aim to generate a certain masterplot, one that utilizes the time-temperature superposition principle of Boltzmann. One of these methods uses the Arrhenius equation and this method will be the basis of this thesis.

THEORY

ELASTOMER DEGRADATION

Elastomer degradation is defined as an irreversible change to the material on a chemical or physical level. These chemical changes include chain scission and crosslinking, the reaction of chains or fillers with molecules. Physical changes include creep, compression set and low temperature stiffing, but extraction of plasticizing agents can be listed here too. Often, to fully understand the mechanism of degradation, more parallel processes are taken into consideration. The driving force behind chemical change is often radical related *in situ*, as it is in the case of thermal oxidation, UV exposure or ozonation which makes for a random degradation along the polymer chain (Brown, 2001).

Time dependent limitation of degradation: diffusion and fluid transfer

When immersed in liquids, chemical ageing depends on the diffusion of the liquid into the material. This may take a long time on the scale of chemical degradation and often a thin specimen is suggested to reach mass transfer equilibria faster. However, once the absorption equilibrium is reached, curve of the registered mechanical property shows an apparent change. Same can be said for oxygen absorption in the case of oxidative ageing, or for any other gas for that matter (Brown, 2001; Gao et al., 2014).

$$\boldsymbol{J} = -D\nabla c, \tag{7}$$

*where **J** is the diffusion flux vector, D is the diffusion coefficient, ∇ is the gradient operator generalizing the time dependent first derivative and c is the concentration.*

Equation 7: Diffusion of liquids, the Fick's law

Other time limiting factor includes a so called induction period. During this time, the material shows little change in mechanical parameters and after the end of the period is reached, the degradation is accelerated. A common example of this is the use of antioxidants which can scout radicals formed inside the material. Once the antioxidants are used up in prevention, the oxidation starts to degrade the material, resulting in severe effects in the rubber. Brown (2001) also warns that *"care must be taken to avoid drawing conclusions from results obtained before equilibrium conditions are reached"*. He adds, that the time to reach maximum absorption is proportional to specimen thickness in a squared fashion as shown by Fick's second law (Equation 8). In case of standard 2 mm thick sample pieces, this may take months or years (Brown, 2001; Gao et al., 2014).

$$\frac{\partial c}{\partial t} = D\frac{\delta^2 c}{\partial x^2}, \tag{8}$$

where x is thickness in the direction of the diffusion and t is the time.

Equation 8: Fick's second law

ARRHENIUS EQUATION

The Arrhenius equation is a widely used kinetic formula that relates the rate of a reaction, the activation energy and temperature. In the case of degradation mechanisms, it is a frequently used tool to estimate the underlying kinetics of a chemically induced degradation. Published by Swedish physicist, Svante Arrhenius in 1889 (Arrhenius, 1889), the equation sought answer to why some molecules participate in a reaction while others do not. He explained that that is because of a certain energy barrier molecules have to overcome, which he called activation energy. All factors of the equation are considered to be non-temperature dependent (Connors, 1990).

$$k = Ae^{-E_a/RT} \tag{9}$$

$$\text{linear form: } \ln k(1/T) = \ln A + \frac{-E_a}{RT} \tag{10}$$

where k is the rate constant, T is the temperature in K, A is the so called pre-exponential factor denoting the frequency of correct molecular collisions, E_a is the activation energy and R is the gas constant.

Equations 9-10: Arrhenius equation and its linearized form

Often the linearized form is used, which is a straight line when ln(k) is shown as a function of 1/T. The slope of such line is $-E_a/R$ and the crosses the y axis at A. There are several things to consider when the equation is used and these considerations shed light on some of the shortcomings of Arrhenius method.

One way to estimate lifetime with the Arrhenius equation

Initially, it was expected that the collected mechanical data could be assessed according to the Arrhenius equation if a failure criterion is set up (Brown, 2001). When using Arrhenius in polymer lifetime estimation, measurements at higher temperatures are extrapolated to fit real life degradation of the material. This means that a certain mechanical failure criteria (end of life criterion) is set before ageing of the material. Once the chemically induced mechanical failure is reached, the data can be correlated to be proportional to the exponential factor of the Arrhenius equation.

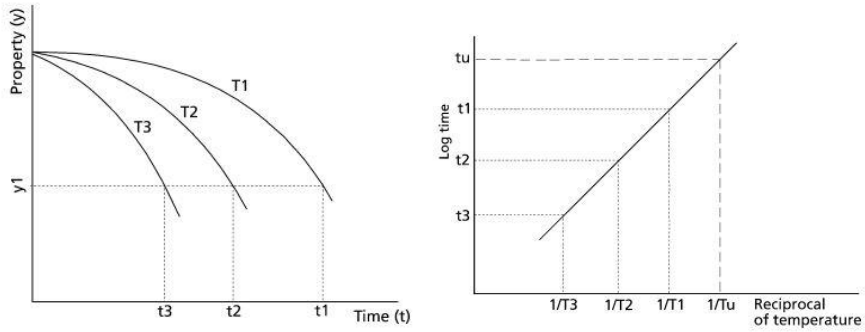

Figure 19: (l) Decreasing evolution of property y of some material recorded at different temperatures (T1<T2<T3) reaching a preset failure criterion y1 after different ageing times (t1>t2>t3) (r) Arrhenius plot constructed from data of the previous graph gets extrapolated to service temperature Tu to yield service time tu (Source: Brown, 2001)

Such correlation assumes that the said mechanical failure was reached independently from temperature; and that E_a is independent of temperature in the region of extrapolation. The former assumption is hard to test as the change in viscoelastic properties may contribute to degradation. The latter is hard to verify beforehand, as it does not allow for e.g. two competing reactions with different E_a-s to drive degradation. A good example for this is polymer oxidation where the oxidation is classically prevented by antioxidants and the mechanical and chemical failure accelerates fast once said antioxidants are fully degraded (Wise et al., 1995; Celina et al., 2005).

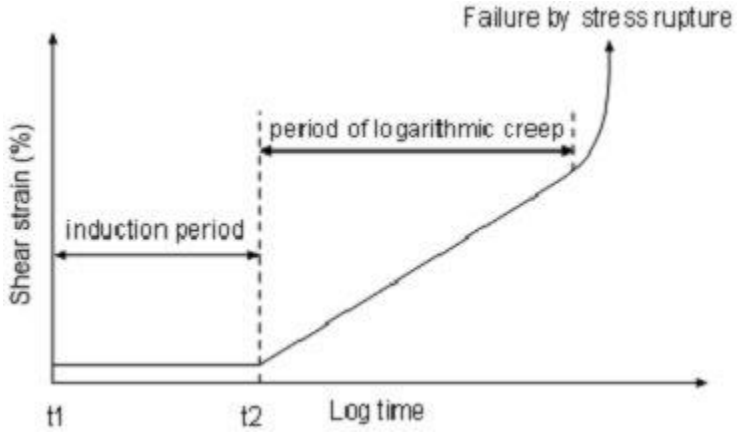

Figure 20: Induction period for the degradation of an adhesive (Source: Adhesives Design Toolkit)

As it was found later, most mechanical degradation was limited in the 90-day period assigned for the experiment. This resulted in many samples not being able to reach an end of life criterion. A new methodology of determining lifetime had to be found.

Following degradation with mechanical and analytical tools

Since the failure criterion method was proven to be less useful, the aim of mechanical testing was reduced to follow several physical properties and their changes over time. These properties and the tests associated with them are often applied to rubbers and are capable of painting a picture of the effect of degradation on the materials. It is worth keeping in mind that degradation may affect one property severely but exert little change to other ones. Consequently, in the case of testing an equipment part, the application of said part has to be taken into account when proposing a design of experiments. E.g. when a seal is tested, compression and hardness tests are more important for determining the useful lifetime of an elastomer as these determine function (Brown, 2001).

Weight change can be useful to follow mass transfer related degradation effects such as swelling or leaching. It is important to mention that degradation is not necessarily followed by weight change and weight change does not imply degradation of any kind (Brown, 2001).

Hardness is a complex mechanical property of a material that can be referred to as the material's resistance to indentation. Hardness can be expressed on several scales using a corresponding durometer. For this experiment, the Shore A scale was chosen as this applies to soft polymers the most. Hardness is easy and to measure, therefore it is frequently used method in the mechanical testing of all plastics. It can also point out some common degradation mechanisms, e.g. crosslinking harden the material, chain scission softens the plastic, deplasticization leads to a harder material too (Brown, 2001).

The tensile test was carried out to measure stress-strain relations of the test piece. Two data will be collected from these curves: the ultimate elongation of the material, i.e. how far can the material be stretched before tearing; and tensile strength, i.e. the materials inherent resistance to stress. These two parameters can change independently during ageing. Crosslinking may result in higher tensile strength due to the increase in entropic resistance against stretching but can lead to lower ultimate elongation since the chains are more restricted in their movement (Brown, 2001).

Compression set measures the ability of an elastomer to recover its original height once the compressive force is removed. It is a frequently used test method for seals and gaskets, as it mimics their application well (Brown, 2001). Unfortunately, in this set of experiments, set has proven to be less reliable due to non-ideal experimental conditions.

Mechanical analysis of the degradation is important to assess in terms of applicability of the material but is incomplete without sophisticated chemical analysis methods. For the sake of getting a picture of the chemical nature of degradation two methods were chosen: thermogravimetric analysis (*TGA*) and Fourier-transform infrared spectroscopy (*FT-IR*). Infrared spectrometer measures the absorbed light of different molecular vibrations. The two beams of light pass through the material with different wavelengths and the interference pattern of these beams are Fourier transformed to get a transmission data. This data can be used to follow dynamic chemical changes (Gabbott, 2010). The spectra of material with different ageing times but with the same ageing conditions can be prepared to see intensified or diminishing peaks as well as new peak formulation. FT-IR is a useful tool to show oxidation or hydrolization of a material's surface.

Thermogravimetric analysis (TGA) consists of the continuous heating and weighing of a polymer sample. It can be used to determine constitution and crystallinity, but in our case, it was the main tool in determining lifetime shortening (Cromton, 2010). In general, TGA can show the material's resistance to thermo-oxidative degradation.

Arrhenius equation of degradation kinetics from TGA data

Ozawa (1965) and Flynn and Wall (1965) describe a way of arriving to activation energies of thermal degradation of materials using thermogravimetric analysis (TGA). This method takes a material, and measures its weight loss over time at different heating rates. The weight loss is then presented with respect to the temperature; such graph is called a thermogram. During the heating process, the material loses weight and the total amount of weight lost is taken as maximum residual loss. The maximum residual loss is correlated to the total amount of degradable components (e.g. bonds) in the material. Therefore, it can be said that:

$$C = \boldsymbol{f}(x) \quad \lim_{T\ (or\ t)\to\infty} C = 100\% \quad C(at\ 120\ °C) = 0\%; \tag{11}$$

where x is the degradable component, C is the residual fraction (or conversion) during degradation. To account for small volatiles that may be present in the material, the degradation was set to start at 120 °C.

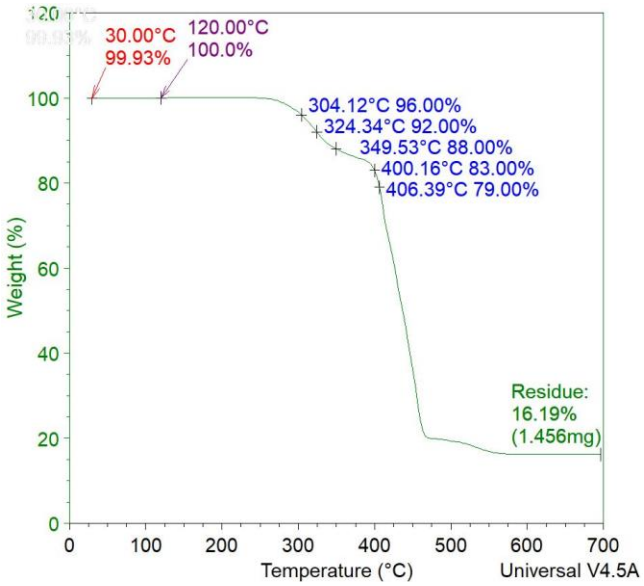

Figure 21: All the data gathered from a single thermogram

The concentration of the degradable component is reduced over time resulting in weight loss. Consequentially, the reactivity of x follows the Arrhenius kinetic equation:

$$-\frac{dx}{dt} = A\exp\left(-\frac{E_a}{RT}\right)\boldsymbol{g}(x); \tag{12}$$

where the g(x) accounts for the order of the reaction. The rest of the equation is same as the Arrhenius equation previously detailed.

Time is then exchanged for temperature as a variable of the above equation. To do this, the heating rate, β is introduced and the integral is formed.

$$-\int_{x_0}^{x}\frac{dx}{g(x)} = A\int_{t_0}^{t}\exp\left(\frac{-E_a}{RT}\right)dt = \frac{A}{\beta}\int_{T_0}^{T}\exp\left(\frac{-E_a}{RT}\right)dT. \tag{13}$$

The above integral cannot be solved numerically, as it would contain the exponential integral. Therefore, it can be written that:

$$\frac{A}{\beta}\int_{T_0}^{T}\exp\left(\frac{-E_a}{RT}\right)dT = \frac{AE_a}{R}\beta^{-1}\boldsymbol{p}\left(\frac{E_a}{RT}\right); \tag{14}$$

where p is a function of the exponential component of the Arrhenius equation containing the exponential integral.

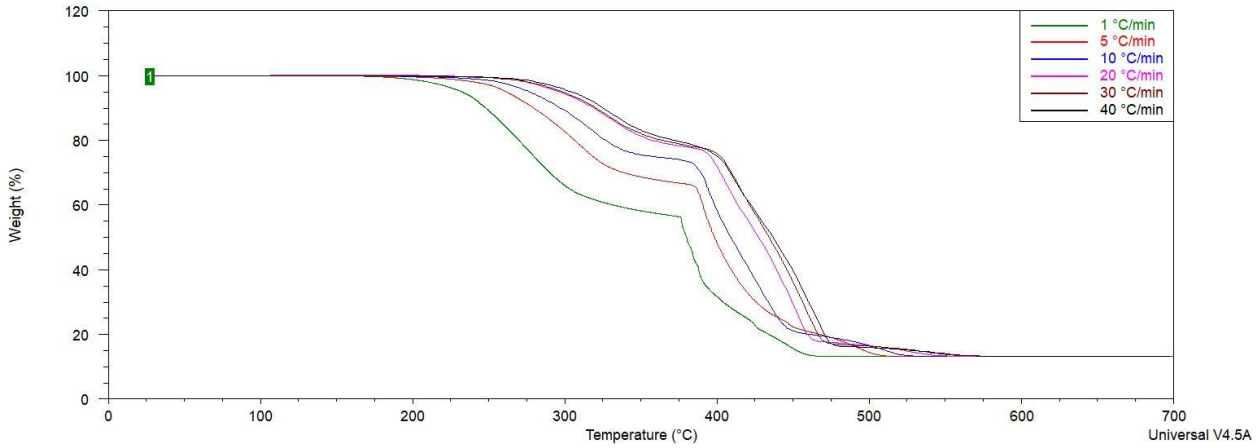

Figure 22: Shifting of the thermograms at higher heating rates

Now conversion is determined but the formula still cannot be solved easily for E_a. Doyle (1962) found that its best to linearize the above function by taking the decadic logarithm of both sides. He found that if $E_a/RT > 20$, then $\log(p(E_a/RT))$ can be closely approximated with an empirical formula, thus arriving to:

$$\log C = \log\left(\frac{AE_a}{R}\right) - \log\beta + \log\left[\boldsymbol{p}\left(\frac{E_a}{RT}\right)\right] = \log\left(\frac{AE_a}{R}\right) - \log\beta - 2.315 - 0.457\frac{E_a}{RT}. \quad (15)$$

Both sides are differentiated with respect to T^{-1}. This simplifies the equation to:

$$\frac{d\log\beta}{d\,T^{-1}} = \left(-0.457\frac{1}{R}\right)E_a = -0.0550\;E_a \; or \; E_a = -18.19\frac{d\log\beta}{d\,T^{-1}}. \quad (16)$$

Essentially, this equation means that on a graph where the reciprocal of the temperature at certain conversion is correlated with the decadic logarithm of the heating rate used to achieve said conversion, the slope of such graph is directly proportional to the activation energy. This activation energy is representative of the material itself, rather than the polymer present in the elastomer. It can be concluded that if the material composition changes, so will the activation energy too.

Once the activation energies were obtained, the kinetic properties of thermo-oxidation of the aged material could be quantitatively compared with that of virgin material. To achieve this, the Arrhenius expression of the kinetic constant of the aged material was divided by that of the virgin material to yield an acceleration factor:

$$\frac{k_{aged}}{k_{virgin}} = \exp\left(\frac{E_{a,virgin}}{RT} - \frac{E_{a,aged}}{RT}\right). \quad (17)$$

Equations 11-17: How to derive the acceleration factor from the Arrhenius equation

Equation 17 above assumes that the pre-exponential factor, A is independent of ageing conditions for the same material. The ratio of the two kinetic constants is expressed as a percentage that shows how much longer or shorter the lifetime of the polymer is after ageing. This method of determining the activation energy, and in turn the acceleration factor, is called the Ozawa method after Takeo Ozawa who developed it along the workings of Doyle (Ozawa, 1965). There are other methods of determining lifetime: the William-Landel-Ferry (*WLF*) method that correlates physical changes according to the time-

temperature superposition principle. The other method also uses the same principals as the WLF, and is called equivalent slope method (*ESM*) (Saboo and Kumar, 2018). These would not work for the same reasons that the original Arrhenius correlation was not working either. Physical changes of the material did not reach a common threshold due to short exposure times from a mechanical degradation point of view.

ACCELERATED AGEING TEST

In this experiment, where the resistance of elastomers is tested towards surface disinfectants, two main accelerative factors were implemented. Firstly, the temperature was increased and the material was aged at 20, 40 and 60 °C. Secondly, several exposure methods were implemented in the scope of this research, most importantly, immersion test. *In situ*, the elastomer parts are wiped with the chemical or dipped into it and left to dry several times over their lifetimes. Immersion assumes continuous exposure, thus a more severe chemically induced degradation is expected. Other methods include dip-and-dry, wet cloth and dry cloth. Dip-and-dry was a cyclical method, where the samples were submerged in the liquids and subsequently lifted out and let to dry. Both wet- and dry cloth procedures utilized a piece of fabric soaked in the disinfectants. The samples were wrapped in said cloth and either let to dry out over the course of one day (dry cloth) or placed in a closed container to maintain their dampness (wet cloth). Fabrics were changed frequently.

What sets immersion apart from the other methods is that immersion does not comprise the contact with air. Results of other methods fall outside of the spectrum of this thesis but will be called upon when relevant information can be extracted from them or when further confirmation of hypothesis is needed.

STATE OF THE ART OF LIFETIME ESTIMATION

Liquid silicone rubber

Kwon, Jun and Song (2015) estimated lifetime of VMQ silicone gaskets by using HALT method. Service time was estimated by setting the 30% compression set failure criteria at 60% for the samples compressed as opposed to the 50% criteria of ISO 11346:2014. Acceleration of ageing was carried out with heating the compression sets at 150-200 °C. Extrapolation was done by three different methods: the Arrhenius equation and two types of a four-parameter method. No significant difference was found In terms of accuracy when the aforementioned methods were compared.

Moghadam et al. (2013) compared three different methods of extrapolating the expected lifetime to low temperatures after thermal ageing of MQ for high voltage applications. Despite of all three methods (Arrhenius, Gillen, Hoang and Lowe) being variants of the Arrhenius equation, the results of them differed. It was concluded that Arrhenius according to ISO 11346:2014 and Gillen give the most accurate estimations for service time.

The Arrhenius equation is often criticized for being inaccurate when multiple reactions are contributing to the degradation of a material. The other main limitation of this process is neglecting physical changes in the material that happen e.g. due to viscoelastic property changes over time.

Mahomed, Hukins and Kukureka (2015) used HALT to follow viscoelastic changes in medical grade silicones by immersing them in physiological saline solution at 70 °C for 38, 76 and 114 days. T_g and T_m (melting point) values, surface and structure properties of the silicone elastomer remained unchanged and the change in viscoelasticity appeared to be not significant.

Yazdan Mehr et al. (2018) were looking into the degradation of optical grade silicones. They found that silicones were unaffected by UV and blue light exposure, immersion into water at 35 °C or 100% RH at 100 °C even after 3000 h of ageing. However, 100 °C saline water contact caused significant changes in the FT-IR spectra due to the reactive Cl^- ions. The change of peaks in the IR spectra was explained by breaking of the Si-O-Si bonds and the decomposition of the hydrocarbon sidechains. This also resulted in a significant change in the light transmission of the samples and lead to embrittlement.

LSR was examined to predict service life of a seal in a future power source for the automotive industry. Cui et al. (2010) used the ISO 11346:2014 compatible Williams-Landel-Ferry (*WLF*) methodology to estimate the lifetime of such seal. This relation as opposed to the Arrhenius equation is only dependent on a reference temperature, i.e. Boltzmann's time-temperature superposition principle applies to this method. This allows for the creation of a so-called master curve, which directly relates change in mechanical properties (in this case stress relaxation) to ageing time. They found that water plays an important role in the stress relaxation of LSR and that the WLF methodology can accurately express lifetime.

Thermoplastic vulcanizate (PP+EPDM)

Mandal et al. (2017) compared the thermal degradation pathways and expected lifetimes of neat PP and acrylic acid grafted PP. They investigated different methods of calculating E_a (activation energy) for this reactions, namely Kissinger, Kim-Park and Flynn-Wall methods. TGA data confirmed that PP degrades in a single step and the degradation products are formed by random chain scission followed by radical transfer reactions. The degradation products vary due to the random reactive radicals being involved. Grafter samples had shorter expected lifetimes than neat PP ones.

The research of Ammala et al. (2002) was investigating UV protective properties of nanoparticulate ZnO light stabilizer additives in high density PE (*HDPE*) and PP plastics. Ageing of the samples were carried out in a QUV accelerated weathering tester. Photolysis of these plastics results in the formation of a radicals which further reacts with the O_2 content of the atmosphere. Therefore, an increased concentration of carbonyl group formation can be examined.

Assink et al. (2002) focused on the thermal degradation of EPDM after the rubber samples have been aged at 140 °C for up to 90 days. The focus of this research was to use ^{1}H-NMR measurements to monitor the degradation of EPDM alongside other mechanical measurements. It was found that in the early stage of degradation, polymeric chains are more prone to scission. On the other hand, after longer ageing, crosslinking becomes the primary degrading effect. The authors claim that of testing ^{1}H-NMR method of testing is a rapid, efficient and reliable tool in determining the degradation of the EPDM rubber.

It can be concluded that most lifetime estimation experiments focus on thermal degradation pathways. Liquid exposure is rarely measured as chemical mechanisms are unclear and can lead to inaccurate Arrhenius plots. Rubbers are inherently complex due to the addition of fillers which further

implies inaccurate lifetime estimation. The author of this thesis is aware of the difficulty of estimating service time but will proceed nonetheless.

HYPOTHESIS

Disinfectants work by damaging cells of germs or by attaching to the cell membrane and inhibiting cell multiplication. The mechanism of protection differs for each disinfectant and thus degradation pathways will differ too. Since four different material contacts were examined in this thesis, four distinct hypotheses can be drawn:

H1. TPV + Isopropyl alcohol 91%

PP+EPDM elastomer will not react with the alcohol. Degradation will be mass diffusion dependent and will result in the absorption of the IPA. Extraction of certain additives is also likely due to the mass transfer mechanisms. However, upon prolonged exposure (especially at elevated temperature) the TPV sample will thermo-oxidize resulting in the formation of radical species from chain scission. The alcohol will also most likely react with the radicals, causing an increase in oxygen containing functional group concentration. Mass transfer degradations can be efficiently followed by weight change and compression set measurements. If thermo-oxidation or alcohol absorption will take place, the IR will show oxygen containing functional groups to confirm such hypothesis.

H2. TPV + DISINF1

Oxygen containing functional group increase can be expected from the other TPV samples due to the oxidative character of the active agent in DISINF1. Paracetic acid is a reactive species around C=O groups (Baeyer-Villiger oxidation) and can also react with double bonds to form epoxy rings. Also, the DISINF1 solution has a slight yellowish hue, which might transfer to the material. Oxidative yellowing is also expected that can be visually confirmed. The oxygen containing functional groups that arise from oxidation will be apparent in the IR spectra of the sample. The change of chemical structure due to oxidation may result in the change of physical properties too. However, the mechanical degradation effects of oxidation can be hard to estimate. If the peroxides cause crosslinking, the material is likely to harden and the change of tensile properties is expected.

H3. LSR + NaOCl 0.5%

Chlorine species are disruptive to silicone rubbers (Yazdan Mehr et al., 2018). The oxidation of sidechains is likely. The degradation will result in changed transparency of samples too. Although not a strong chlorinating agent, hypochlorite is capable of chlorination which can be determined by IR spectroscopy. Due to the degrading effect of the chlorine species present in the NaOCl solution, the tensile strength of the LSR is expected to decrease significantly.

H4. LSR + DISINF2

DISINF2 is a complex disinfectant containing alcohols and a quaternary amine. At elevated temperatures, some oxidation of the hydrocarbon chains may be observed but the majority of the degradation will be mass transfer limited. The significance of this mass transfer depends on whether the silicone has any additives that are capable of migrating into the solution. Also, due to the stability of quaternary amines, negatively charged species will be stabilized and absorbed into the material. Due to the large molecular weight of such amines, a mass increase is likely to arise. Absorbed species can be seen in the IR spectra and the TGA thermogram.

EXPERIMENTAL

SAMPLE PREPARATION

The elastomer samples were provided by Philips and ordered directly from the manufacturer in 2 mm sheets. A leveraged cutter was used to cut out the sample specimens in four different sizes. The tensile bars were ISO 37 compliant and fell under the Type II category. The width of the narrow part was 4 mm, resulting in a cross-sectional area of 8 mm^2. This was later checked and adjusted to fit volume loss in cases where it was apparent. Overall specimen length was 75 mm (ISO 37, 2011).

Compression set was measured at constant 25% strain in accordance with ISO 815-1. For this, 13 mm diameter cylinders were cut out. To reduce deviation between samples, each disk's thickness was measured to 0.01 mm accuracy and the samples were stacked in threes to reach the recommended 6 (±0.02) mm thickness. One compression disk held three samples and the 4.5 mm spacers were used to achieve 25% compression. The screws were tightened by hand and with a hex key. For samples immersed in NaOCl at elevated temperatures, *PEEK* (polyether ether ketone) compression disks were used. This decision was made due to the oxidizing effect of NaOCl that caused rust to appear on the disks and spacers at room temperature. Rust not only degraded the disks, rendering them unusable after the experiments but also affected the measurements. With these disks, extra care was taken to avoid breaking of the screws upon tightening them. Samples immersed in DISINF1 also showed copper oxidation (bluish color change) of the brass spacers but the effect was less severe and due to the limited number of PEEK disks available, the same change was not made (ISO 815-1, 2014).

For the weight and hardness tests, the same 25 mm diameter samples were used. The samples were differentiated by piercing holes in them with a leather hole punch. To measure the hardness, again, 6 mm thick samples were recommended. This was again achieved by stacking the samples for the measurement (ISO 868, 2003).

To follow chemical degradation, an analytical sample piece was also cut out. The analytical piece was an unspecified piece cut out from between tensile bar shapes. This was used to measure TGA, DSC in some cases, and surface IR.

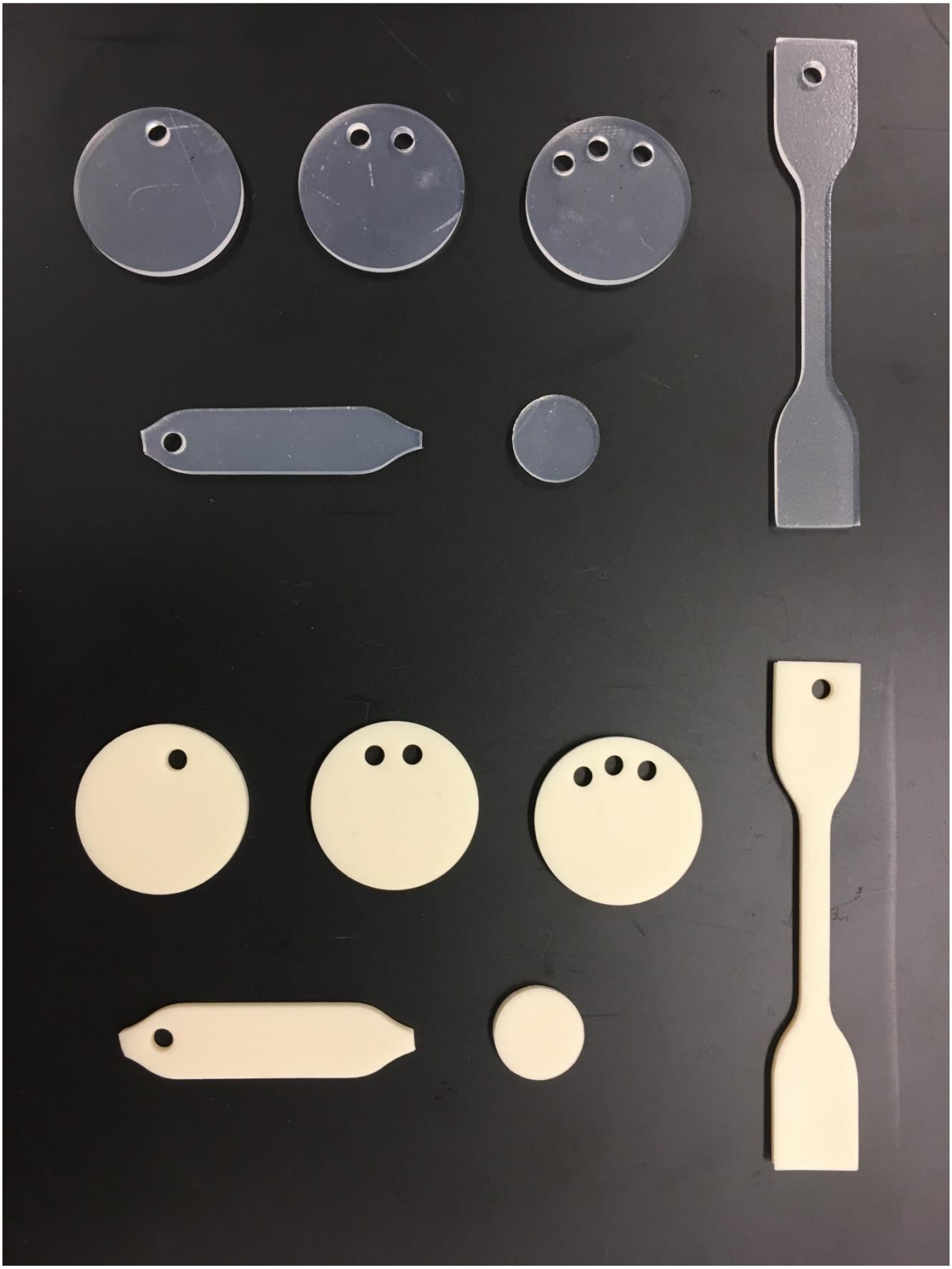

Figure 23: All sample specimens, above for LSR and below for TPV

Sample nomenclature

Due to the scope of the research, many samples were made. These samples were tested at different temperatures, with different contact methods, after different ageing times. To avoid confusion, a precise nomenclature method was developed early on to follow mechanical property evolution. Some contact methods fall outside of the spectrum of this research but were included in the naming process nonetheless. Untreated samples were marked with a "V" that stands for virgin. The diagram below (Table 5) elaborates on this nomenclature.

"TPV_ M_ I_ 40_ 21"

Material_	Contact method_	Liquid_	Temperature_	Ageing time
TPV *LSR*	*M* – immersion *D* – dip-and-dry *OC* – open/dry cloth *CC* – closed/wet cloth	*I* – IPA 91% *N* – NaOCl 0.5% *A* – DISINF1 3% *C* – DISINF2™	*RT* (20 °C) *40* (°C) *60* (°C)	in days *(3, 7, 14, 21, 60, 90)* in case of dip-and-dry: number of dips *(150, 300, 450, 900)*

Table 5: Sample nomenclature

SOLUTION PREPARATION

DISINF2™ was used as is, from the bottle. Pouring of the liquid was done in the fume hood to avoid inhaling the vapors of 2-butoxyethan-1-ol.

30 g DISINF1 was mixed with almost 1 L of distilled water in a 1 L volumetric flask. The solution was pale green and showed foam and gas formation. The flask was placed on a magnetic stirrer with a stirring rod and stirred until all solids disappeared. Then the flask was topped off to the 1 L mark and stirred some more to achieve homogeneity. When poured over the TPV samples the elastomers floated on the surface. Therefore, the jars used for aging were filled quite high to ensure proper immersion. At higher temperatures, the solution turned dark yellow over the course of a few hours. Excess was labeled, closed off and stored in a fridge to prevent the peracetic acid decomposition.

IPA was mixed with distilled water to create a 91 wt% solution. The solution was stored in the flammable cabinet and labeled for flammability hazard.

NaOCl was supplied in a jerry can as an 11% solution. The solution was diluted 20-fold: a 100 mL cylinder was filled and the contents were carefully funneled into a 2 L volumetric flast. The cylinder was washed with distilled water and emptied into the flask to wash out the remaining NaOCl. While stirring the flask, distilled water was added to fill the flask until the 2 L mark. The solution smelled of bleach and had a dirty, pale yellow color. Much like the DISINF1 solution, excess was labeled, closed off and stored in the fridge. To further prevent the UV catalyzed decomposition of the hypochlorite ions, all transparent glassware containing the solution was wrapped in aluminum foil.

Changing the liquids

NaOCl and DISINF1 were more reactive than the alcohol based solutions, in turn these needed to be changed less frequently. In the beginning of the experiment, DISINF2™ and IPA were changed twice a week. This was later reduced to a biweekly change due to the shortage of supplies. The change was considered necessary and was estimated to be non-significant in terms of degradation.

Shortage of supplies was also a factor for NaOCl and DISINF1 solutions. While they were changed daily in the start of the experiment, the changes were rescheduled to be three times and twice a week for NaOCl and DISINF1, respectively. This reduced consumption and thus the stock lasted for the duration of the experiment. Important to mention, that an estimation has been made to calculate assumed raw material consumption. This step is crucial for any ageing experiment, as these last a long time and can be quite pricey for the executing company. When discarding old liquids, care was taken to accurately dispose of them.

SAMPLE SETS AND START OF EXPERIMENT

As suggested under “Sample nomenclature”, the test specimens were grouped together under one service condition that depended on material, contact method, the liquid that the material was exposed to, the ageing temperature and the ageing time. The name denoted what will be referred to as a sample set. A sample set consisted of nine 2 mm thick cylinders of 13 mm diameter; three, distinguishable 2 mm thick cylinders of 25 mm diameter; four ISO 37 type II tensile bars and a random analytical piece. All but the compression samples were pierced with a hole punch. The hole was used to thread the pieces together, thus the sample sets became easily distinguishable and accessible in a crowded container. This trick was important in the case of e.g. weight samples but also helped the collection of other samples. A fishing string made from nylon 6,6 was used to connect the samples. A high pressure resistant, hard polyurethane (*PU*) tube was cut up into ~5 mm rings and placed between each sample. This was done to prevent sticking of the specimens to each other and hence generate and even degradation across all samples. Only problem of this approach was that the nylon and PU spacers degraded in NaOCl causing a flakey solution. The DISINF2™ turned the spacers brittle. The latter was not replaced as only some spacers were broken off the chain well after 2 months of exposure. The NaOCl sample sets were re-threaded after each month due to the thinning of the nylon thread which made sample collection complicated.

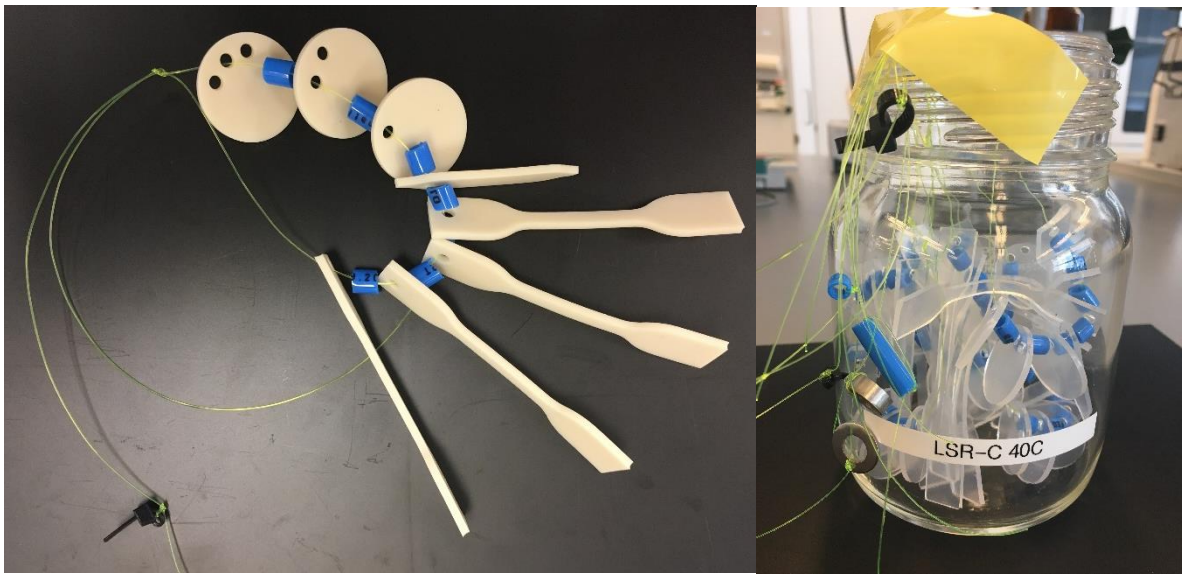

Figure 24: (l) A sample set of TPV on nylon 6,6 thread with the PU spacers and a distinguishing zip tie (r) Distinguishing the sample sets in the case of LSR_M_C_40

At the end of each sample set, a distinguishing piece was connected (e.g. washer, compression spacer, aforementioned PU tube piece). When the samples were placed in the jar, these were hanging out from it, making sample collection easier to follow. The thread made it easier to allow for an even distribution of samples inside the jar. Threading was only done for elevated temperature aging; at ambient temperatures the sample pieces were all directly immersed in the liquid in a PE bottle. Therefore, a side etching method was developed to distinguish between ambient temperature aged samples (see Figure 25). The side of the disks was marked with a handheld electric saw. The PE bottles could not be used inside the ovens due to the pressure buildup.

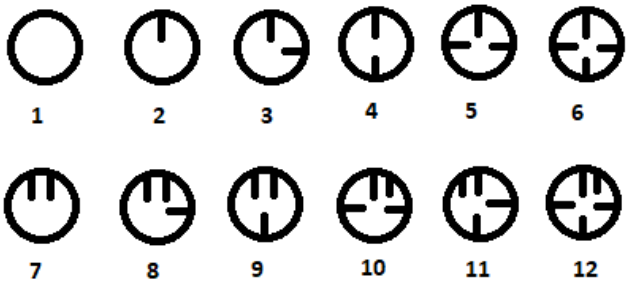

Figure 25: Side-etching technique used on room temperature aged weight samples

The jars were placed in the oven at 40 and 60 °C. The oven was set to have the fan on with high ventilation to assure even temperature distribution inside. The temperature inside the oven was checked periodically to match the temperature displayed on the screen with an electric thermometer. The PE bottles containing the room temperature aged samples were left on the laboratory working surface.

Figure 26: (l) At ambient temperature the samples were placed on a desk in a closed PE container (m) Each oven contained four closed jars of each sample (r) The ovens were marked with my name and closed with a preset temperature

Compression disks, once closed, were treated similarly to the regular sample sets. Room temperature aged samples were immersed in a PE bottle and elevated temperature samples were closed in a glass jar. As mentioned previously, due to the limited number of compression disks available, two compression disks of each liquid contact was measured simultaneously.

Figure 27: Compression set triplets for elevated temperature ageing grouped to match the 6±0.02 mm height criteria

COLLECTING THE SAMPLES

Once the samples needed to be collected, the thread connecting the sample sets was lifted out of the solution and cut. Weight samples were patted dry and weighed. Subsequently, their hardness was measured. Tensile bars and the analytical sample were washed under running cold water, dried and wrapped in aluminum foil to circumvent further degradation. Compression disks were opened and a recovery time of 30 minutes was waited out. After that time had passed, the samples were measured for their height.

MECHANICAL ANALYSIS OF MATERIAL DEGRADATION

All analytical data was processed with respect to the sample set in Excel and partially in MiniTab 18. Standard deviation was calculated where multiple data points were turned into mean values. Said values with their corresponding standard deviations were presented on a graph with respect to the ageing time. If applicable, untreated material's properties were shown too which allowed for a quick visual comparison upon primary inspection of data.

Weight change

Prior to submersion, the samples were measured using the Mettler Toledo XPE205 scale and their weight was recorded with 0.01 mg accuracy. As mentioned before, the three weight specimens were distinguishable from each other according to the number of holes pierced into them. After the ageing process, the samples were gently patted dry and weighed again. The percentage weight change was determined using Equation 18.

$$\%\, weight\ change \ \equiv\ 100\% * \frac{m_{aged} - m_{initial}}{m_{initial}}, \tag{18}$$

where m_x denotes the mass of the specimen before or after ageing.

Equation 18: Percentage weight change over the ageing period

Hardness

After the samples were weighed, they were transported and their hardness was measured with a Zwick/Roell Shore A durometer. After lowering the durometer on the samples, the hardness value was read and recorded following a 15-second relaxation time.

Tensile strength

In this measurement, the specimen is fixed between two self-enforcing clamps in a Zwick/Roell Z030 tensile testing machine. Using these clamps was essential due to the thinning of the test subject at high stress. To prevent slipping (which happened for most NaOCl aged LSR samples), an additional spring clamp was used if necessary. During the tensile test, two parameters of the rubbers were recorded: ultimate elongation and tensile strength. Untreated samples were measured too and compared with data from manufacturer.

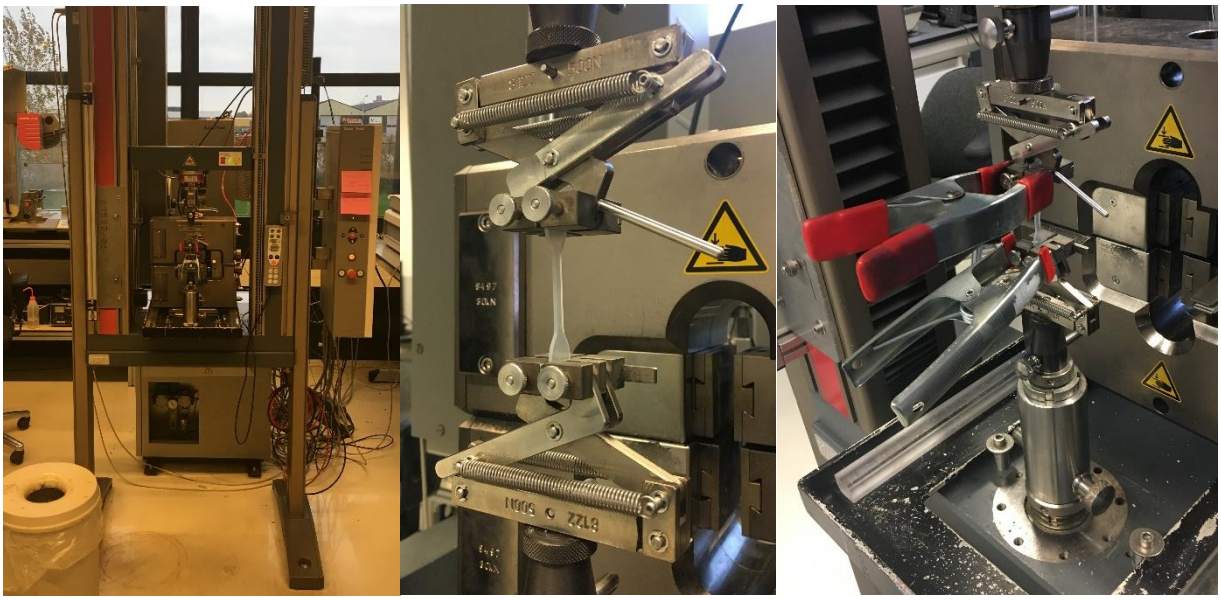

Figure 28: The tensile machine (l) The Zwick/Roell tensile machine (m) Self-enforcing clamps (r) Fixation of NaOCl aged LSR tensile speciment with spring clamps

The tensile machine operated with a 500 mm/min pull speed after the pre-load of 0.1 MPa was reached. The initial clamp distance was 45 mm and the rest of the setting were all complient with ISO 37 (ISO 37, 2011).

Compression set

The unique specimens were stacked and closed in a compression disk at 25% compression. The height of the immersed specimens was measured using a Heidenhain ND280 position display unit after 3, 7, 14 and 21 days. To allow for comparison, untreated samples were also compressed under ambient conditions and their set was measured after equivalent time intervals.

$$\%\, recovery\ loss\ \equiv 100\% * \frac{h_{aged} - h_{initial}}{h_{initial}}, \tag{19}$$

where h_x denotes the height of the compression set before and after ageing.

Equation 19: Percentage recovery loss over the ageing period

Due to the lack of 6 mm thick compression specimens, the accuracy of this method is questionable. The stacking of the samples gives for a lot of inherent error thus compression recovery data was considered with caution.

CHEMICAL ANALYSIS OF MATERIAL DEGRADATION

The collection of mechanical data only explains physical changes of the material. Thus, analysis of the plastics is incomplete without assessing chemical changes. These two methods were selected to be complementary to each other. Fourier-transform infrared spectroscopy (FT-IR) showed surface degradation. This is important knowing that the degradation in the bulk of the material was limited by mass transfer. Thermogravimetric analysis (TGA) has proved to be an interesting tool not only to see how the thermo-oxidative behavior of the elastomer changed. Ultimately, this analytical method became a way to measure lifetime.

Fourier-transform infrared spectroscopy (FT-IR)

Figure 29: The Thermo Scientific Nicolet iZ10 IR module (Source: Thermo Fisher)

The sample was carefully placed over the "split-pea" crystal of Thermo Scientific Nicolet iZ10 IR spectrometer. The surface of the analytical sample was measured and checked for characteristic peaks between 650-4000 cm^{-1}. The machine was set to have an accuracy of 4 cm^{-1} and the run was repeated 16-fold. When the spectra is presented, the red line always correlates to the most recent (longest ageing time) one. The asymmetric stretching of the CO_2 molecule at around 2400 cm^{-1} wavenumber is ignored from spectra analysis as it is an present in air and creates noise for sample measurements.

Thermogravimetric analysis (TGA)

Figure 30: TA Instruments TGA Q5000 (Source: TA Instruments)

All thermogravimetric data was collected using a TA Instruments TGA Q5000. Only TPV samples were measured with a TGA. A small piece of the random analytical sample was cut off and the sides were removed to expose as much of the bulk material as possible. The piece was about 8-12 mg and cut into 6-8 smaller bits. These were placed onto the pre-weighed, cleaned, cleaved pan. The sample was matched with a protocol, named accordingly. Protocols of 5 and 10 °C/min ran until 500 °C, the fastest (40 °C/min) ran until 700 °C to guarantee an accurate residue percentage. All samples were chosen to run under compressed air flow, as it was most representative of the real life media that the elastomer has to endure during its lifetime. Once the sample finished the procedure, the pan was removed, cleaned and the process was repeated until all measurements were completed.

RESULTS

Collecting all the data of all four samples was a lengthy process that required organized safekeeping of data. One data set usually consisted of multiple measurements, therefore the average of the data was represented in Excel. The graphs of averages were shown in the same graph as a function of ageing time. Different heat aged samples were put on the same graph to assess the effect of temperature on degradation of mechanical and chemical properties. The standard deviation of the data was introduced in the form of error bars, and in some cases, even the data set is shown in a table below the graph.

FTIR data is shown on for each temperature that the sample was aged at. This shows the evolution of the sample's chemical structure. If interesting conclusion could be drawn from it, the thermograms were also represented. Occasionally, thermograms are coupled with their respective derivatives according to temperature. The visual observations are shown on a photograph of the weight samples that shows the virgin material too. Unfortunately, the images are affected by the flash and bad lighting but the most important changes are still observable. The first 4 weight samples (20 °C aged for 3/7/14/21 days) are missing due to them also being part of another experiment.

TPV AGED IN IPA 91%

Visual observations

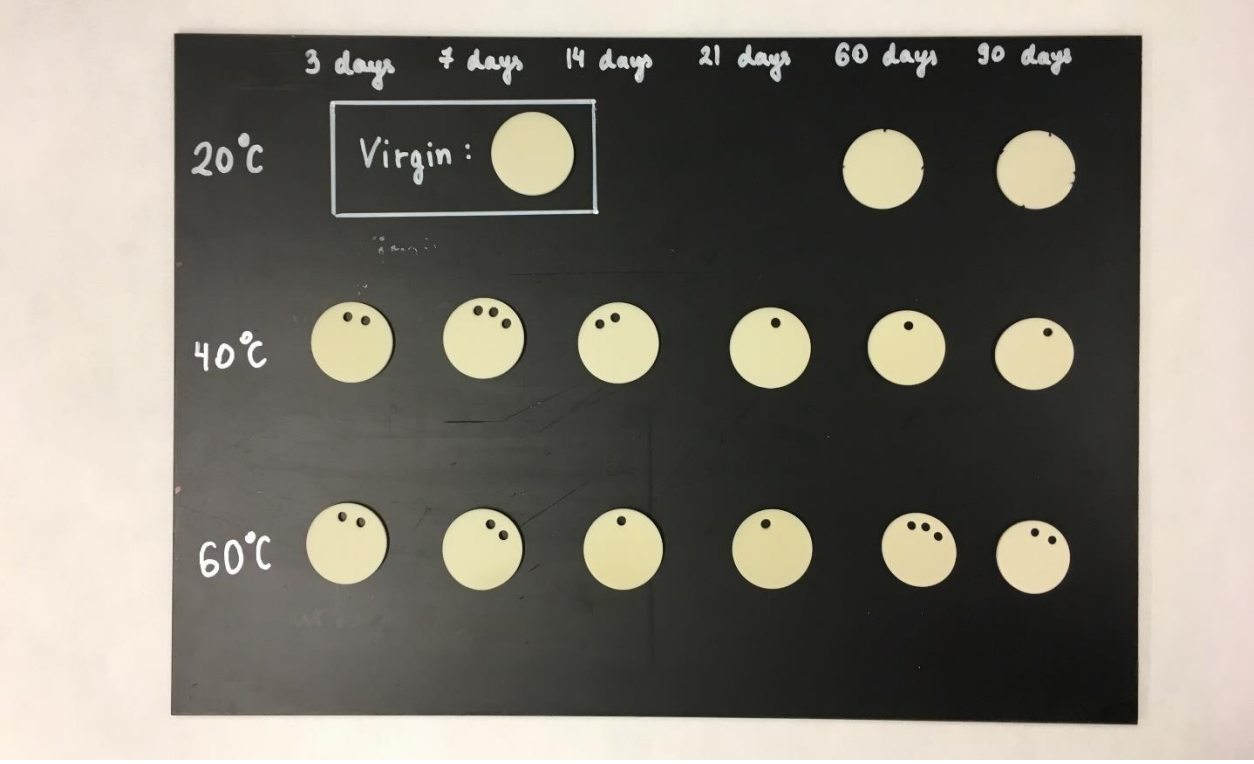

Figure 31: Visual observation of IPA 91% aged TPV

Upon closer inspection of IPA aged TPV, the volume loss of samples is trivial. The longer the exposure and the higher the temperature, the smaller the samples were. This can be easily seen when TPV_M_I_60_90 is compared with the Virgin sample. Discoloration of the samples was minimal, a slight brightening of the material can be observed. The volume loss is not uniform throughout the material that can be the result of the holes as they create a larger surface are for the mass transfer processes playing a role in this particular ageing method. The samples felt harder and less elastic. Due to the mass loss being so apparent, the leaching of the materials is very likely, and this assumption is further supported by other measurements.

Weight change

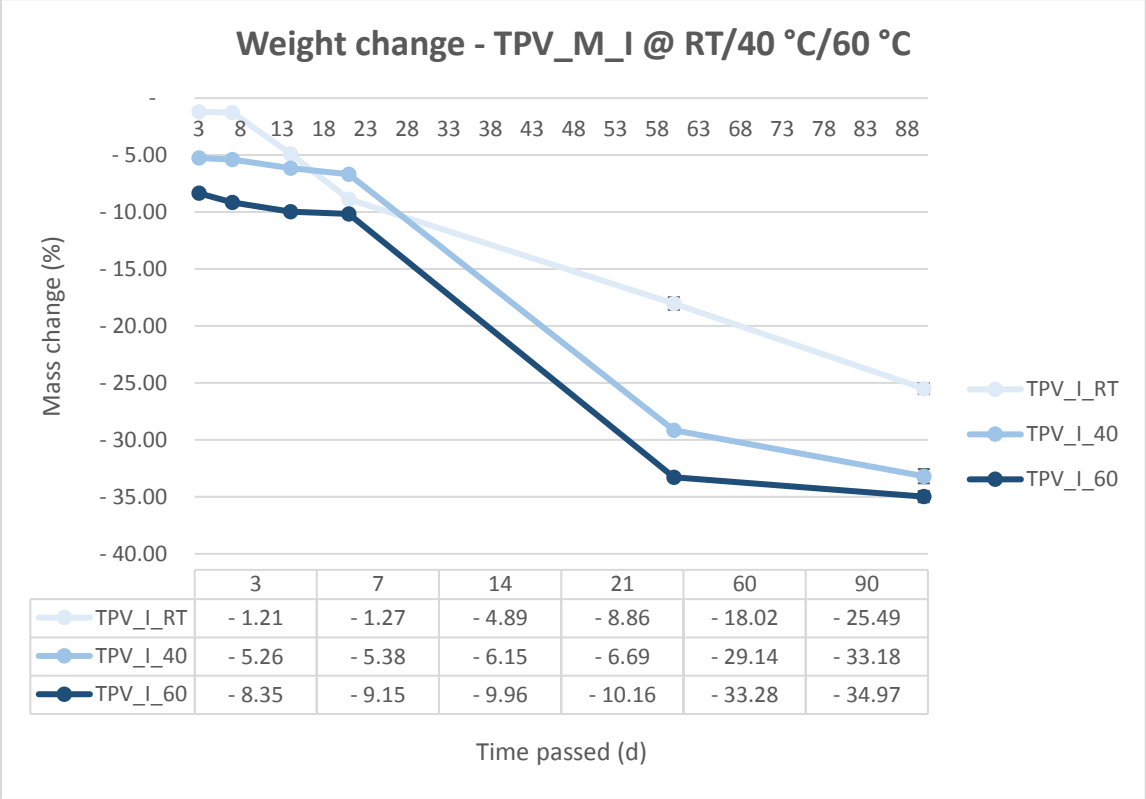

	3	7	14	21	60	90
TPV_I_RT	- 1.21	- 1.27	- 4.89	- 8.86	- 18.02	- 25.49
TPV_I_40	- 5.26	- 5.38	- 6.15	- 6.69	- 29.14	- 33.18
TPV_I_60	- 8.35	- 9.15	- 9.96	- 10.16	- 33.28	- 34.97

Figure 32: Weight change of IPA 91% aged TPV

The weight loss is also supporting the volume loss suspicion: the material is losing some of its constituents. This is accelerated by temperature. These claim are confirmed when the data concerning liquid contacts published by COMPOUNDER2 (COMPOUNDER2, 2017) is also considered. This compatibility chart does not include specific measurements for the TPV. Similar TPVs also show weight loss after 7 days of room temperature exposure with IPA. The harder 201-73 loses 13% and the softer 201-55 does 19%. Although our measurements are less drastic after 7 days (-8.4% for the most severe case), there seems to be a correlation between initial hardness and susceptibility to weight loss among TPV materials. The harder the material, the less weight it loses upon exposure to IPA. Softer grades of TPV also contain more oil (US 4,130,535, 1978) and this is expected to be the main leaching component of the material.

Hardness change

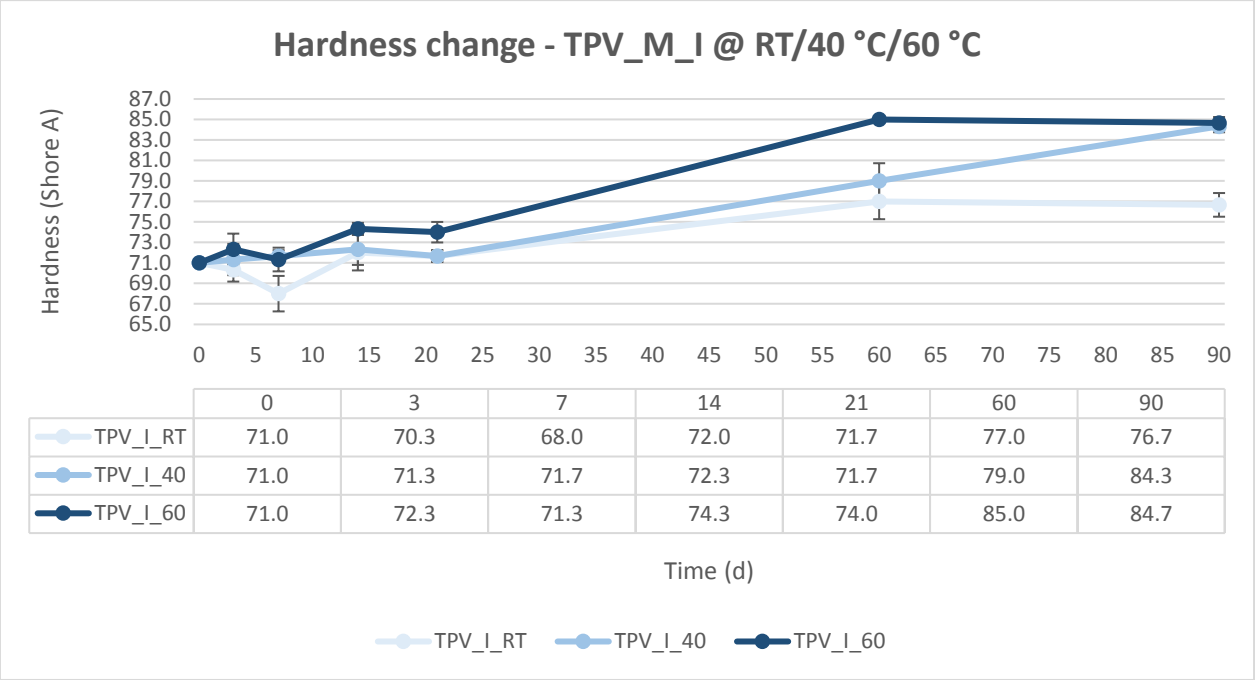

	0	3	7	14	21	60	90
TPV_I_RT	71.0	70.3	68.0	72.0	71.7	77.0	76.7
TPV_I_40	71.0	71.3	71.7	72.3	71.7	79.0	84.3
TPV_I_60	71.0	72.3	71.3	74.3	74.0	85.0	84.7

Figure 33: Hardness change of IPA 91% aged TPV

Knowing that the material is leaching, a change in hardness is no surprise. The material is hardening at a similar rate regarding the ageing temperature. This makes the suspicion for the leaching of plasticizers oils that much more likely. Due to the leaching effect of these oils, the material goes through a deplasticization step which results in the hardening of the material. Similarly to weight and visual changes, the hardness also seems to show a minimal 21 day induction period for this degradation. After 21 days, the material starts to lose its mechanical characteristics a lot faster. The induction period is between 7 and 14 days for 60 °C aged samples. These samples reach a plateau at 60 days with a maximal hardness of 84.7 Shore A. The induction period can be assigned to the mass transfer reaching the bulk of the material and thus, allowing the leaching to happen throughout the material. Once the equilibrium is reached, the material's hardness change comes to a halt.

Compression set

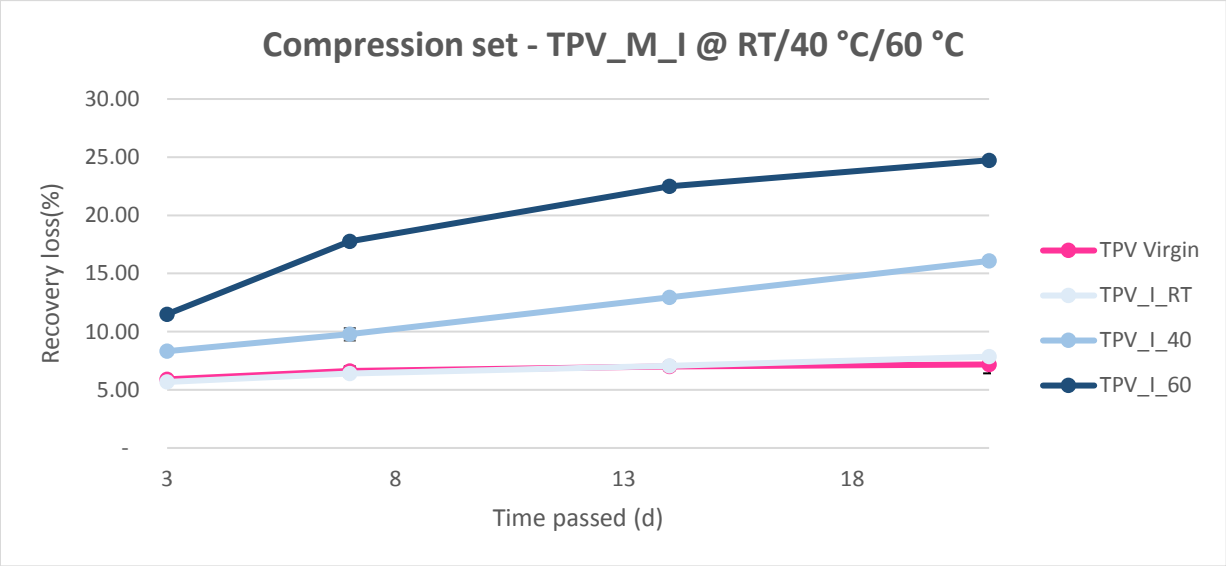

Figure 34: Compression set change of IPA 91% aged TPV

As mentioned previously, compression data is rather unreliable. In this case however, it further confirms the previous findings. Deplasticization of the material and the volume loss are all negatively affecting set. Conclusively, it is no surprise that the recovery loss is increasing in the observation period until it reaches the possible maximum for TPV_I_60 at 25%. One interesting observation though, is that the virgin set does not seem to be deviating a lot from the room-temperature aged TPV's. However, it is speculated that upon longer exposure, i.e. past the 21 day induction period, the deviation from the virgin material would be more apparent.

Tensile strength, ultimate elongation

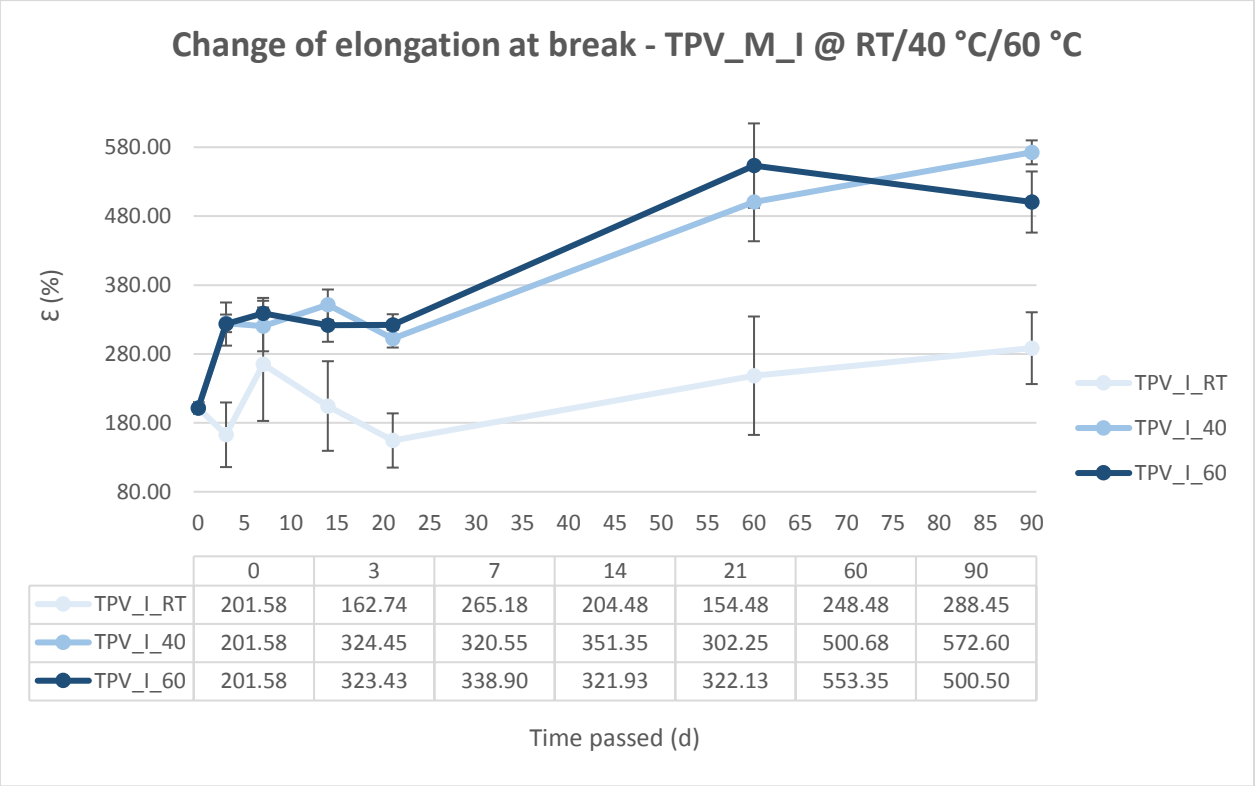

	0	3	7	14	21	60	90
TPV_I_RT	201.58	162.74	265.18	204.48	154.48	248.48	288.45
TPV_I_40	201.58	324.45	320.55	351.35	302.25	500.68	572.60
TPV_I_60	201.58	323.43	338.90	321.93	322.13	553.35	500.50

Figure 35: Ultimate elongation change of IPA 91% aged TPV

Due to how the tensile bars were tested in comparison with weight and hardness, data regarding elongation and strength should be considered carefully. The tensile bars were washed and wrapped in aluminum foil until they were stretched as opposed to other measurements that were carried out immediately after the removal from the liquid. This probably contributed to degradation effects but their severity is estimated to be almost negligible. That is because mass transfer equilibrium is reached rapidly with a small continuous phase, i.e. the remaining IPA on the surface. The material hardening is further confirmed to be a result of deplasticization. The leaching of the oils did not make the material brittle, quite the opposite, the plastic became stronger and could be stretched longer than the unaged material. It seems that the elevated temperature accelerated the arrival to the mass transfer equilibrium but the rate of this acceleration does not differ significantly for 40 °C and 60 °C aged specimens. This aligns with the product datasheets found on harder grades of TPV. These grades contain less oil and have higher elongation at break and tensile strength values. TPV_I_60_90 loosely correlates to the same grade of TPV but Shore A hardness 93 (COMPOUNDER2, 2014). The tensile bars showed tensile whitening, as shown on Figure 36.

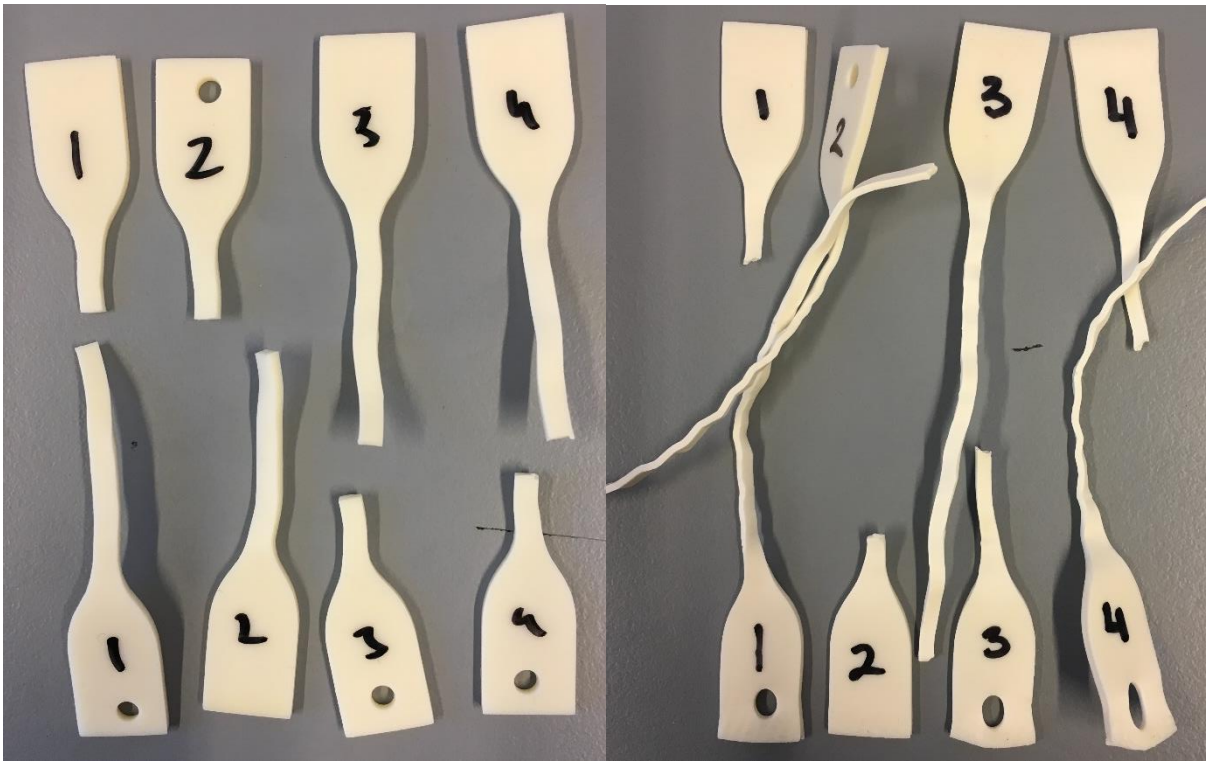

Figure 36: Change in tensile behavior (l) TPV_I_60_3 shows small amount of permanent elongation (r) TPV_I_60_90 shows tensile whitening and crystallization due to deplasticization

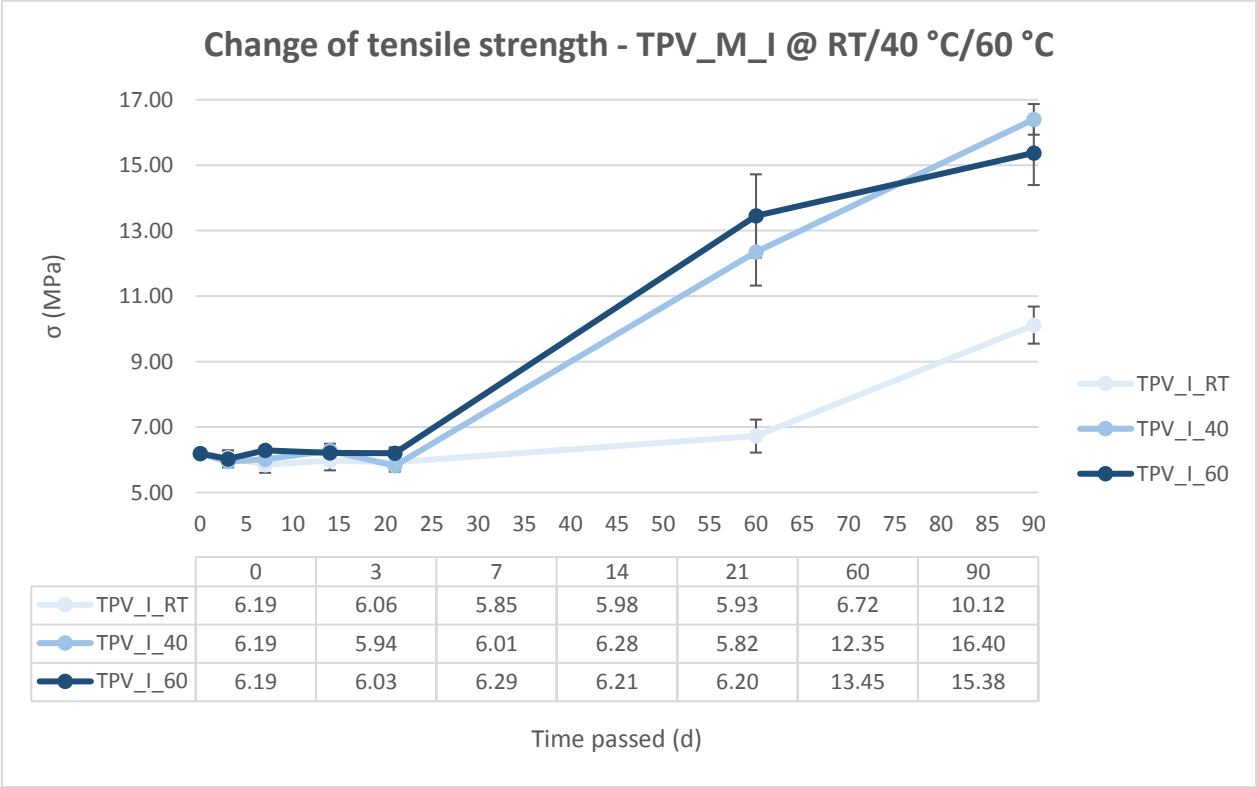

	0	3	7	14	21	60	90
TPV_I_RT	6.19	6.06	5.85	5.98	5.93	6.72	10.12
TPV_I_40	6.19	5.94	6.01	6.28	5.82	12.35	16.40
TPV_I_60	6.19	6.03	6.29	6.21	6.20	13.45	15.38

Figure 37: Tensile strength change of IPA 91% aged TPV

Infrared spectra

TPV_I_RT	TPV_I_40	TPV_I_60	Deformation
cm^{-1}	cm^{-1}	cm^{-1}	
3400			O-H stretch
2955	2955	2957	C-H stretch, various changes but weaker peak
2925	2925	2927	C-H stretch, various changes but stronger peak
2855	2855	2852	C-H stretch, various changes but stronger peak
1654		1647	Unidentifiable peak
1460	1465	1463	C-H bend
1381	1380	1377	C-H bend in CH_3
1097	1094	1094	O=C-O-C stretch
800-	800-	800-	C-H bend of CH_2

Table 6: Peaks of FT-IR in TPV_I

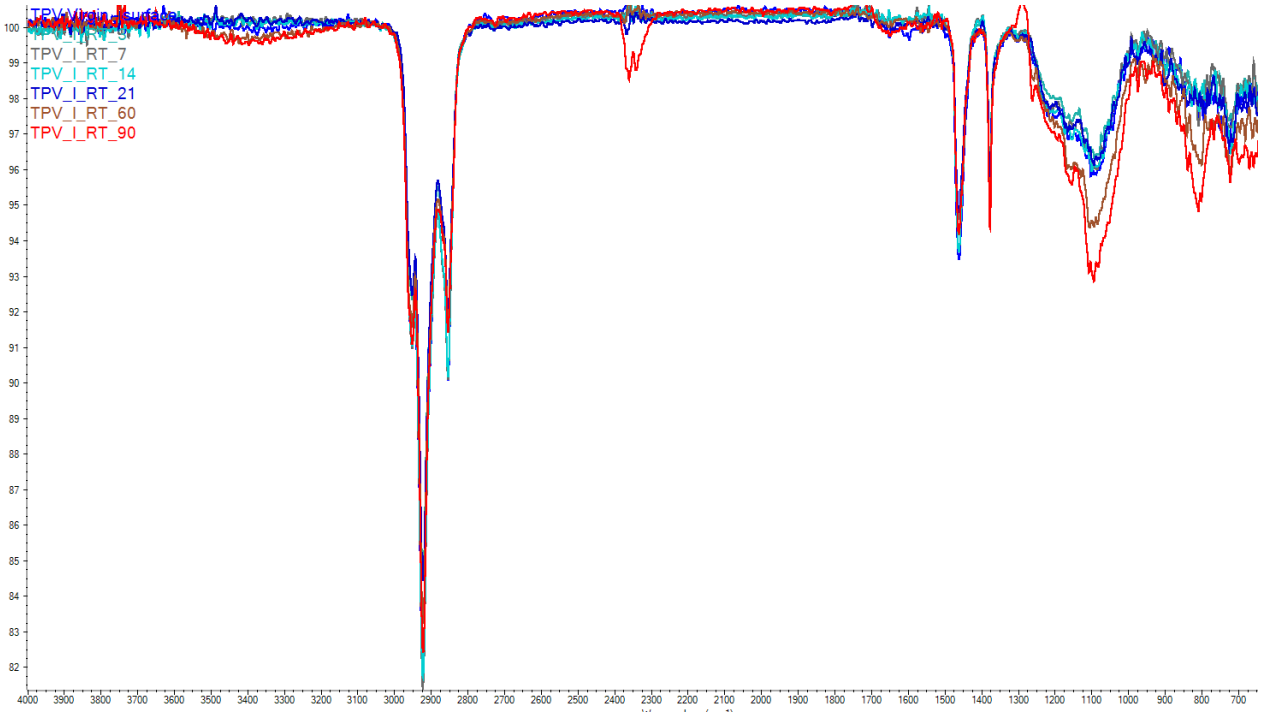

Figure 38: Fourier-transform infrared spectra of TPV aged in IPA 91% at 20 °C

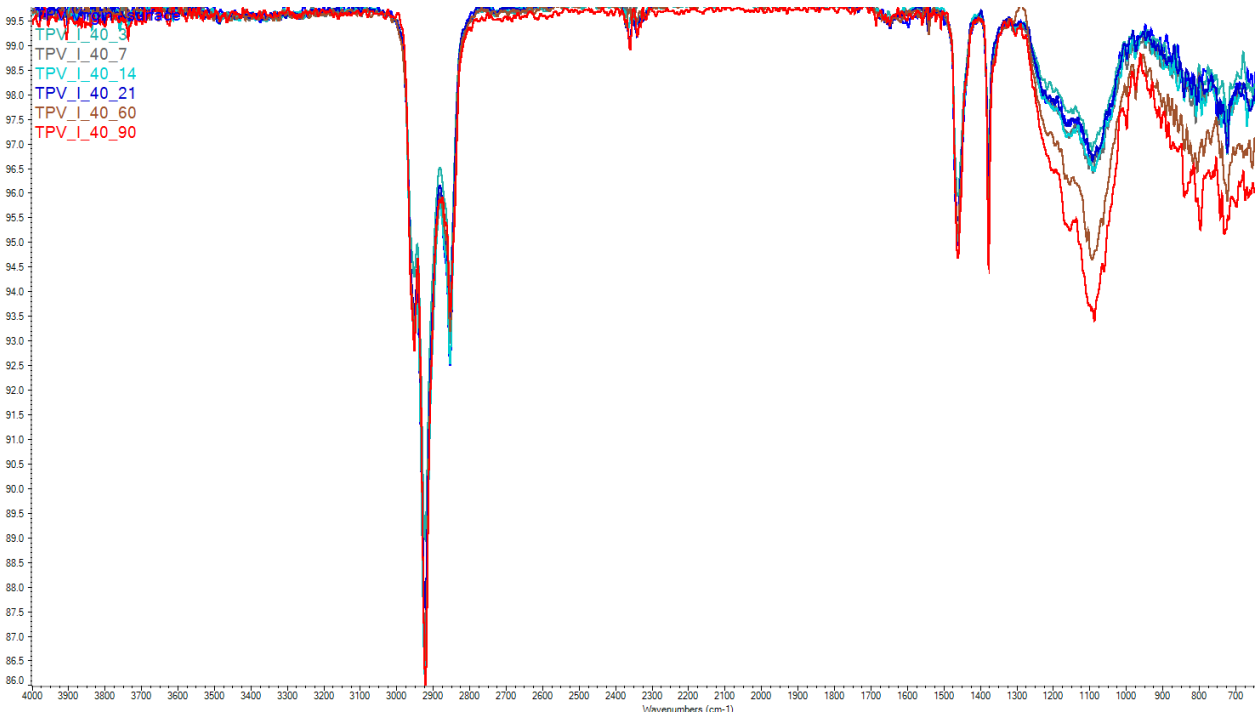

Figure 39: Fourier-transform infrared spectra of TPV aged in IPA 91% at 40 °C

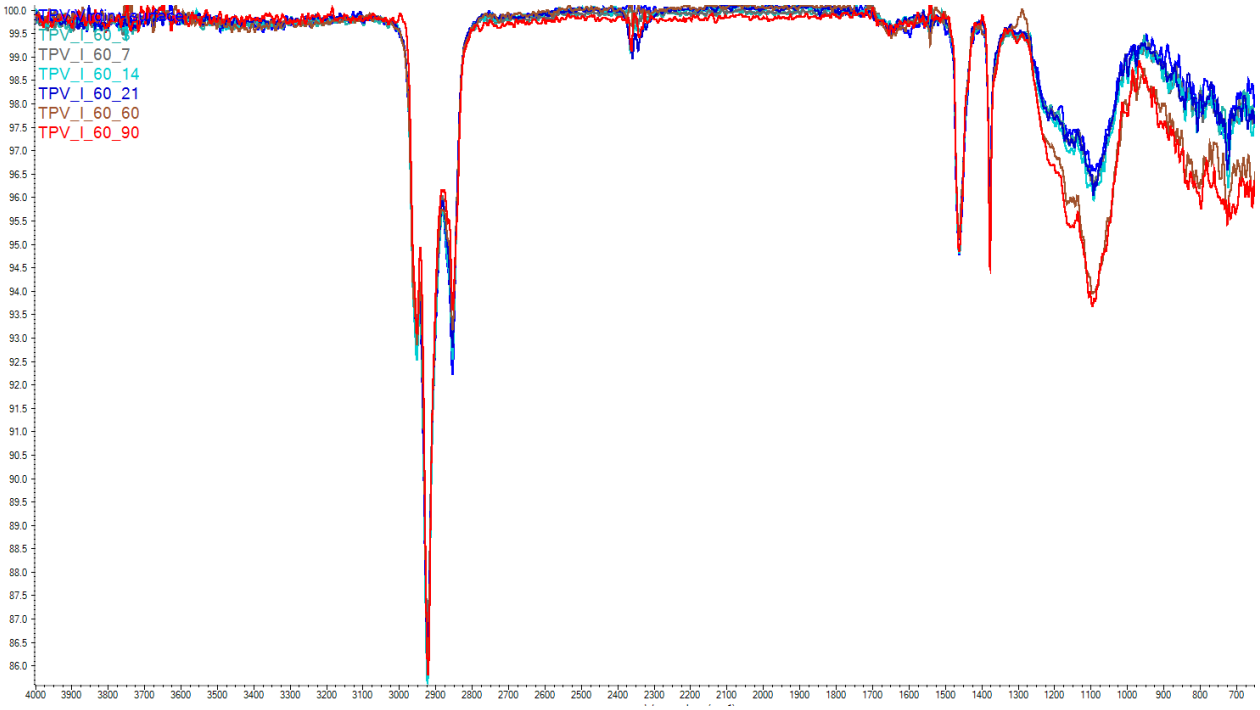

Figure 40: Fourier-transform infrared spectra of TPV aged in IPA 91% at 60 °C

The IR spectra of the material is less informative in the case of a mass transfer related degradation, as it mainly translates to peak intensity changes rather than new peak formation. The room temperature aged TPV shows slightly increased absorption in the 3400 cm^{-1} region where the O-H stretch is present. This is probably some residual, superficial IPA that does not show up on the other aged material's spectra.

Therefore, reaction with the material can be excluded. The saturated C-H stretching at 2900 cm^{-1} shows a characteristic triplet of CH_3, CH_2 and CH groups found in PE, PP and the filler oils (Krimm, 1956). The change of these peaks is apparent as their intensity decreases over time. Since the TPV matrix is unaffected, we can conclude that this is a sign of oil leaching. The oils are often triglycerides, much like in the case of castor oil (Lisa.chem, 2015), and are in turn aliphatic esters that show a broad peak for stretching of the O=C-O-C structure at 1100 cm^{-1}. The reason why we see an increase in the intensity of this stretching is because the remaining oils migrate to the surface. It can assumed that the ester bond is being hydrolyzed at higher temperatures in contact with alcohols. The reason we do not see any strong peaks associated with carboxylic acids is that the so formed acids leached into the ageing solution. Other peaks are observable at 1500 cm^{-1} for C-H bends of mainly the PP/EPDM matrix; at 1380 cm^{-1} for the CH_3 C-H bend in PP and at 700-800 cm^{-1} for the CH_2 C-H bend from the polymer backbone (Roeges, 1994).

Thermogravimetric residue analysis

The residue after the full thermolysis of the TPV shows how the proportion of inert and residual molecules to combustible components changed over the course of ageing. The samples were heated with the fastest heating rate, 40 °C/min until 700 °C. At this point two assumptions were made. On one hand, that the residue is independent of the heating rate and that at 700 °C all that is volatile or prone to pyrolysis has evaporated or reacted away. This would mean that the mass of this residual fraction is constant throughout ageing but their corresponding mass fraction is not. A graph was constructed to show how the residual fraction changed as a function of ageing conditions, time and temperature.

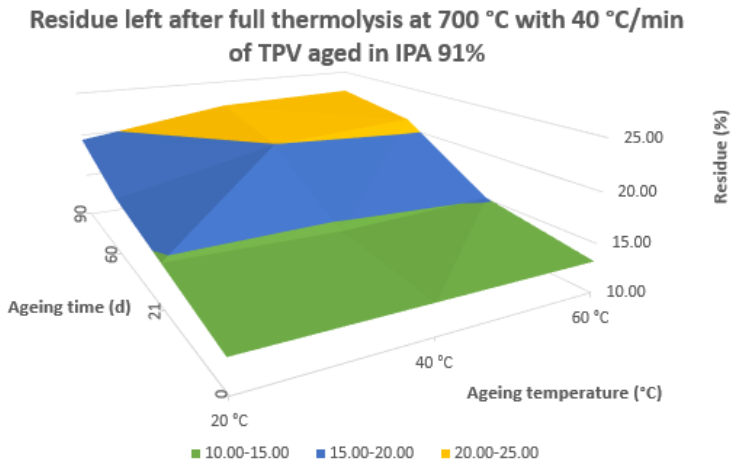

Figure 41: Residual fraction change in aged TPV_I

The residue remaining after the TGA was measured increased as a function of time and temperature. This shows that the material in fact lost weight, and this loss was supplied by plasticizer components only. This is further confirmed when the thermograms of the elastomer, and the temperature derivatives of those is inspected. Below, the thermogram for the unaged material and the material after the maximum ageing time at the three different temperatures is compared. The derivative of the thermogram is with respect to time, but since all above thermograms were generated with a heating rate of 5 °C/min, the time is analogous to temperature. This was done because the program (TA Universal Analysis) has trouble integrating the peaks with respect to temperature.

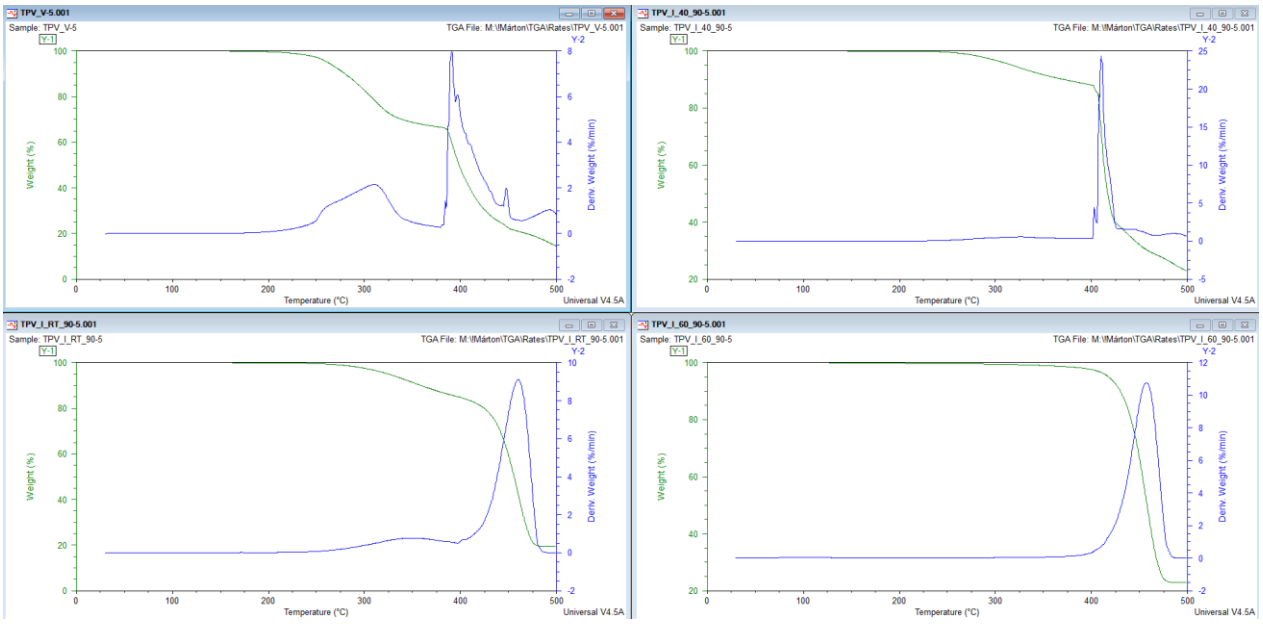

Figure 42: Thermograms with their respective time derivative (l-top) Virgin TPV (l-bottom) TPV_I_60_90 (r-top) TPV_I_RT_90 (r-bottom) TPV_I_40_90

One striking observation is that in the virgin material, the weight loss is a two-step process. First, plasticizer oils leave the material. Then the PP/EPDM matrix starts to degrade around 400 °C (Crompton, 2010). The intensity of the first step is decreasing over time until it is virtually diminished in TPV_I_60_90. As a consequence of this, the degradation of the second step contributes to more weight loss over the weight of the sample. This can be interpreted as a conformation for leaching of components more volatile than PP or EPDM which, in the case of TPV, is oil. This leads to the weight loss fractions inspected are being pushed to higher temperatures, in turn granting the material a higher thermo-oxidative resistance.

	TPV_I
Visual	Shrinking, whitening
Weight	Decreasing
Hardness	Increasing
Elongation	Increasing
Tensile strength	Increasing
Compression set	Increasing
Thermogram	Decrease in oil fraction, more residue fraction
Infrared	Small increase in O-H, decrease in C-H intensity, increase in CH_2 intensity

Table 7: Assessing all the changes of TPV_I

TPV AGED IN DISINF1

Visual observations

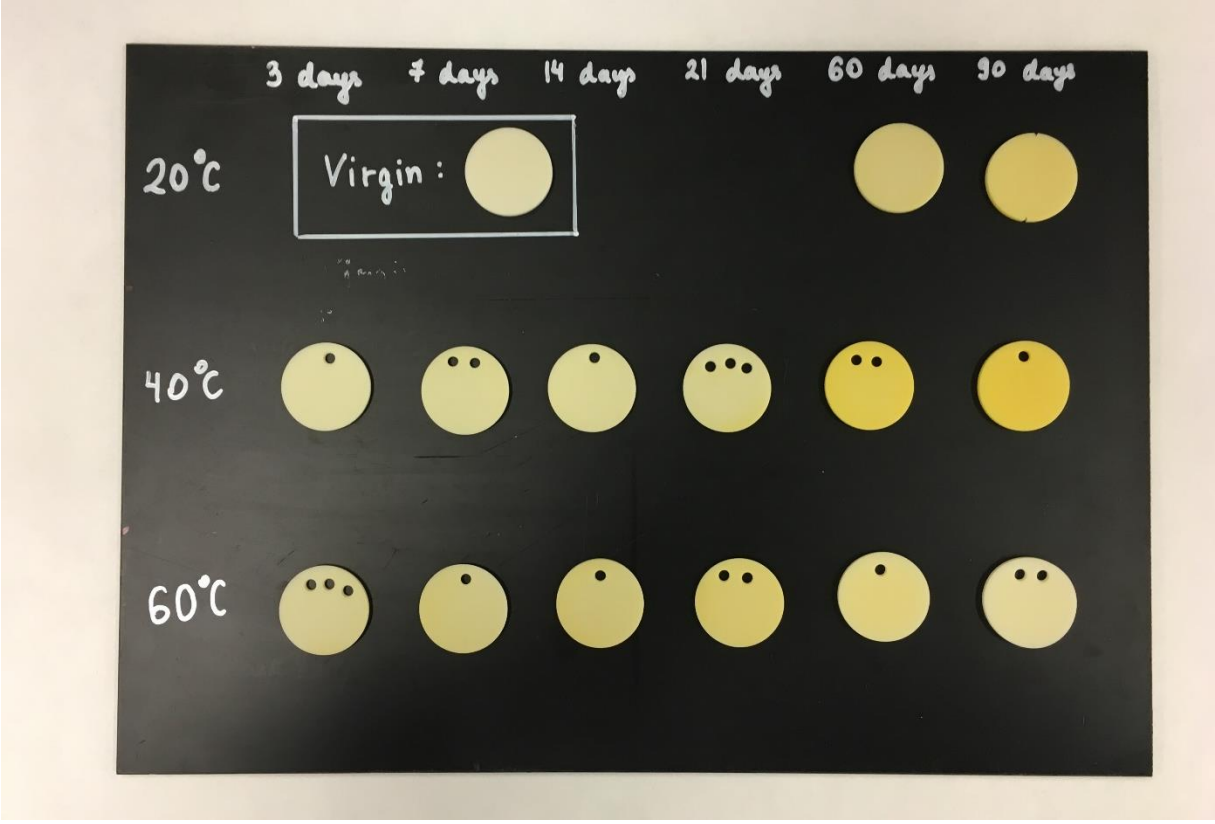

Figure 43: Visual observation of DISINF1 aged TPV

The first thing that can be observed about the peroxide aged plastic is the heavy discoloration of the samples at higher temperatures and long exposure times. The haptics of the samples did not change. It is surprising to see that the discoloration affected the 40 °C samples more than it did with the 60 °C aged ones. That is contrary to the general observation of longer oxidation results in darker yellowing. Assuming that this difference was not caused by human error (mixing up the samples between 21 and 60 days), one could reason that due to the color of the DISINF1 solution, the transferred some of its yellowish tones to the material. A slight increase in volume is also observable but it is hard to justify without quantitative measures.

Weight change

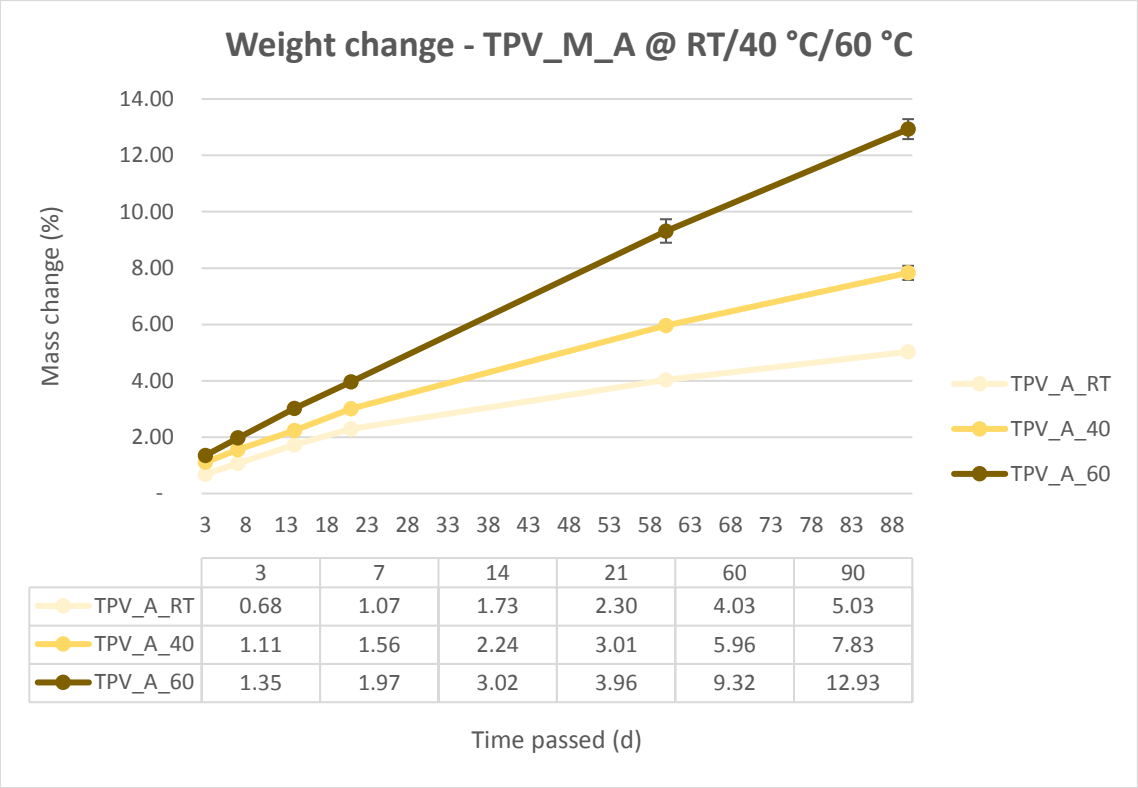

	3	7	14	21	60	90
TPV_A_RT	0.68	1.07	1.73	2.30	4.03	5.03
TPV_A_40	1.11	1.56	2.24	3.01	5.96	7.83
TPV_A_60	1.35	1.97	3.02	3.96	9.32	12.93

Figure 44: Weight change of DISINF1 aged TPV

Boiling deionized water has little effect on the weight of TPVs of similar grade (COMPOUNDER2, 2017). It can be said that the steady weight increase we see here is not just due to the absorption of some volatile into the material but there is a greater effect playing a role here. It is also unlikely that this much weight increase would be the result of solely the peroxidic oxidation of the TPV. Therefore, the most likely scenario would be that the due to the change in chemical constitution, the aged TPV is more susceptible to absorption. The trajectory of the weight increase is very linear and seems to be increasingly accelerated for increased temperatures.

Hardness change

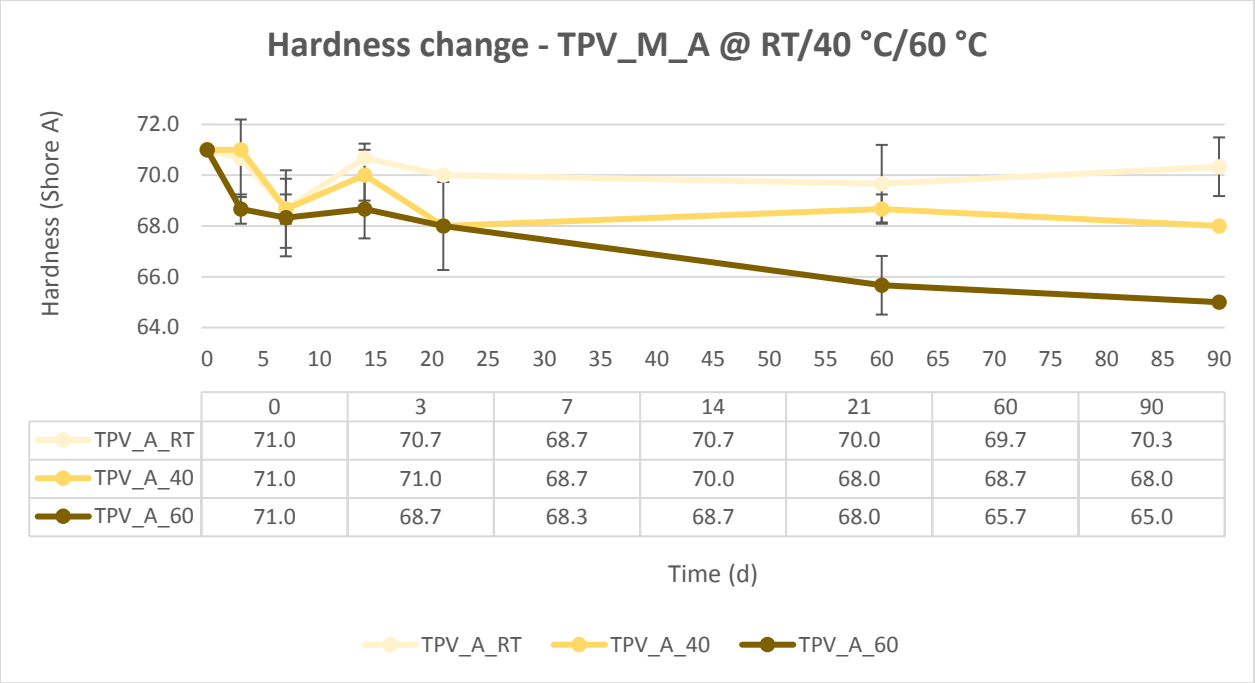

	0	3	7	14	21	60	90
TPV_A_RT	71.0	70.7	68.7	70.7	70.0	69.7	70.3
TPV_A_40	71.0	71.0	68.7	70.0	68.0	68.7	68.0
TPV_A_60	71.0	68.7	68.3	68.7	68.0	65.7	65.0

Figure 45: Hardness change of DISINF1 aged TPV

The TPV also little softer during ageing, but the extent of this is less severe and hard to justify with only three samples. Hardness measurements are quick and efficient way to follow the evolution of an elastomer's property, but also carry the possibility of measurement inconsistency and non-reproducibility. This effect is further magnified thanks to the holes pierced into the samples. These inconsistencies result in relatively large standard deviations. However, for long-term ageing, the effect is severe enough (-6 and -3 Shore A for 60 °C and 40 °C aged samples, respectively) that softening will be considered as a valid result of degradation.

Compression set

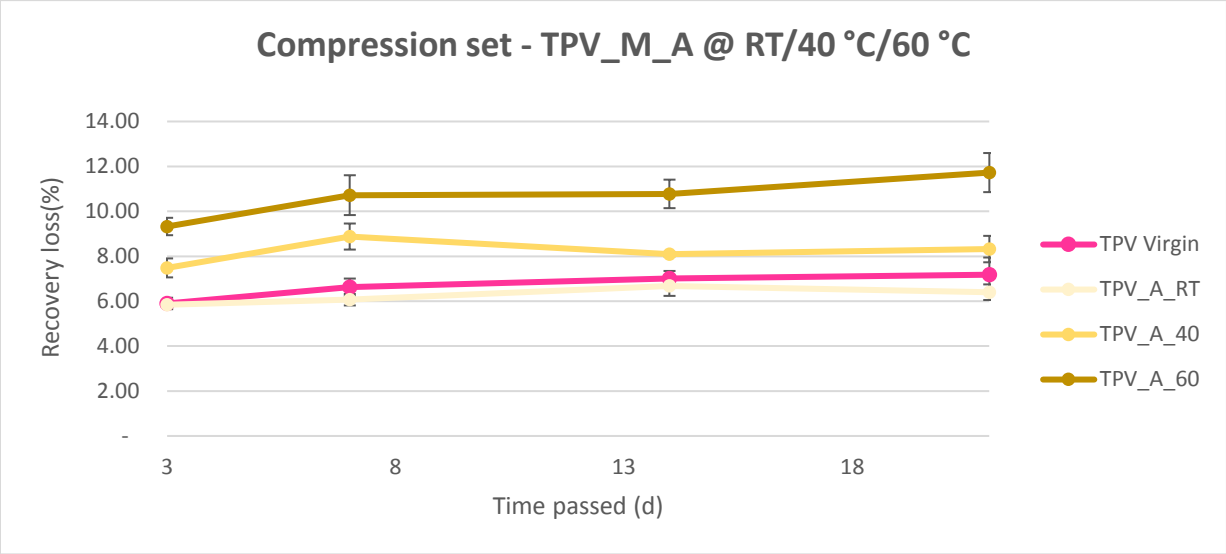

Figure 46: Compression set change of DISINF1 aged TPV

Compression data shows that during the inspection period the material lost its compression recovery in a parallel manner. After 3 days, the difference between the three lines is almost identical to that after 21 days and the virgin sample is similar to the room temperature aged one's trajectory. This tells us that, with the inaccuracy of compression set measurements in mind, the set was more temperature dependent. No further general trend of degradation can be assumed from the presented data.

Tensile strength, ultimate elongation

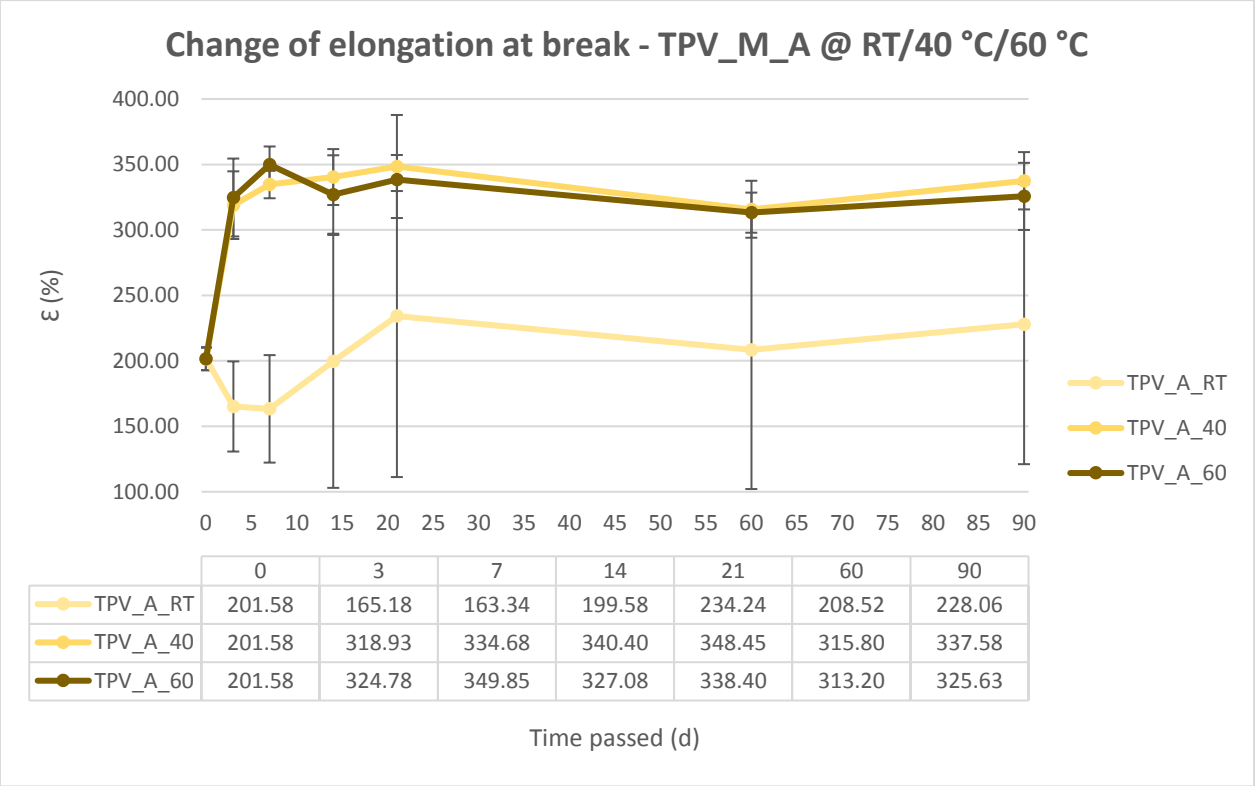

	0	3	7	14	21	60	90
TPV_A_RT	201.58	165.18	163.34	199.58	234.24	208.52	228.06
TPV_A_40	201.58	318.93	334.68	340.40	348.45	315.80	337.58
TPV_A_60	201.58	324.78	349.85	327.08	338.40	313.20	325.63

Figure 47: Ultimate elongation change of DISINF1 aged TPV

The tensile test showed variance in both observed properties. Conclusion, however, is very hard to draw due to the high standard deviation of the samples. As mentioned before, these data points are a mean values of the performance of 4-5 tensile bars. In the case of the room temperature ageing, two out of five bars of the four longest ageing times showed elongation around 120% thus creating very large standard deviations and pushing the mean of these measurements lower. These many bars are not enough to conclude degradation. The samples aged at elevated temperatures show more homogeneity. They have nearly doubled their ultimate elongation in a short period of time. Tensile strength of the material decreased over time by 0.5-1 MPa.

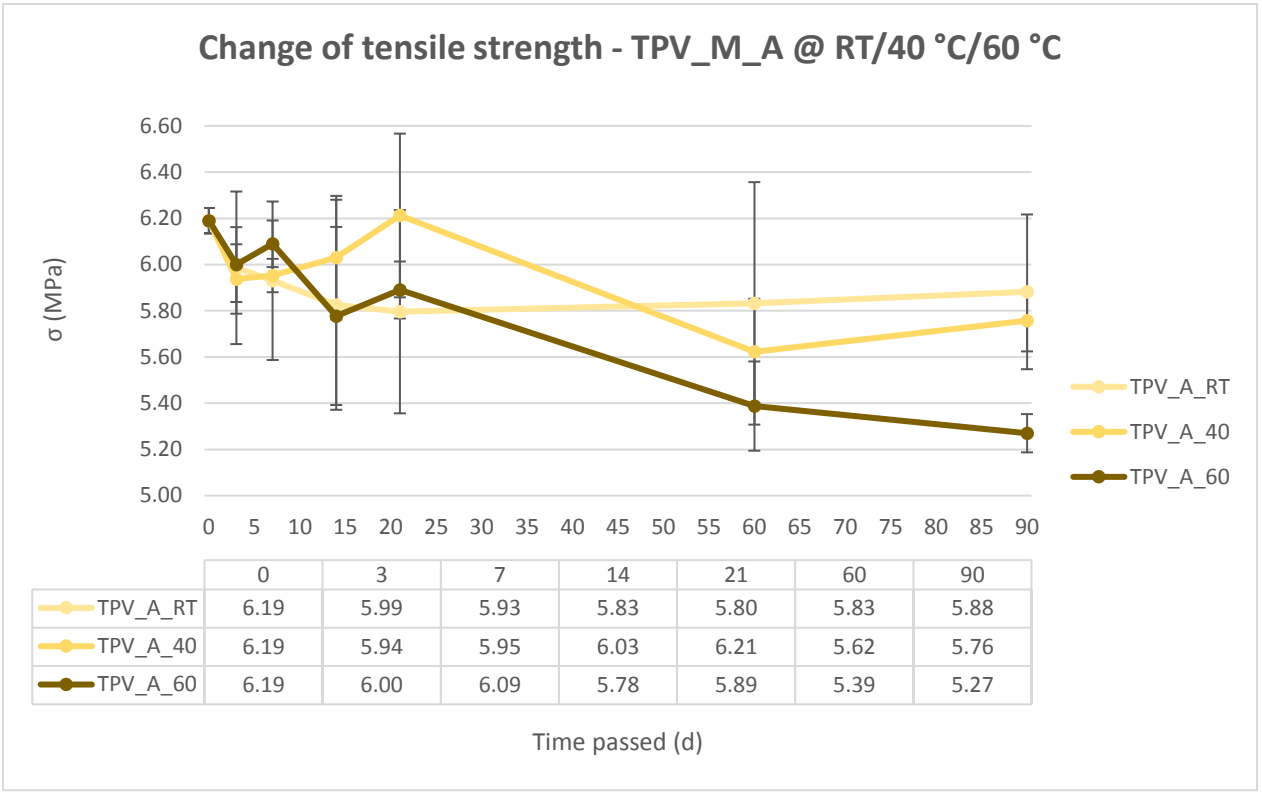

	0	3	7	14	21	60	90
TPV_A_RT	6.19	5.99	5.93	5.83	5.80	5.83	5.88
TPV_A_40	6.19	5.94	5.95	6.03	6.21	5.62	5.76
TPV_A_60	6.19	6.00	6.09	5.78	5.89	5.39	5.27

Figure 48: Tensile strength change of DISINF1 aged TPV

Infrared spectra

TPV_A_RT	TPV_A_40	TPV_A_60	Deformation
cm^{-1}	cm^{-1}	cm^{-1}	
3435			O-H stretch
2955	2955	2955	C-H stretch weakening signal
2927	2925	2925	C-H stretch weakening signal
2855	2857	2857	C-H stretch weakening signal
		1745	C=O stretch appearing
	1600	1603	C=O stretch of COO^- appearing
	1577		C=O stretch of COO^- appearing
	1544		C=O stretch of COO^- appearing
1463	1465	1465	C-H bend
		1416	C=O stretch of COO^- appearing
1379	1377	1379	C-H bend in CH_3
1108	1108	1100	O=C-O-C stretch
800-	800-	800-	C-H bend of CH_2

Table 8: Peaks of FT-IR in TPV_A

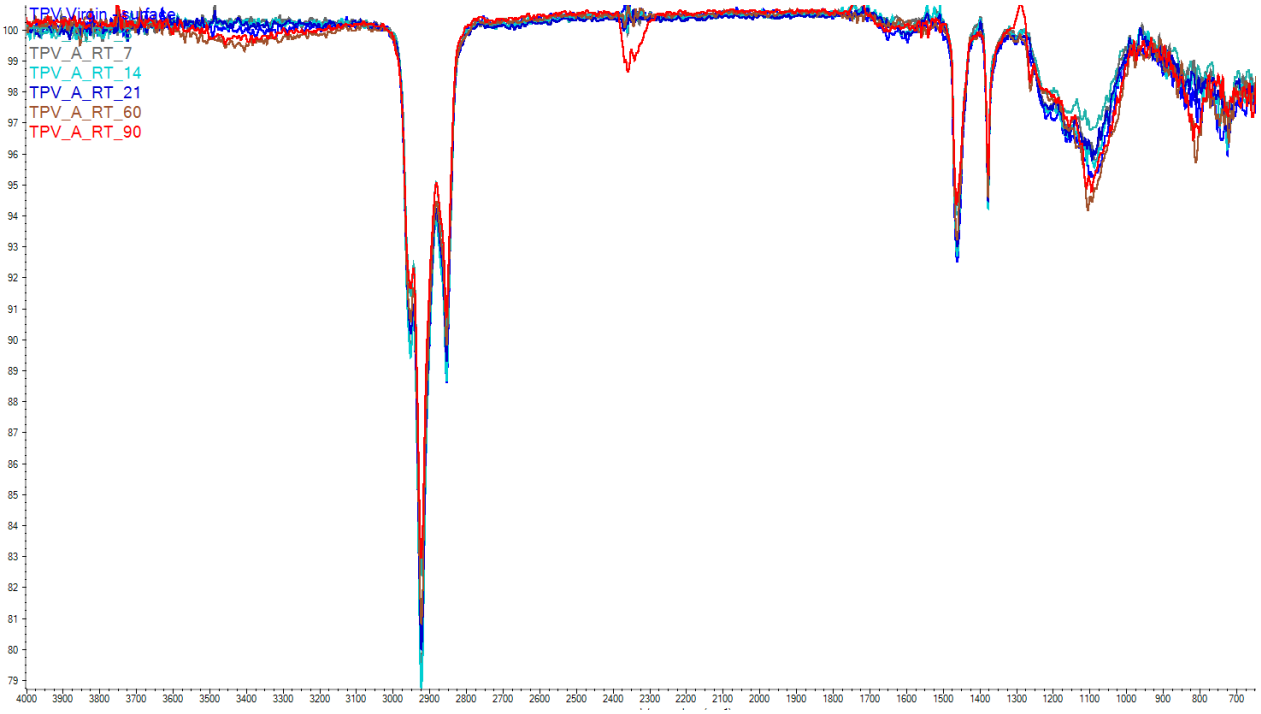

Figure 49: Fourier-transform infrared spectra of TPV aged in DISINF1 at 20 °C

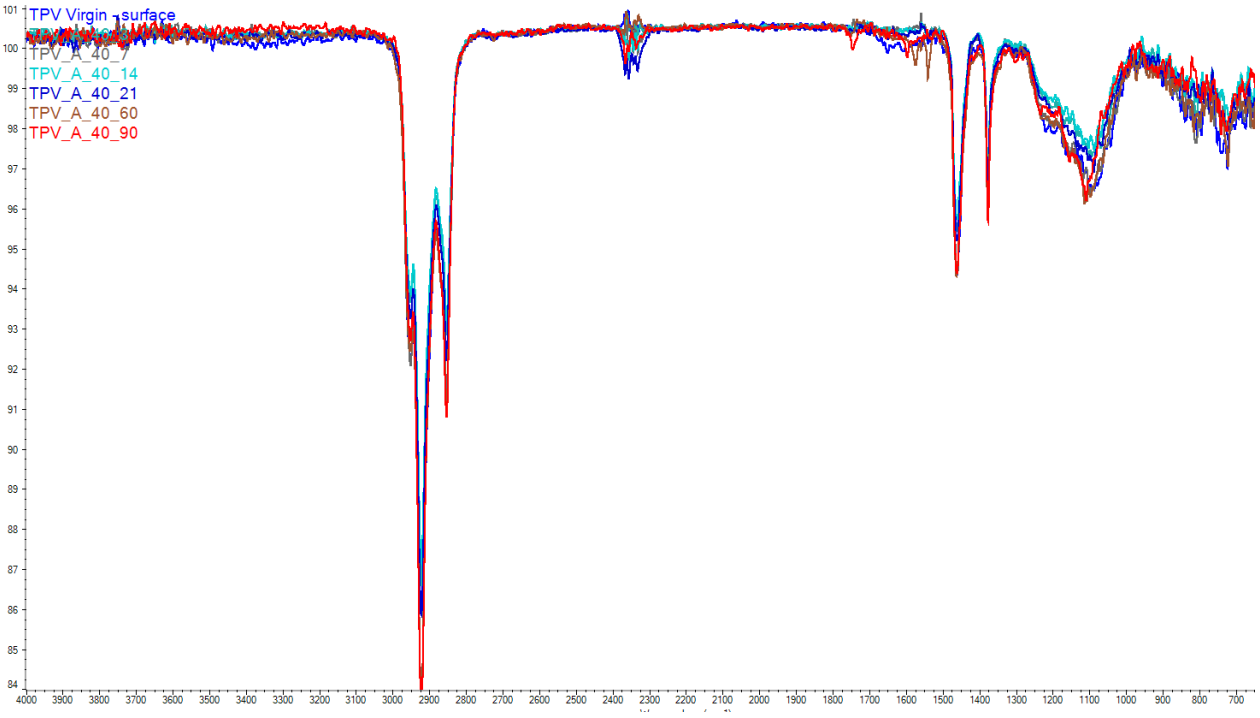

Figure 50: Fourier-transform infrared spectra of TPV aged in DISINF1 at 40 °C

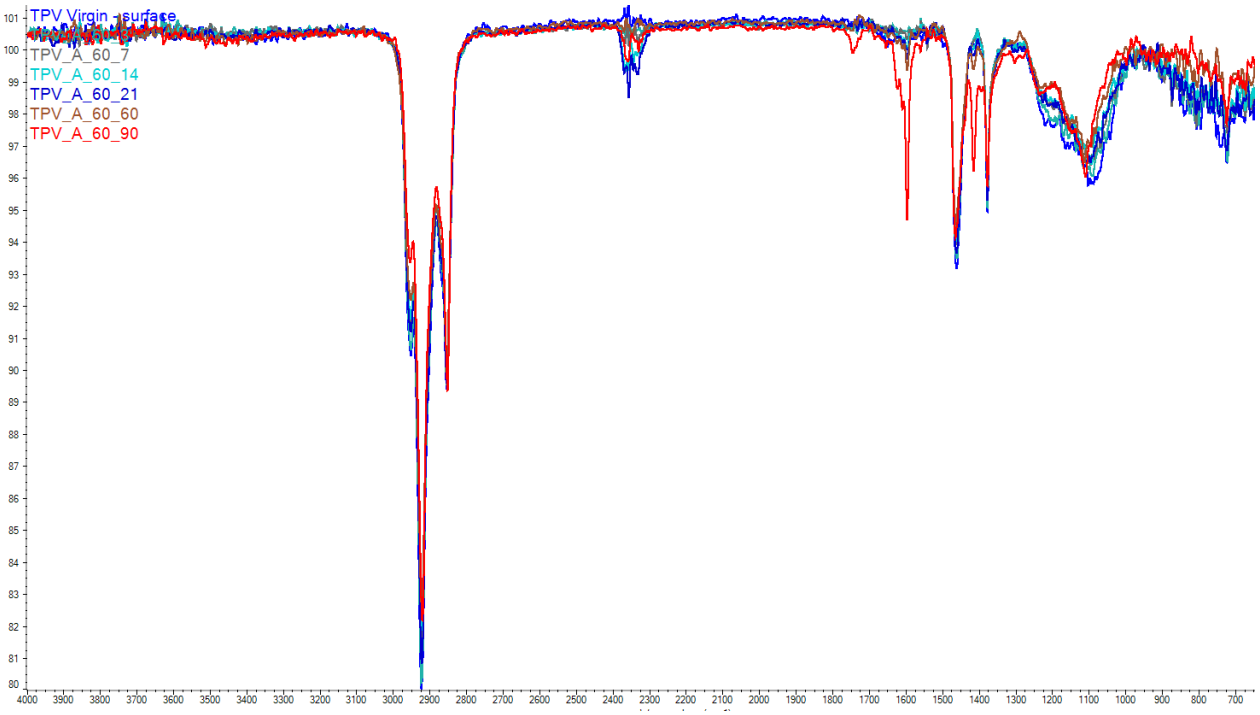

Figure 51: Fourier-transform infrared spectra of TPV aged in DISINF1 at 60 °C

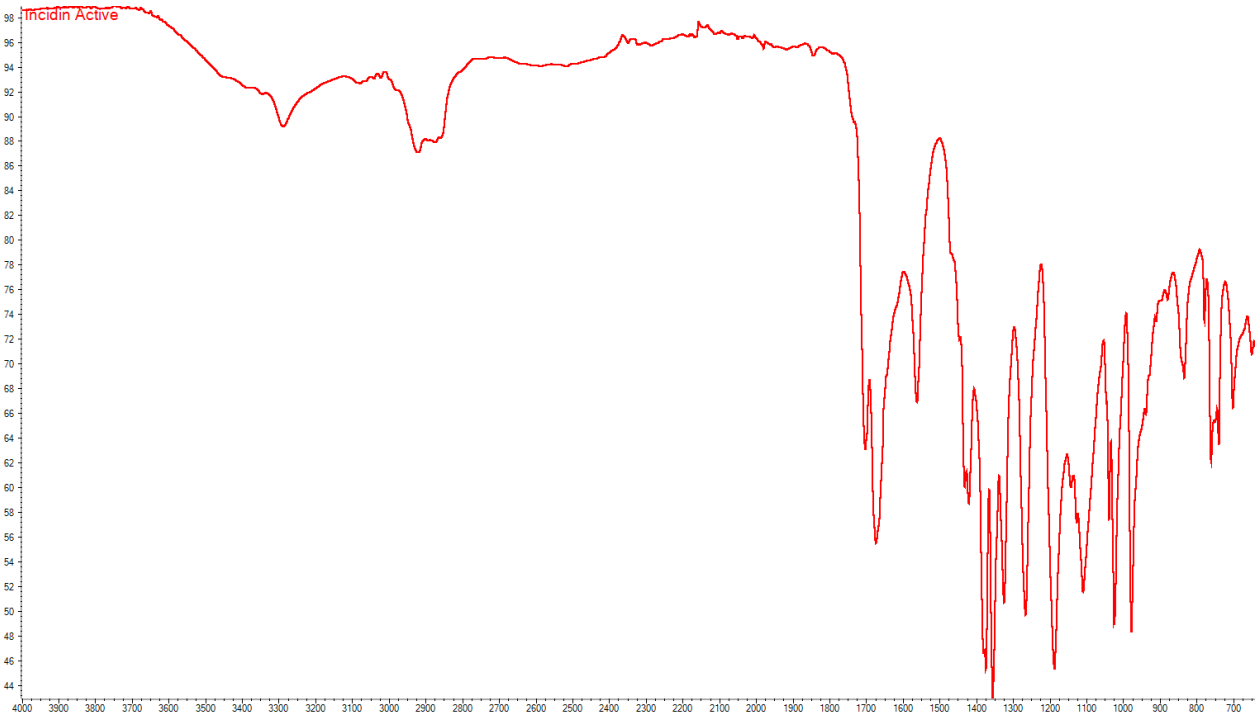

Figure 52: Fourier-transform infrared spectra of DISINF1

At room temperature, we can observe a slight increase in the O-H stretch at 3400 cm^{-1}. This is paired with the increase of intensity of C-O stretching observable around the 1100 cm^{-1} wavenumber. Therefore, it is fair to assume that at room temperature hydroxyl group formation is the result of oxidative degradation.

At higher temperatures, the sample shows a different degradation prevail. To a smaller extent, ketones are formed. Their presence is confirmed by a small peak increase at 1750 cm^{-1}. The chemical change of the material is more profound when the spectra of the 60 °C aged TPV is inspected. Two new peaks appear between 60 and 90 days of immersion: one at 1600 cm^{-1} and the other at 1400 cm^{-1}. It can be interpreted as carboxylic acid salt formation with the peroxide. These peaks would regard the O-C=O stretch. Other peaks are observable at 1500 cm^{-1} for C-H bends of mainly the PP/EPDM matrix; at 1350 cm^{-1} for the CH_3 C-H bend in PP and at 700-800 cm^{-1} for the CH_2 C-H bend from the polymer backbone. The IR spectra of DISINF1 is also shown too, where a really broad O-H stretch band can be seen that stretches between 3600 cm^{-1} and 2600 cm^{-1}. This is only an approximate value as the spectra is complex and it is hard to single out a signal. The other striking peak observable is at 1700 cm^{-1} regarding the C=O stretches. This broad peak thus can be interpreted as a carboxylic acid species, and the broadness of the peak is justified by the various H-bonding of the molecules (Roeges, 1994).

Thermogravimetric changes

The residue graph can be created for TPV_A too but the change is not significant, as residual weight percent remains around 11-13% of initial sample weight. Also, comparing the thermograms and their time derivatives, it can be concluded that the material did not leach as the two distinct degradation steps are still present after ageing. However, the peak associated with the PP/EPDM matrix suffered structural changes. It can also be said, that the onset temperature of the oil degradation was pushed to lower temperature. As mentioned before, the filler oils used in TPV are likely to contain double bonds and these bonds are more chemically active. These bonds were responsible for the oxidation of the material and thus made it weaker against further thermo-oxidation.

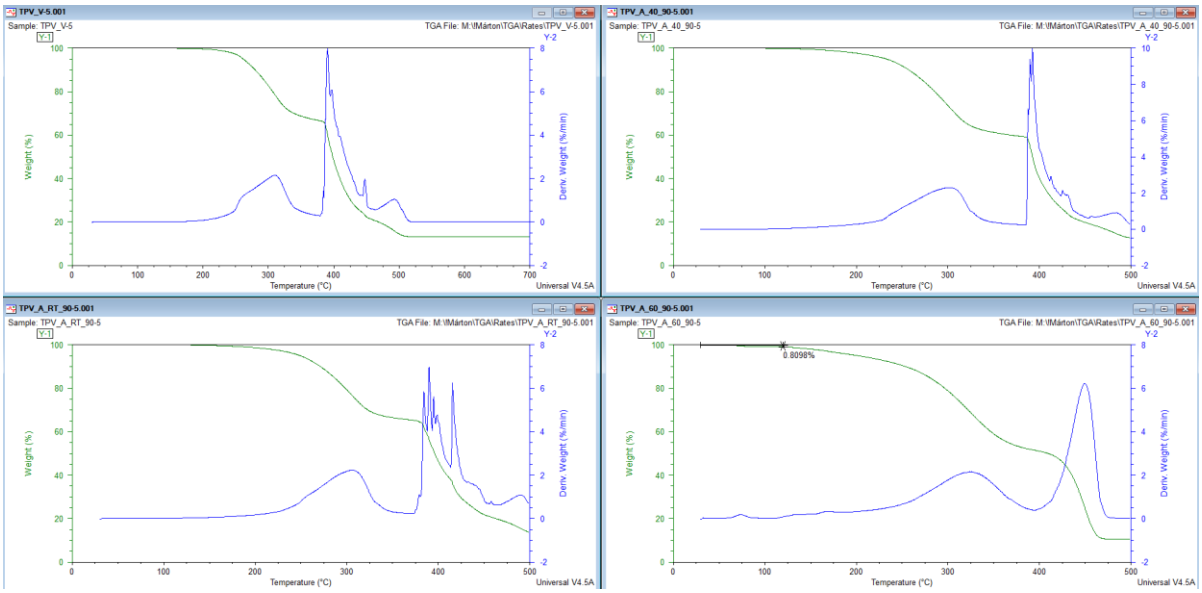

Figure 53: Thermograms with their respective time derivative (l-top) Virgin TPV (l-bottom) TPV_A_RT_90 (r-top) TPV_A_60_90 (r-bottom) TPV_A_40_90

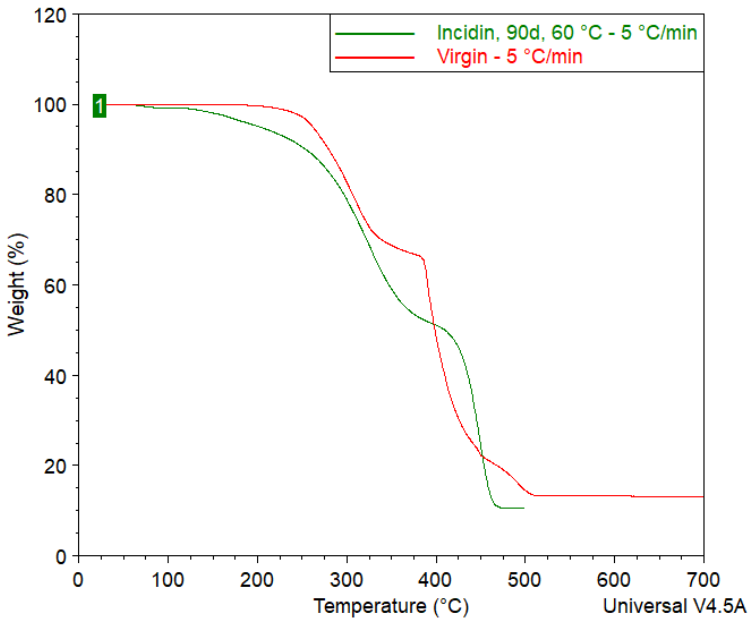

Figure 54: TPV_A_60_90 compared with unaged TPV

When the aged sample's thermogram is compared with that of the virgin material, a shift to lower temperatures can be observed. This means lower thermo-oxidative resistance for the material. This comes as no surprise, since the oxidation of the material was already initiated by the DISINF1 ageing. The antioxidant mixture added to the TPV during compounding is fully reduced. We can also conclude that the weight fraction associated with the oils increased over time by 13%, most likely due to oxidation. However, this showed no time nor temperature dependence, thus was non-conclusive.

	TPV_A
Visual	Yellowing
Weight	Increasing
Hardness	Decreasing
Elongation	Increase but unreliable results
Tensile strength	Small decrease but unreliable results
Compression set	Increasing
Thermogram	Shift to lower temperatures, lower activation energy
Infrared	COO^- peak appears, decreasing C-H peak intensity

Table 9: Assessing all the changes of TPV_A

LSR AGED IN NAOCL

Visual observations

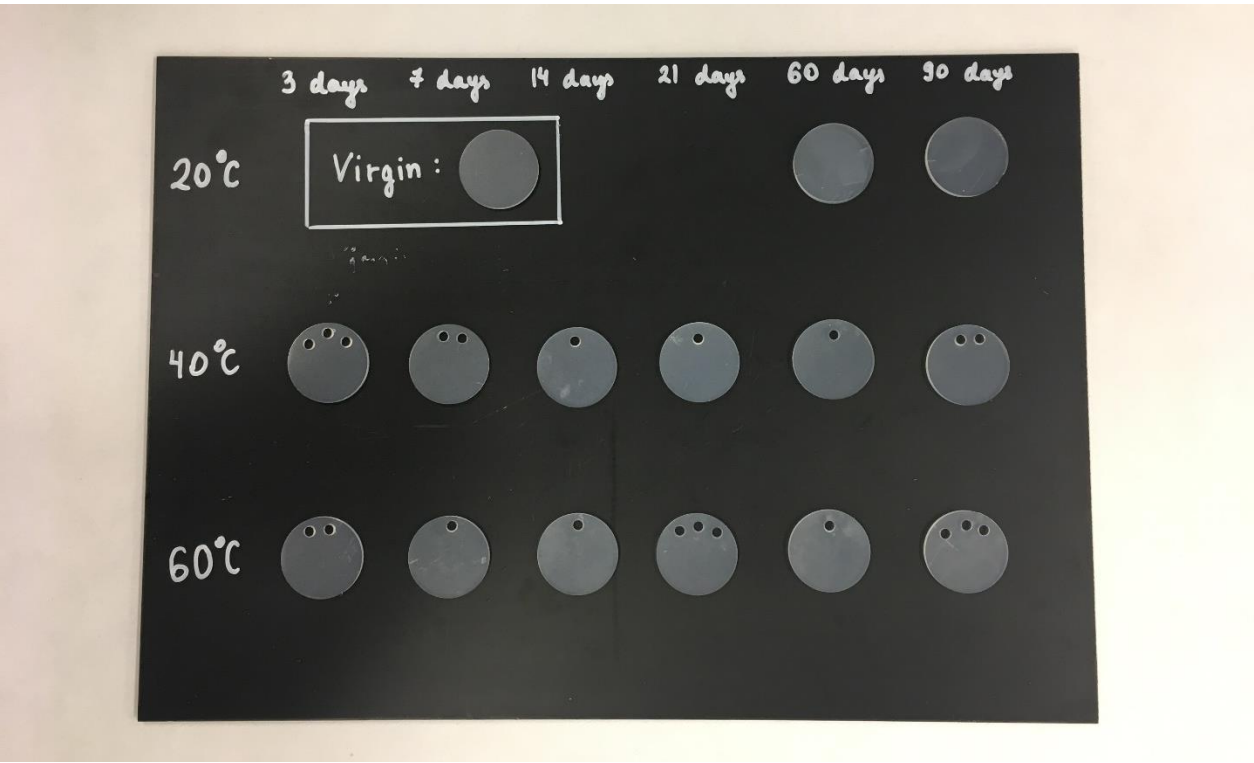

Figure 55: Visual observation of NaOCl aged LSR

The degradation of silicone was a lot harder to assess than that of TPV. Both visually and measurably, the samples showed less severe changes. This aligns with silicone's unreactive nature (Wacker, NA) and also calls for a longer ageing experiment to properly understand the ageing behavior of silicone.

Firstly, some visual degradation can be observed. Samples aged longer show a loss in transparency and the surface of the elastomer is stickier than before and lost its haptic behavior. When taken out of the solution, the samples often resembled a whiter disk inside a more transparent outer layer. This feature was temporary, as presented on Figure 56, but the loss of transparency stayed. This confirms that the material is still in the diffusion-limited stage.

Figure 56: LSR_N_60_90 tensile bar with a diffusion limitation profile

Weight change

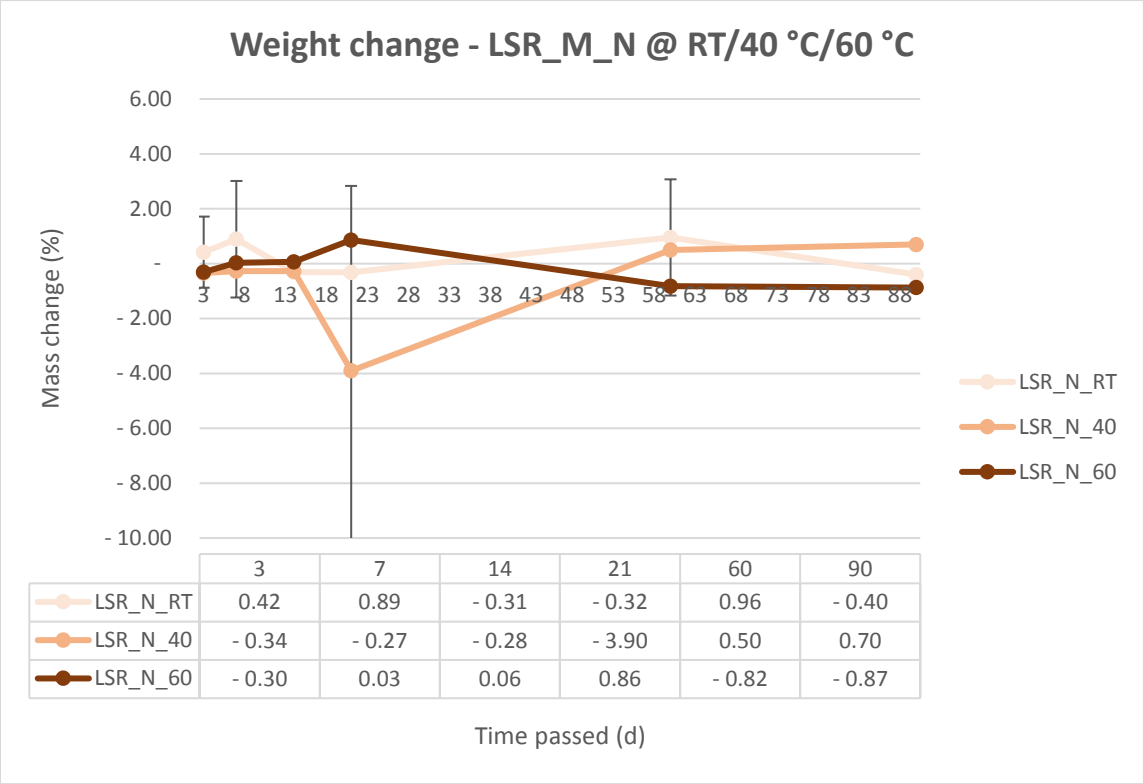

	3	7	14	21	60	90
LSR_N_RT	0.42	0.89	- 0.31	- 0.32	0.96	- 0.40
LSR_N_40	- 0.34	- 0.27	- 0.28	- 3.90	0.50	0.70
LSR_N_60	- 0.30	0.03	0.06	0.86	- 0.82	- 0.87

Figure 57: Weight change of NaOCl aged LSR

Weight change has proven to be less useful when following the degradation of LSR species. The weight change is insignificant, and shows little promise to derive conclusions from. There seems to be a decrease in weight for the 40 °C aged material after 21 days of exposure, however, when the standard deviation associated with this measurement is considered, the unreliability of this measurement prevails.

Hardness change

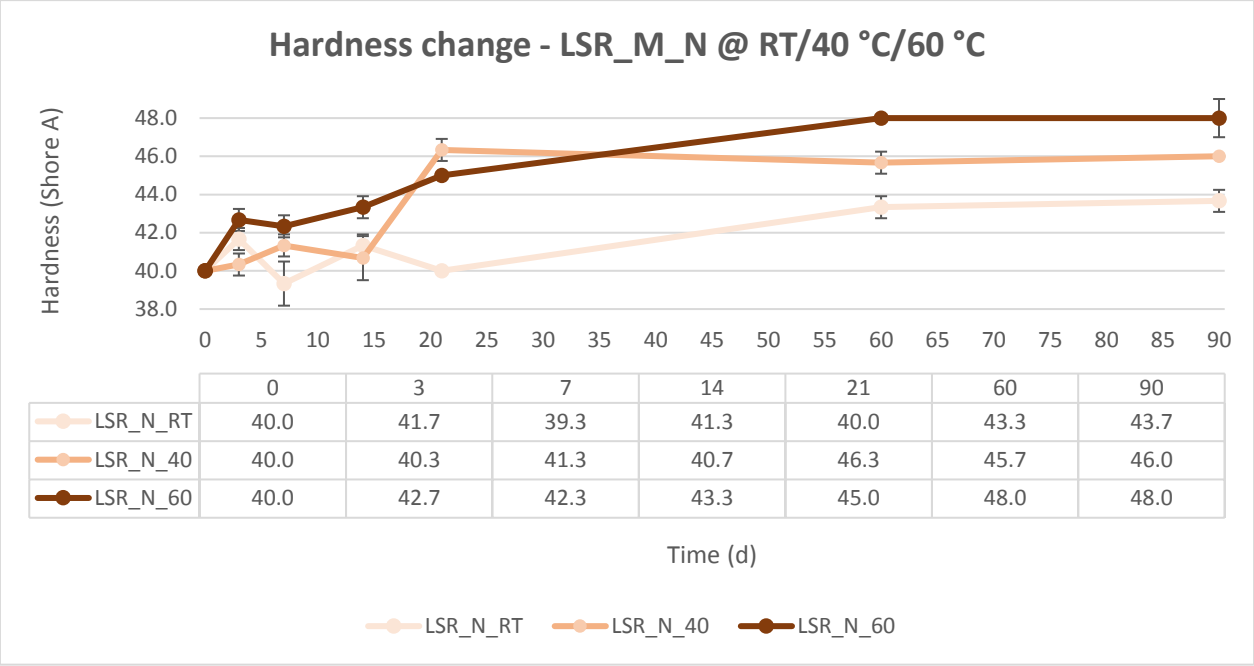

	0	3	7	14	21	60	90
LSR_N_RT	40.0	41.7	39.3	41.3	40.0	43.3	43.7
LSR_N_40	40.0	40.3	41.3	40.7	46.3	45.7	46.0
LSR_N_60	40.0	42.7	42.3	43.3	45.0	48.0	48.0

Figure 58: Hardness change of NaOCl aged LSR

As mentioned before, the samples changed their haptic characteristics. This also manifested in an increase of hardness. The hardness increased slowly in the first 60-day period but stagnated between the last to measurements. The hardening may be a result of some oxidative crosslinking reaction happening with the hypochlorites being so chemically active (Wacker, NA). Further conformation is needed for this hypothesis.

Compression set

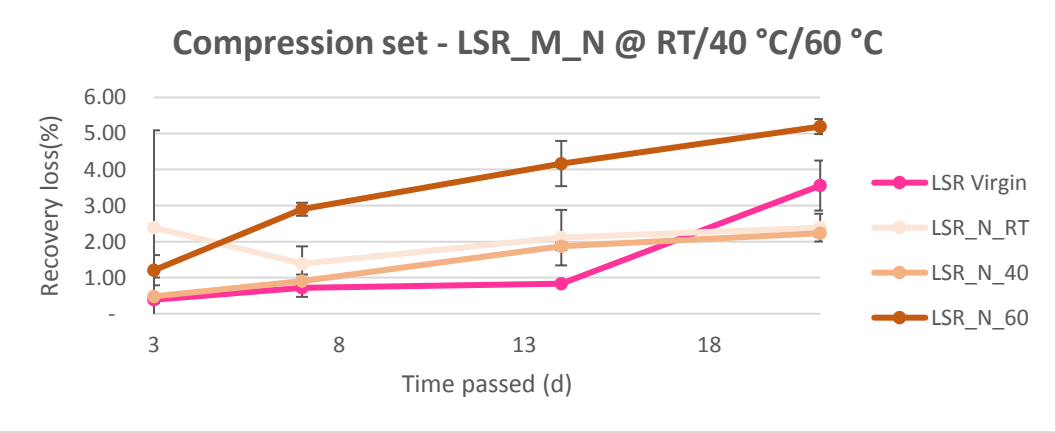

Figure 59: Compression set change of NaOCl aged LSR compared to unaged LSR

Compression data shows no significant degradation. Almost all data points are below 5% change and this is still insignificant when the accuracy of the test is considered.

Tensile strength, ultimate elongation

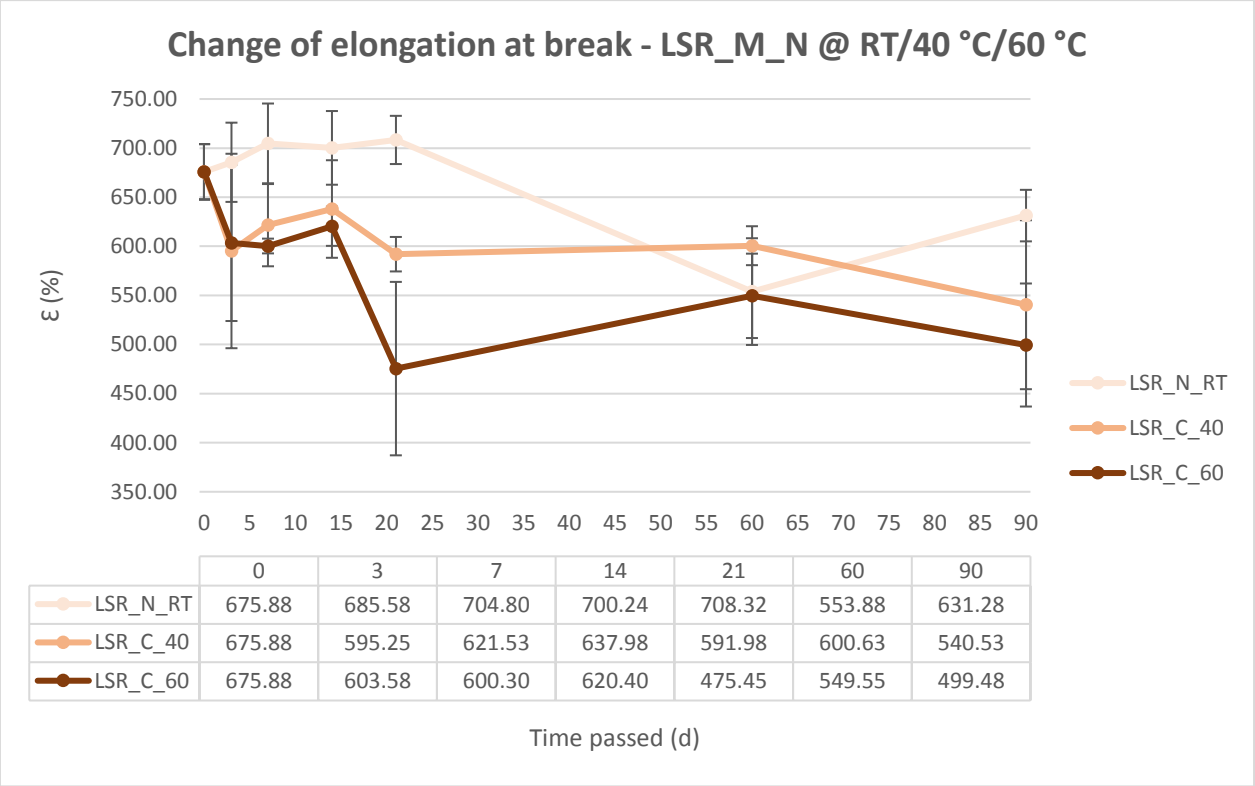

	0	3	7	14	21	60	90
LSR_N_RT	675.88	685.58	704.80	700.24	708.32	553.88	631.28
LSR_C_40	675.88	595.25	621.53	637.98	591.98	600.63	540.53
LSR_C_60	675.88	603.58	600.30	620.40	475.45	549.55	499.48

Figure 60: Ultimate elongation change of NaOCl aged LSR

Again, highly inconsistent data with huge standard deviations that allow for little to be concluded from the tensile experiments of LSR. The ultimate elongation seems to decrease while tensile strength is also slightly decreasing. Due to the inconsistent trajectory of the tensile strength graph, this decrease is hard to justify in magnitude and its temperature dependency is also hard to assess.

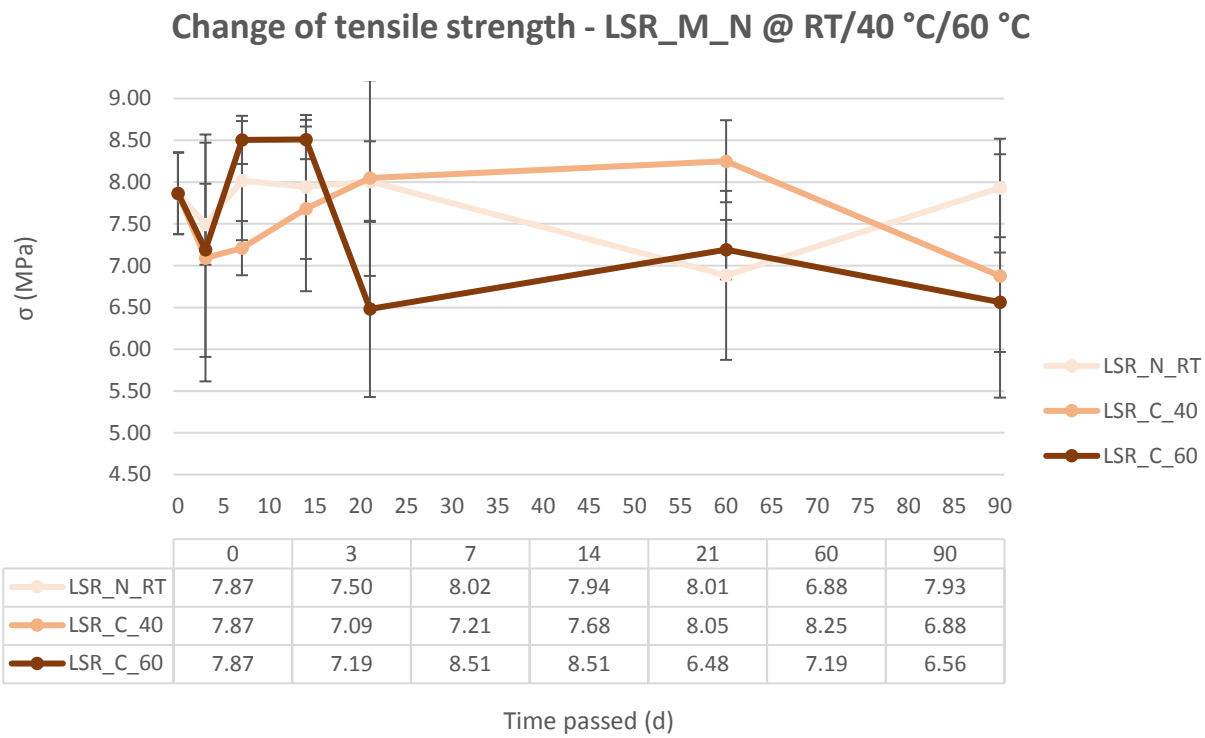

	0	3	7	14	21	60	90
LSR_N_RT	7.87	7.50	8.02	7.94	8.01	6.88	7.93
LSR_C_40	7.87	7.09	7.21	7.68	8.05	8.25	6.88
LSR_C_60	7.87	7.19	8.51	8.51	6.48	7.19	6.56

Figure 61: Tensile strength change of NaOCl aged LSR

Infrared spectra

LSR_N_RT	LSR_N_40	LSR_N_60	Deformation
cm^{-1}	cm^{-1}	cm^{-1}	
3416	3387	3388	O-H stretch, non-time dependent
2967	2967	2967	C-H stretch
	1650	1642	Unknown increasing peak (C=O stretch)
1416	1414	1418	C-H bend of CH_3
1265	1265	1262	Si-CH_3
1085	1080	1083	Si-O-Si, decreasing over time
1020	1017	1015	Si-O-Si
866	866	864	Si-$(CH_3)_2$
796	798	798	Si-$(CH_3)_2$

Table 10: Peaks of FT-IR in LSR_N

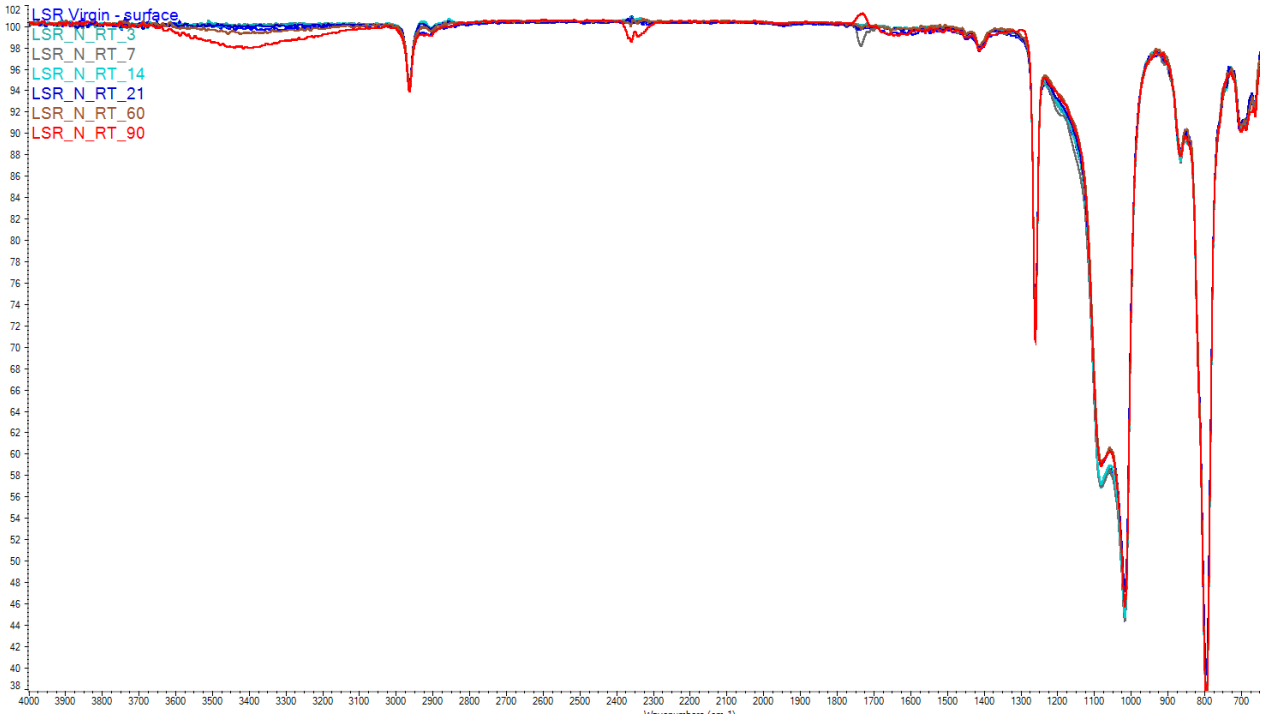

Figure 62: Fourier-transform infrared spectra of LSR aged in NaOCl at 20 °C

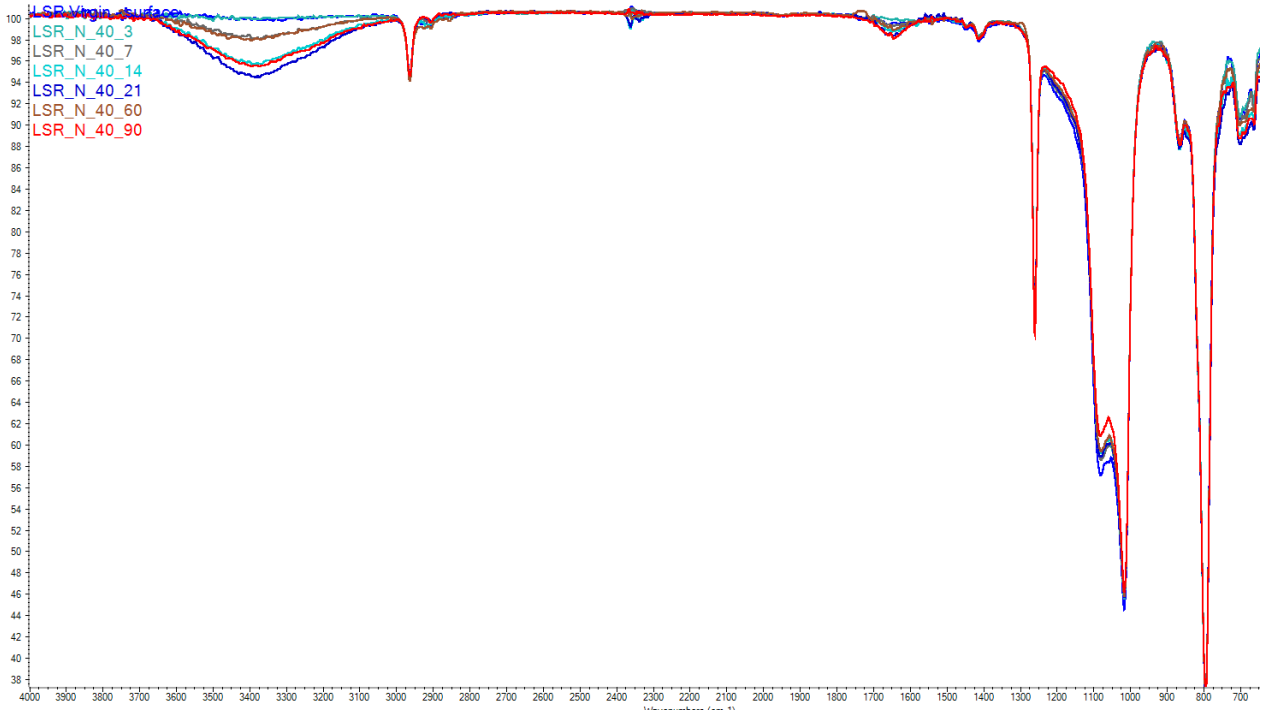

Figure 63: Fourier-transform infrared spectra of LSR aged in NaOCl at 40 °C

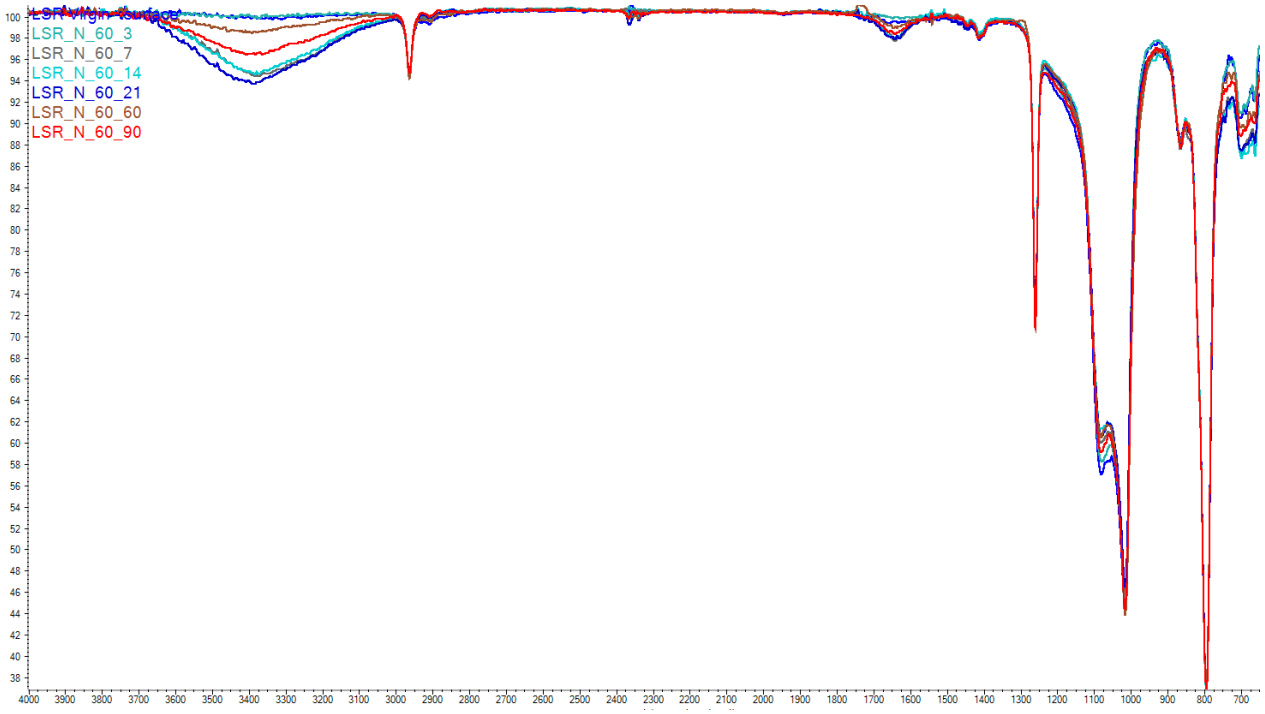

Figure 64: Fourier-transform infrared spectra of LSR aged in NaOCl at 60 °C

As opposed to previous experimental data, IR spectra of aged LSR gives a more helpful view on what the material degradation entails. Independent of time, the increase of the O-H stretch peak at 3400 cm^{-1} is evident. The peak intensifies when the samples is aged at higher temperatures. It is speculated that the dimethyl siloxane is not affected: the Si-CH_3 stretch at 1300 cm^{-1}, the C-H stretch at 3000 cm^{-1} and the Si-$(CH_3)_2$ bend at 800 cm^{-1} is intact. However, the broad peak of Si-O-Si stretch is disrupted after ageing. A small but hard to identify peak at 1650 cm^{-1} might refer to C=O stretching as an effect of oxidation (Roeges, 1994). This allows for scission of the chains to be considered as a degradation mechanism (Gao et. al, 2014). This would explain the increasing OH concentration and the change observed regarding the Si-O-Si backbone. This would result in the shortening of the polymer chains and the narrowing of the doublet peak (Launer, 2013). Unfortunately, there is not enough data to support this. In the case of chain shortening, a method to measure molecular weight distribution would confirm the suspicion.

	LSR_N
Visual	Diffusion phenomena, slight loss of transparency
Weight	Insignificant
Hardness	Increasing
Elongation	Decreasing but hard to signify
Tensile strength	Non-conclusive
Compression set	Increasing
Thermogram	Non-conclusive
Infrared	Si-O-Si and O-H peaks change are non-time dependent

Table 11: Assessing all the changes of LSR_N

LSR AGED IN DISINF2

Visual observations

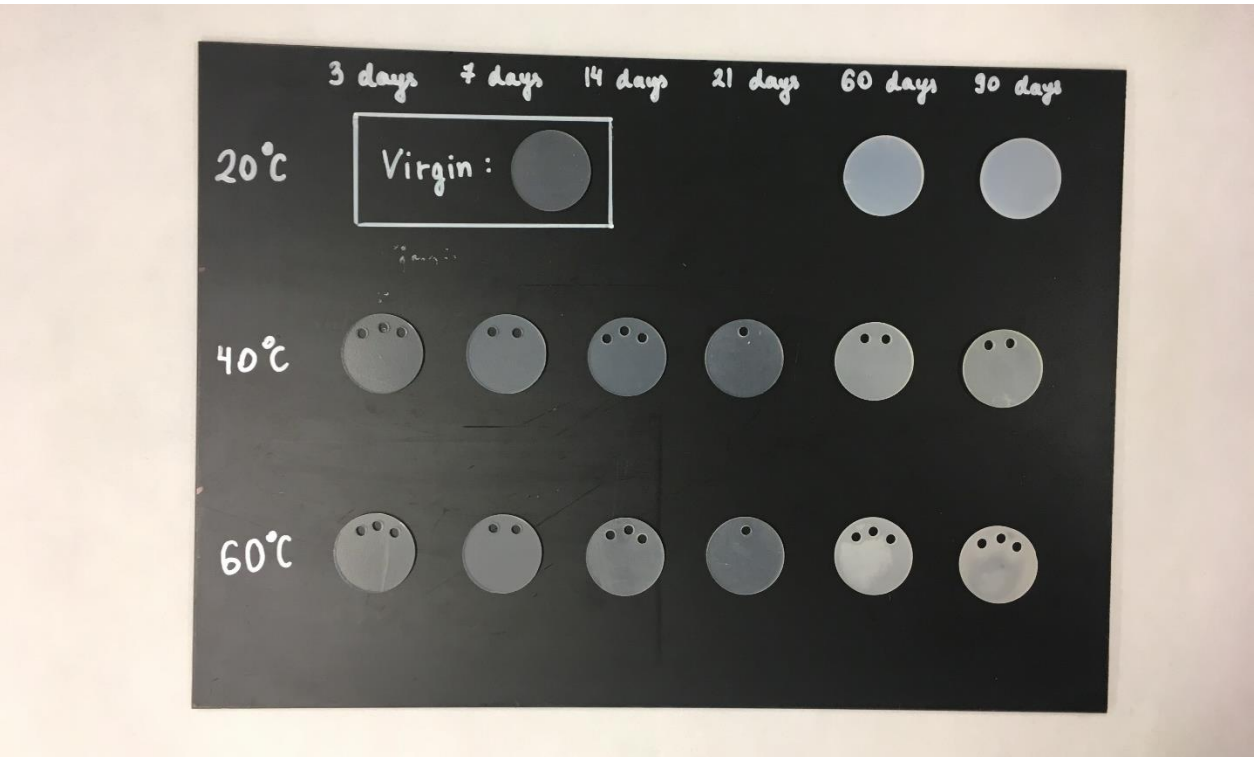

Figure 65: Visual observation of DISINF2 aged LSR

Little change can be observed for samples that were aged for 21 days of shorter. However, the change in transparency for longer exposure times and the slight browning of the samples aged at higher temperatures is striking. The samples became firmer and more leathery to the touch.

Weight change

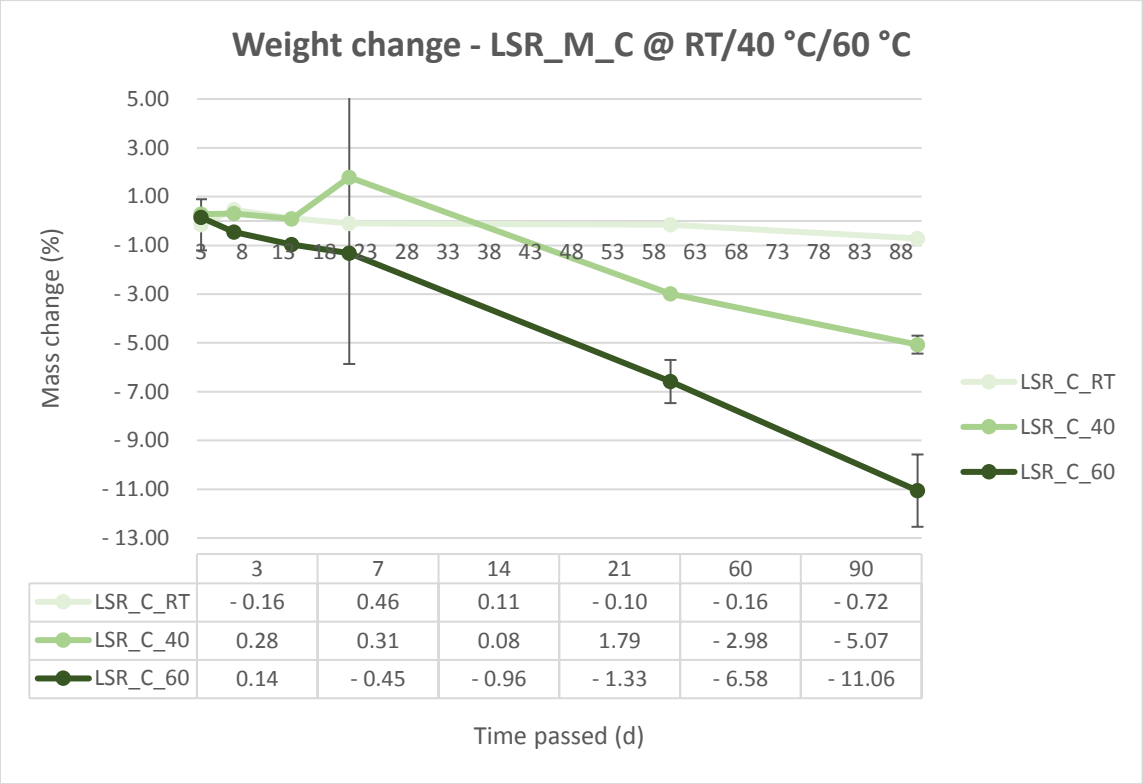

	3	7	14	21	60	90
LSR_C_RT	- 0.16	0.46	0.11	- 0.10	- 0.16	- 0.72
LSR_C_40	0.28	0.31	0.08	1.79	- 2.98	- 5.07
LSR_C_60	0.14	- 0.45	- 0.96	- 1.33	- 6.58	- 11.06

Figure 66: Weight change of DISINF2 aged LSR

Weight of room temperature aged samples are stagnant during the period observed. The samples aged at elevated temperature give a sense of degradation that is to be expected from the material after longer exposure times. The weight decrease is very slow in the first 21-day period but reaches a considerable level after 60 days. This could mean that the induction period for such ageing is around 21 days long for elevated temperatures and after that the solvent reaches the bulk of the material. In the bulk, something dissolves out of the material into the solution. LSR does not contain oil, so either other substances are leaching out or the weight loss is a direct result of some chemical degradation. Unfortunately, no convincing explanation can be assigned to reason with the weight decrease other than the leaching of small chain silicones.

Hardness change

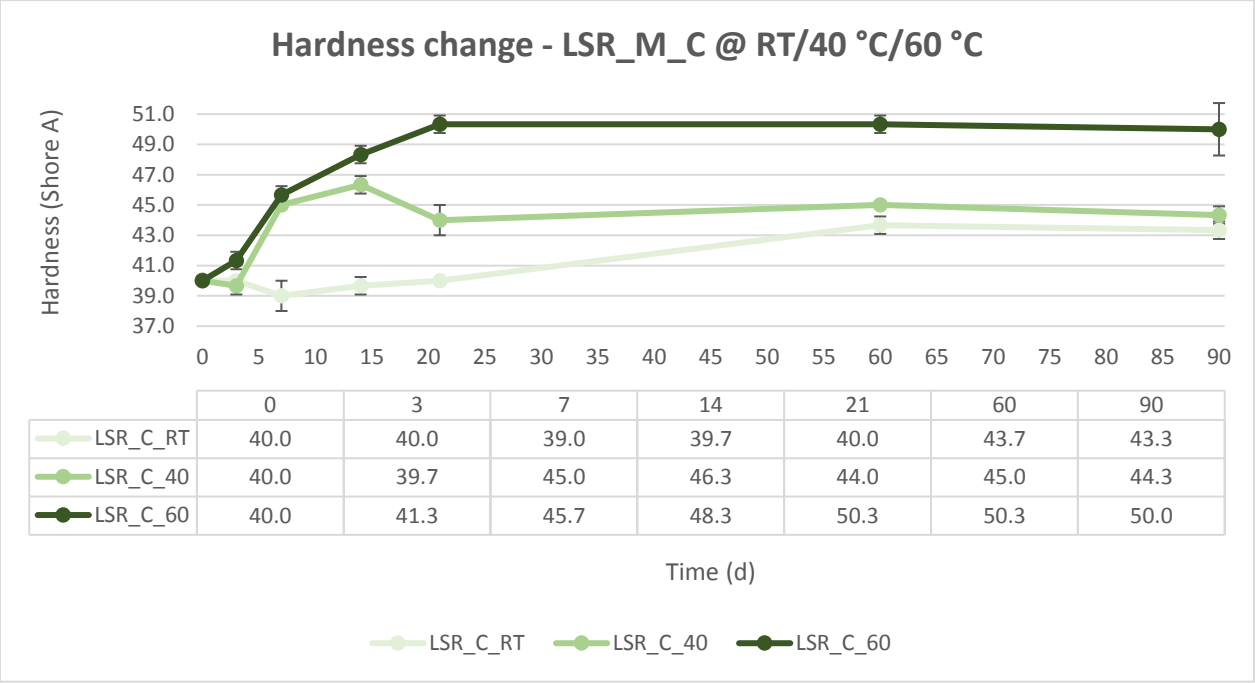

	0	3	7	14	21	60	90
LSR_C_RT	40.0	40.0	39.0	39.7	40.0	43.7	43.3
LSR_C_40	40.0	39.7	45.0	46.3	44.0	45.0	44.3
LSR_C_60	40.0	41.3	45.7	48.3	50.3	50.3	50.0

Figure 67: Hardness change of DISINF2 aged LSR

The sign of hardening is trivial in the case of DISINF2 aged LSR. This hardening seems to be significantly faster in the first 21-day period of elevated temperature ageing. After 21 days, the hardness change levels out and reaches a plateau. This could be reasoned with a mass transfer limitation where the surface of the material hardens followed by the bulk degradation of the material. Maybe this limitation is what allows the mass to decrease rapidly. Short chain silicones act as a plasticizer for LSR and the leaching of them leads to material hardening.

Compression set

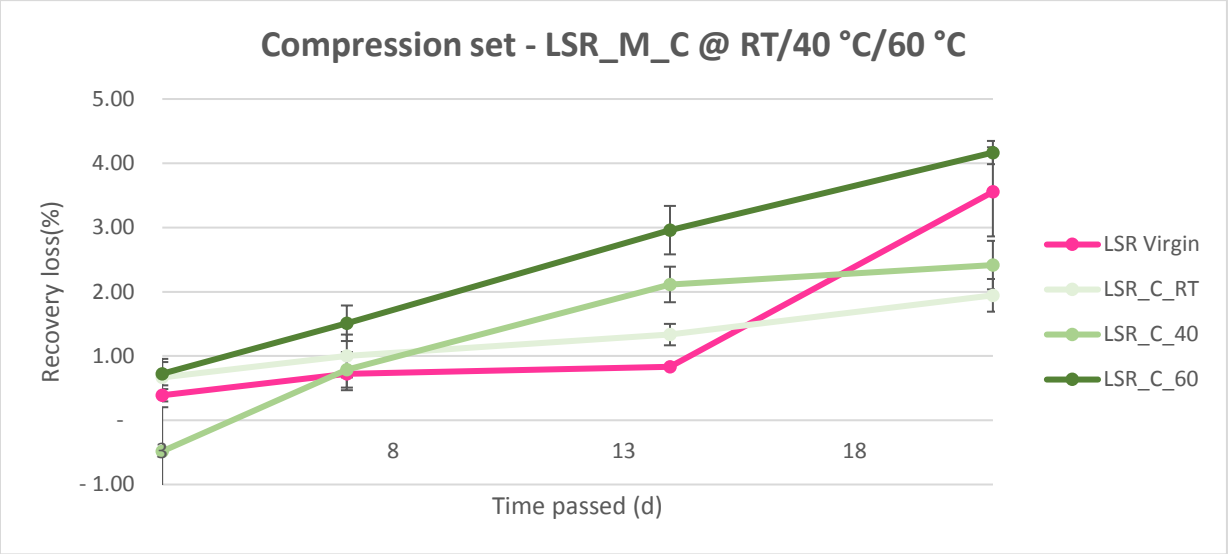

Figure 68: Compression set change of DISINF2 aged LSR compared to unaged LSR

Much like for the NaOCl aged LSR, compression set data is non-conclusive. The set is below the accuracy of the test and therefore, is considered to be an insignificant change.

Tensile strength, ultimate elongation

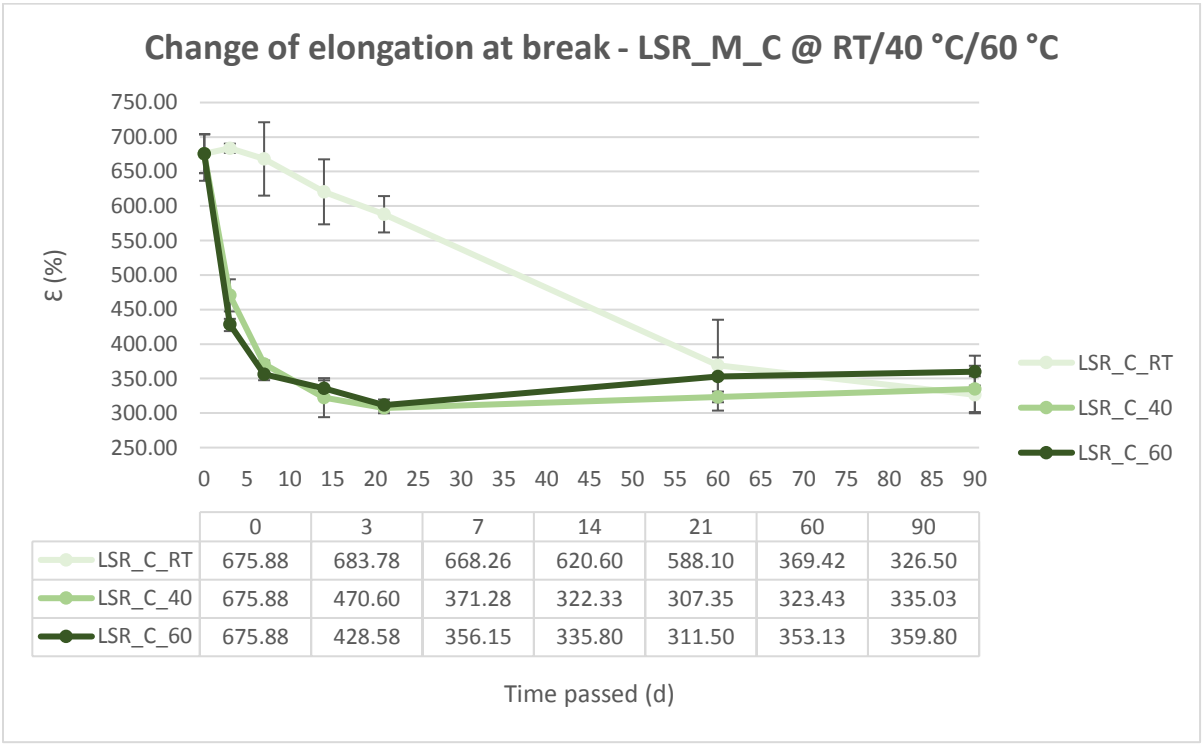

	0	3	7	14	21	60	90
LSR_C_RT	675.88	683.78	668.26	620.60	588.10	369.42	326.50
LSR_C_40	675.88	470.60	371.28	322.33	307.35	323.43	335.03
LSR_C_60	675.88	428.58	356.15	335.80	311.50	353.13	359.80

Figure 69: Ultimate elongation change of DISINF2 aged LSR

Again, a rapid decreases in tensile properties can be observed at higher temperature ageing in the first 21 days. After that, similarly to the hardness, the tensile strength and the ultimate elongation both reach a plateau. Knowing that silicone has a low tear strength, it can be said that surface degradation has a serious effect on tensile properties. The crazes that form due to the harder outer shell are propagation sites for tear, thus the tensile failure happens earlier. This is further supported by looking at the evolution of break sites. Early stages of ageing show that the specimens are more likely to snap neatly at the base of the bar. Later, when mass transfer equilibrium is settled, the thinner elongation part of the bars break and show tearing (Le Huy and Evrard, 1998).

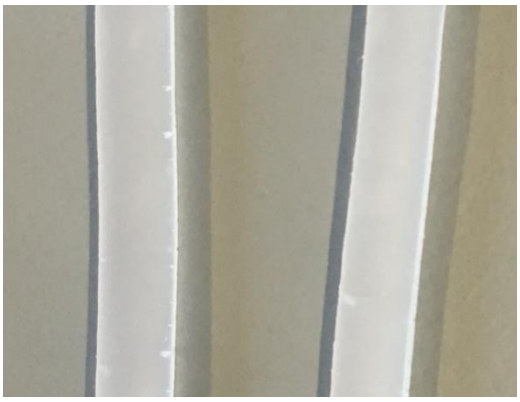

Figure 70: Crazing caused by tensile stress in LSR_C_40_90 samples

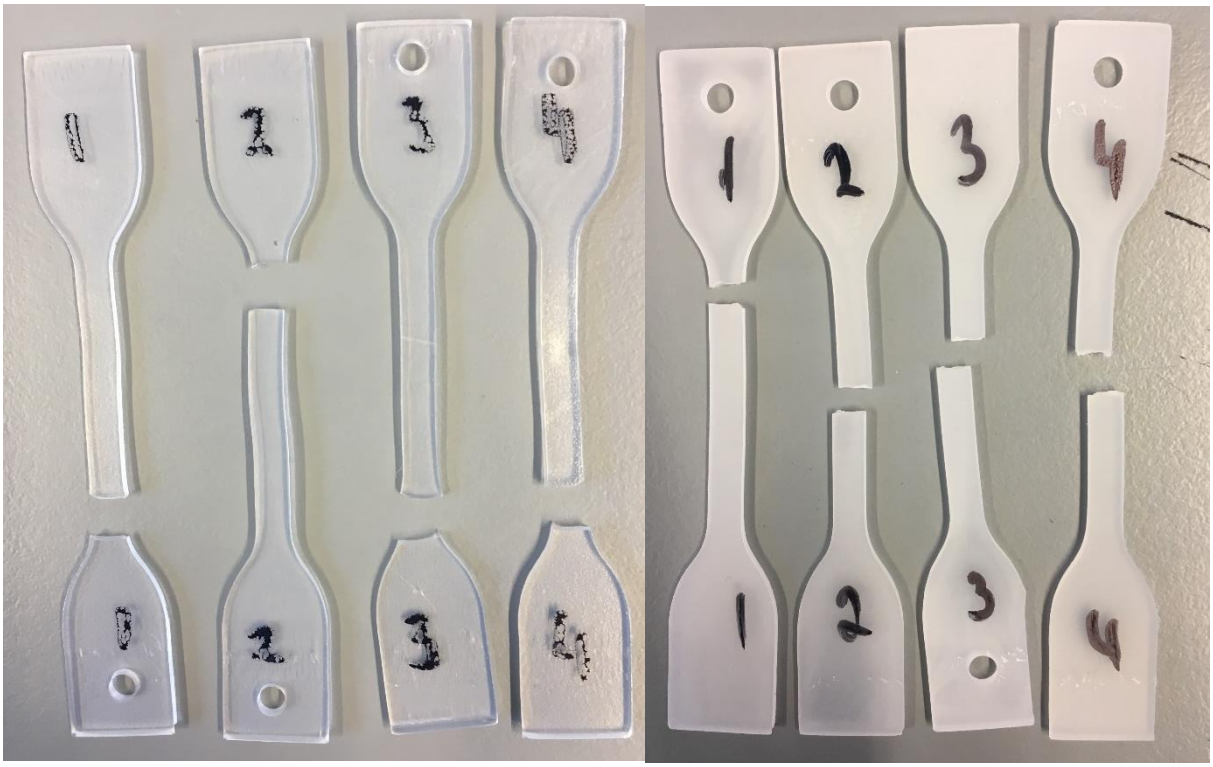

Figure 71: (l) LSR_C_40_3 shows tensile break close to the base of the tensile bar (r) LSR_C_60_90 shows crazing, and more central breakage

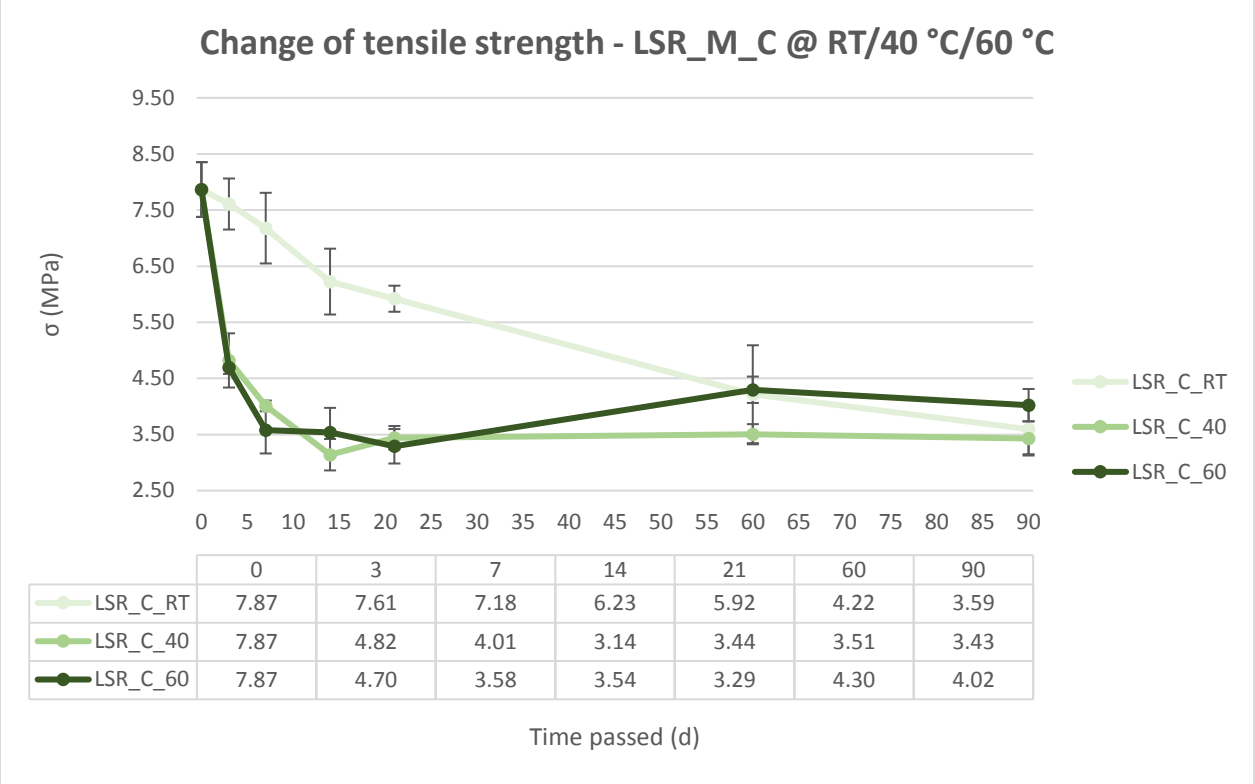

	0	3	7	14	21	60	90
LSR_C_RT	7.87	7.61	7.18	6.23	5.92	4.22	3.59
LSR_C_40	7.87	4.82	4.01	3.14	3.44	3.51	3.43
LSR_C_60	7.87	4.70	3.58	3.54	3.29	4.30	4.02

Figure 72: Tensile strength change of DISINF2 aged LSR

Infrared spectra

LSR_C_RT	LSR_C_40	LSR_C_60	Deformation
cm^{-1}	cm^{-1}	cm^{-1}	
3375	3402	3391	O-H stretch, only present in 90 day samples
2967	2967	2965	C-H stretch
1409	1416	1416	C-H bend of CH_3
1262	1265	1265	Si-CH_3
1083	1090	1085	Si-O-Si, decreasing over time
1020	1022	1018	Si-O-Si, decreasing over time
871	866	868	Si-$(CH_3)_2$
799	796	796	Si-$(CH_3)_2$

Table 12: Peaks of FT-IR in LSR_C

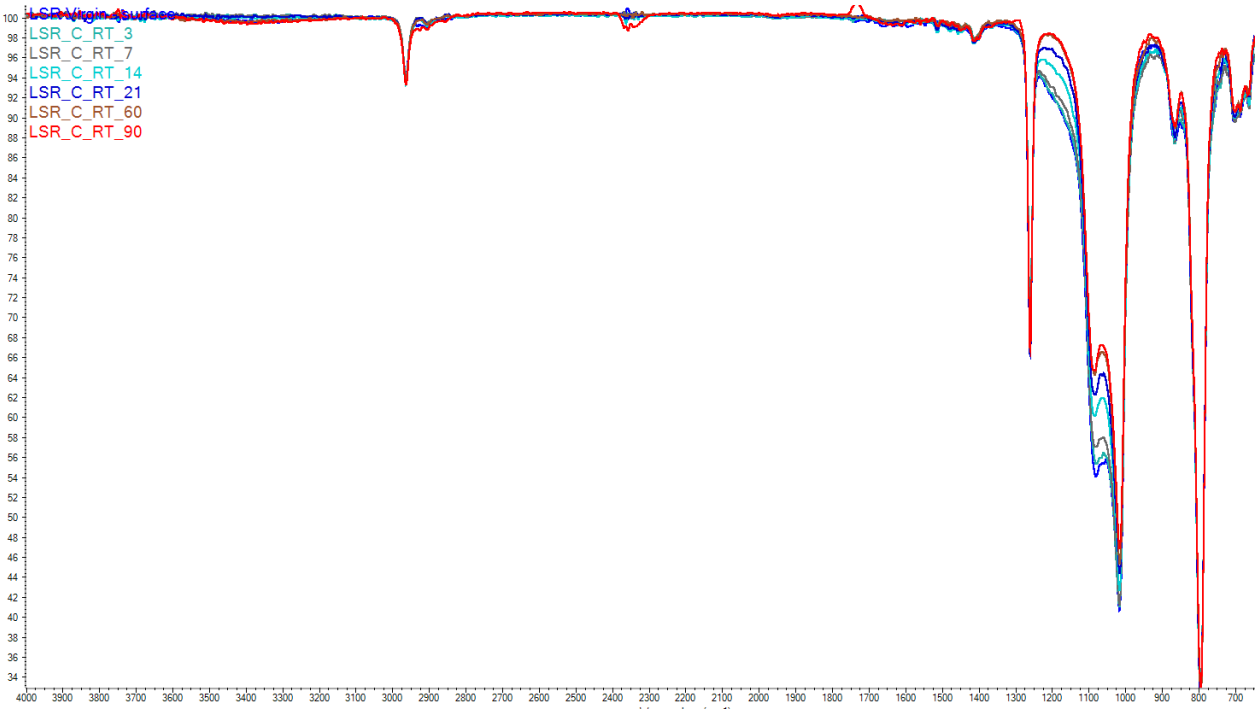

Figure 73: Fourier-transform infrared spectra of LSR aged in DISINF2 at 20 °C

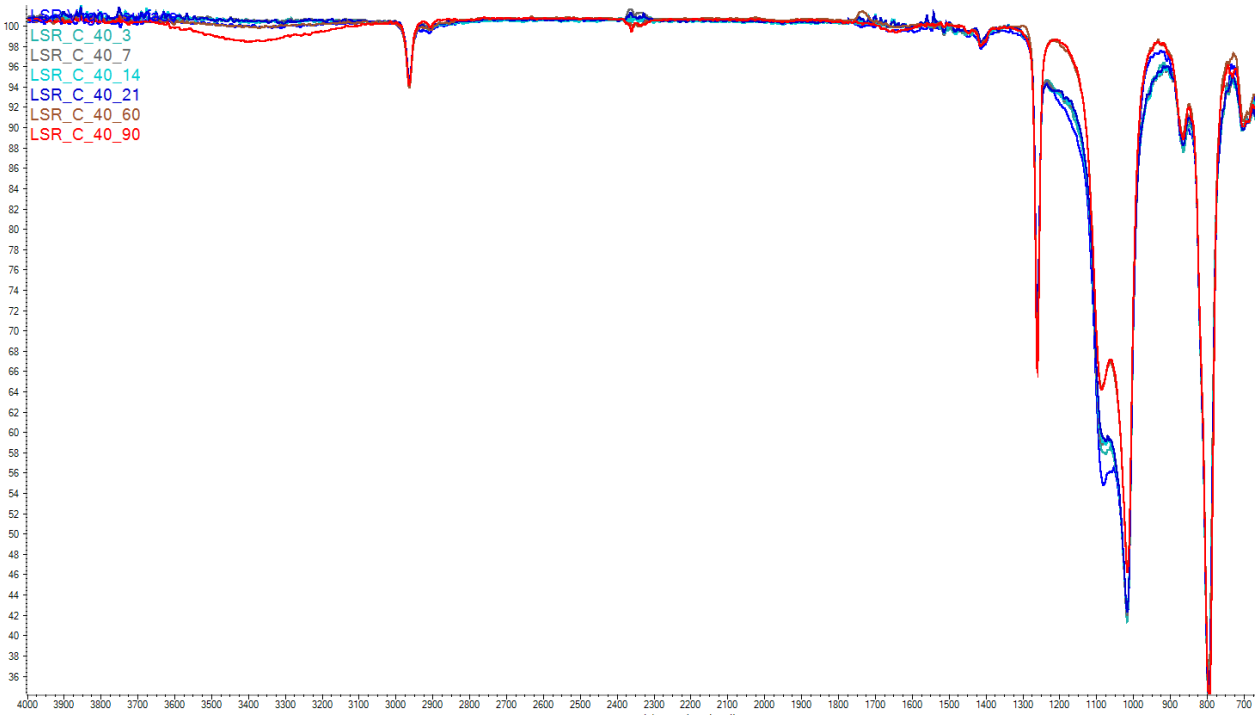

Figure 74: Fourier-transform infrared spectra of LSR aged in DISINF2 at 40 °C

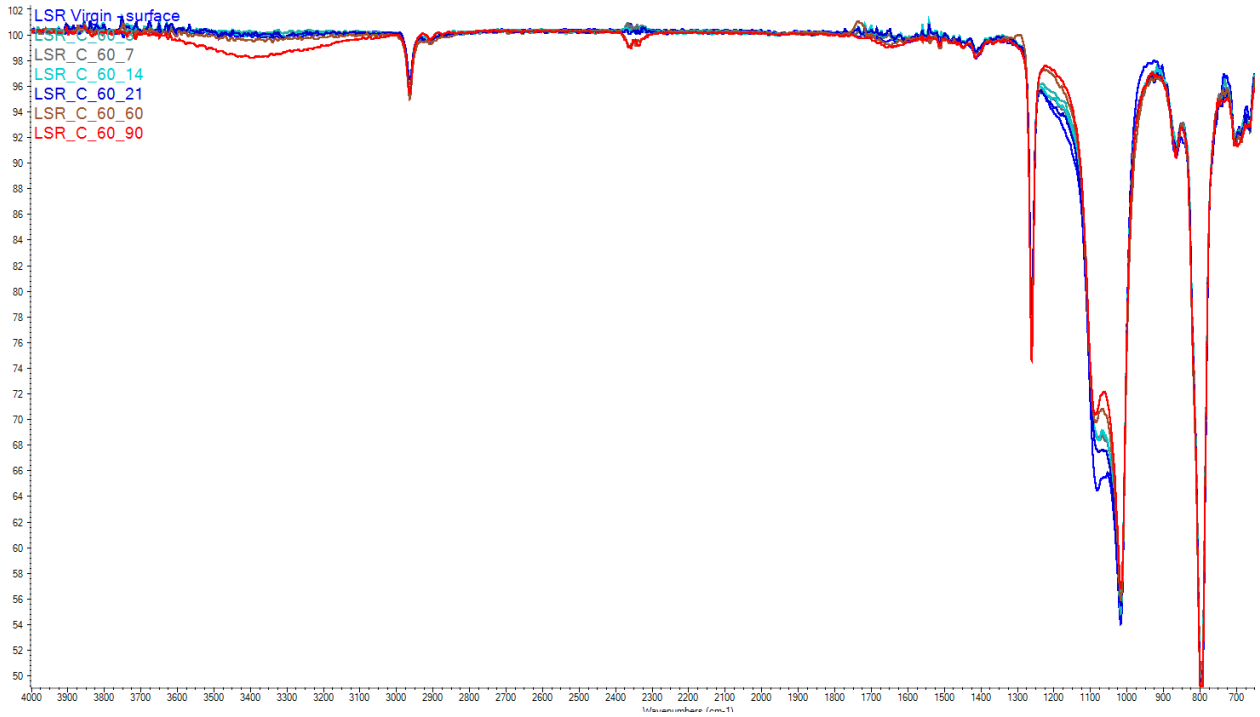

Figure 75: Fourier-transform infrared spectra of LSR aged in DISINF2 at 60 °C

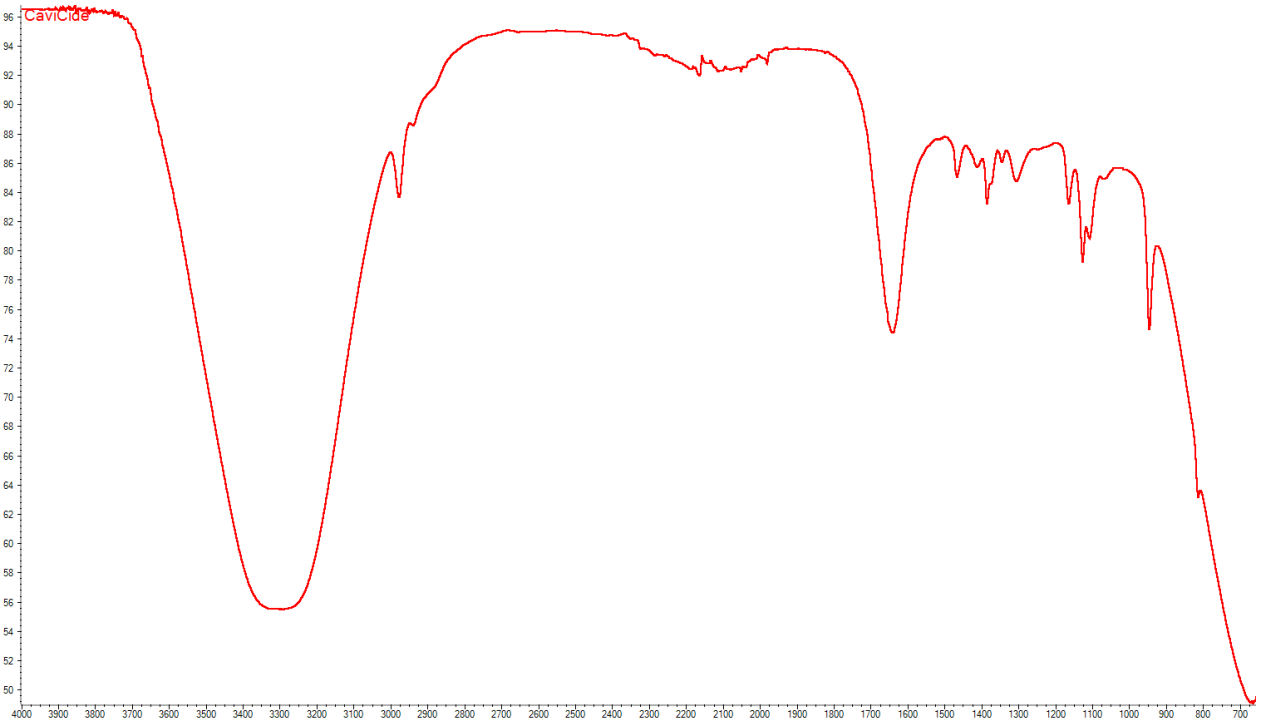

Figure 76: Fourier-transform infrared spectra of DISINF2

The IR spectra of room temperature aged LSR shows that the first things to be affected by degradation are the Si-O-Si (1000-1100 cm^{-1}) structures of the polymer. The peak in all cases becomes less intense and narrower (Launer, 2013). O-H stretch peak appears only late in the degradation of the material at 3400 cm^{-1} and are likely to be originating from the absorbed DISINF2. The IR of DISINF2 shows a violent

O-H band which is likely to show on the spectra of the aged material. The second most intense peak of DISINF2 is at 1650 cm^{-1} and it can also be seen to show up in aged material spectra. Superficial crosslinking is a possible degradation mechanism (Wen et al., 2017) that may be helped by the stability of the positively charged quaternary amine (Roeges, 1994).

	LSR_C
Visual	Loss of transparency, slight browning
Weight	Decreasing
Hardness	Increasing
Elongation	Decreasing
Tensile strength	Decreasing
Compression set	Increasing
Thermogram	Non-conclusive
Infrared	Change in Si-O-Si peak, O-H peak appears

Table 13: Assessing all the changes of LSR_C

THERMOGRAVIMETRIC LIFETIME ANALYSIS

As explained previously, a method utilizing different heating rates was used to determine the effect of ageing on the material's lifetime for TPV. The weight loss was shown as a function of temperature and the temperatures correlating to 5-25% thermal conversion was used to draw an Arrhenius graph. The slope of this graph gave rise to the activation energy of thermo-oxidative degradation of the aged material. The activation energies could be compared to arrive to the acceleration factor, a dimensionless indicator expressed as a percentage of how much faster (or slower) the thermo-oxidative end-of-life of the material can be reached. To demonstrate the process of this, the method will be explained step-by-step for TPV_I_60_21.

First, the sample was heated at 5, 10 and 40 °C/min heating rate in the TGA. The results of these were shown in a thermogram. The degradation was adjusted to start at 100% weight at 120 °C and the residue was read from the sample with the fastest heating rate. It was assumed that the same sample at other heating rates has the same amount of residue left after full thermolysis.

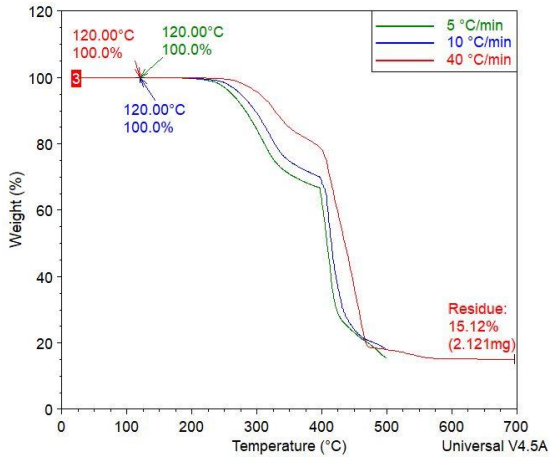

Figure 77: The graphs are adjusted to 120 °C and the residue is determined

Unfortunately, the same could not be done for LSR. LSR experiences cyclic volatile formation through a radical process that happens at random (Crompton, 2010). This determines the residue after thermolysis to be random too and creates sharp drops in the thermograms. Unaged LSR was tested at different heating rates twice, to support this claim. Below the thermograms of both runs will be presented to support the randomness claim.

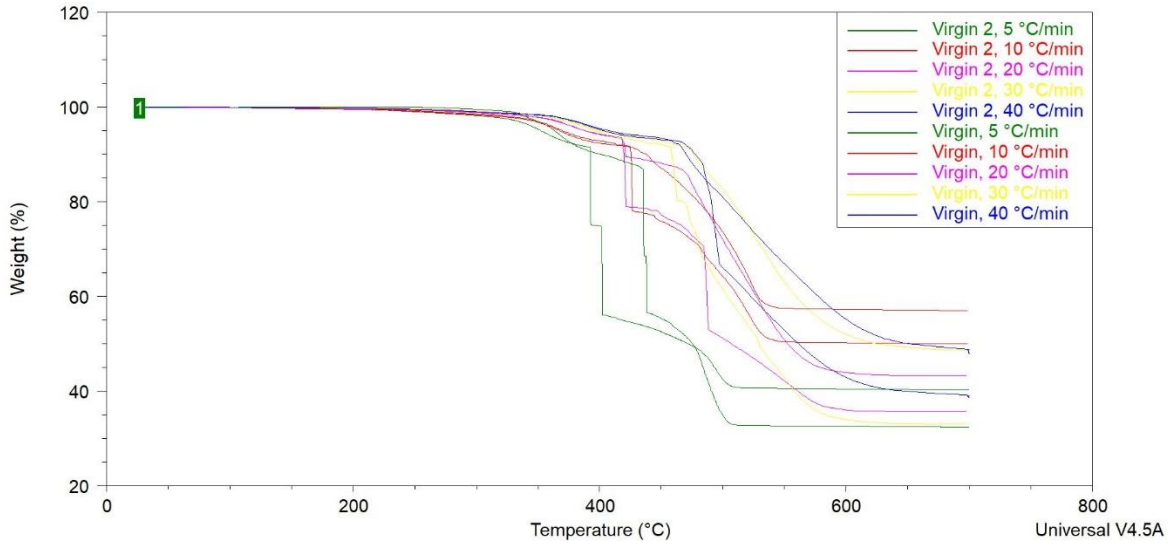

Figure 78: Virgin LSR at different heating rates shows unpredictability

Secondly, 5-25% weight conversion was calculated according to these two parameters and was given as total weight loss. This method is shown for the 40 °C/min sample but the same technique was used for all thermograms.

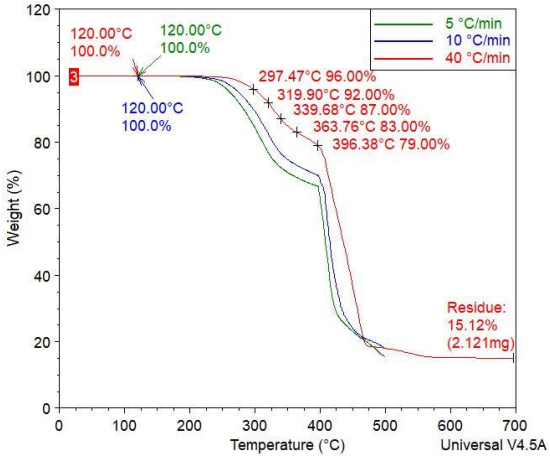

Figure 79: The second step collected the temperatures associated with the weight conversion

Thirdly, all this data was collected in an Excel sheet that contained the name of the sample, all ageing parameters of the sample, the heating rate, the conversion and the temperature where said conversion was achieved. The reciprocal of this temperature was then calculated and so was the decadic logarithm of the heating rate. These were then presented in the same graph and a linear approximation using the minimum of R^2 method was drawn. The two parameters of the linear graph was collected and so was the R^2 of the linear approximation.

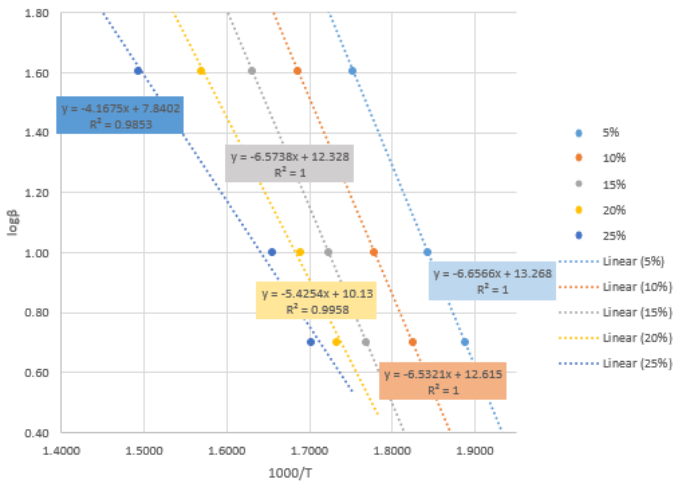

Figure 80: Linear approximation of the thermal data collected from the thermograms

The slope was multiplied by 18.19 to arrive to activation energy expressed in kJ/mol for each conversion. The mean of these activation energies represented the activation energy of the first 25% of thermal weight conversion. In the case of TPV_I_60_21 this value was 106.80 kJ/mol. This was then compared to the activation energy determined for the unaged sample, and thus the acceleration factor was determined. Two graphs were generated from this data: one showing the activation energies and another showing the kinetic acceleration. The linear approximation was less accurate (low R^2 values considering that there were only 3 points to draw the linear approximation) for TPV_I samples where the inflection point between the thermal degradation of the leachables and the thermal degradation of the PP/EPDM matrix was included in the first 25% weight conversion interval.

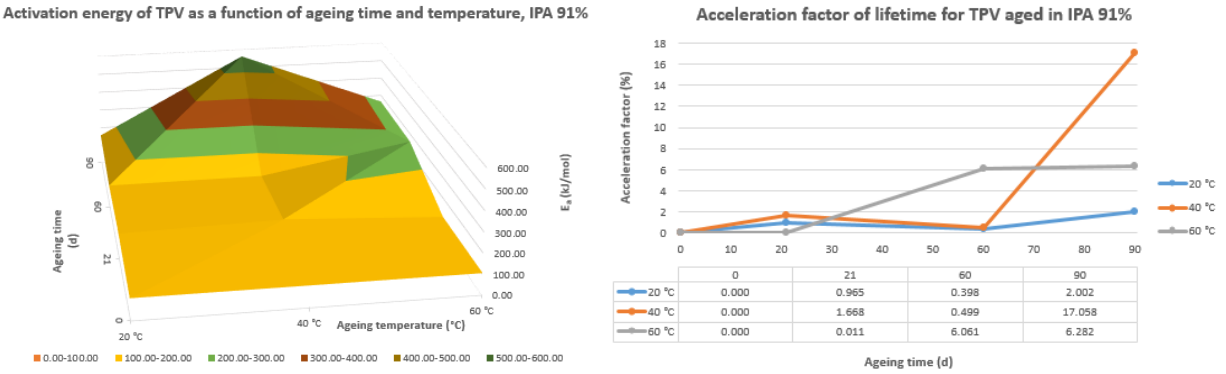

Figure 81: (l) Activation energy shown as a function of ageing time and temperature for TPV_I (r) Acceleration factor for end-of-life criterion

This inaccuracy was what resulted in the big increase of activation energy calculated for TPV_I_40_90. Activation energy was determined to be 106.53 kJ/mol for the virgin material. This was increased to 155.80, 562.12 and 264.58 kJ/mol after 90-day-long ageing at 20, 40 and 60 °C, respectively. This translates to a 2.0, 17.1 and 6.3% increase in lifetime. An increase in activation energy means an increased expected lifetime. This can be reasoned with the leaching of oils from the TPV. Many oils contain unsaturated bonds which are more prone to thermo-oxidation due to the increased reactivity of a π bond. Once these oils were consumed in the ageing process, the material became more stable towards oxidation. To demonstrate this, unaged TPV is compared with TPV aged in IPA 91% at 60 °C for 90 days.

Figure 82 shows the comparison of these two thermograms. Around 70 °C, the aged sample is losing weight compared to the virgin material. This is due to the residual absorbed IPA in the material. For this reason, degradation was only examined after 120 °C to account for the absorbed low temperature volatiles. Other notable difference is that the aged sample shows one weight loss step while the virgin material degrades in two distinct steps. Knowing that the material is also losing weight while the residue after full thermolysis at 700 °C has increased, we can conclude that during this ageing period the material leached some of its constituents into the solution. Therefore, the quantitative determination of the activation energy is also shifted from referring to the leachables, to PP/EPDM.

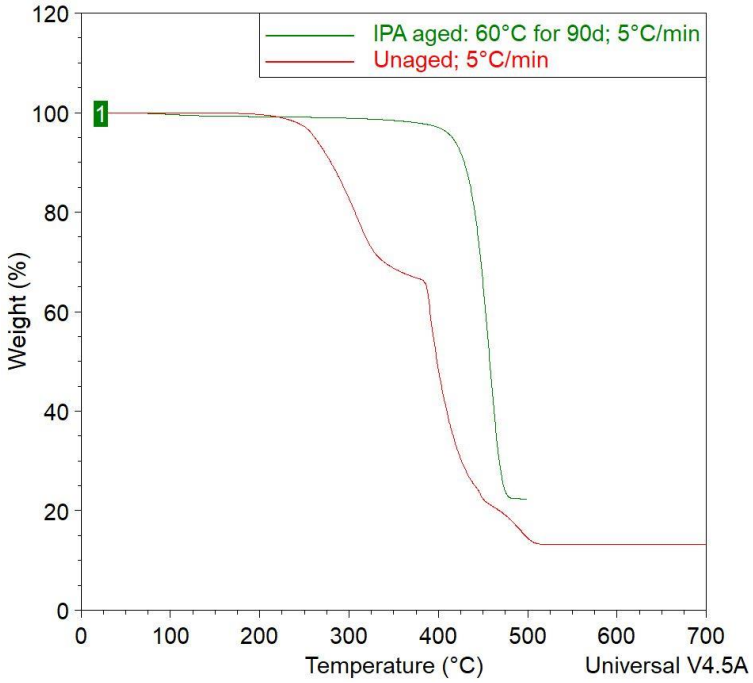

Figure 82: Comparing the thermograms of aged and unaged TPV

This resulted in an increased lifetime from a thermo-oxidative perspective. After 90 days, the thermal behavior of TPV_I changed to favor longer service life. However, TPV also lost its initial tensile properties and volume, and weight loss was significant enough to assume that in certain uses, the end-of-life criterion would have been realized faster.

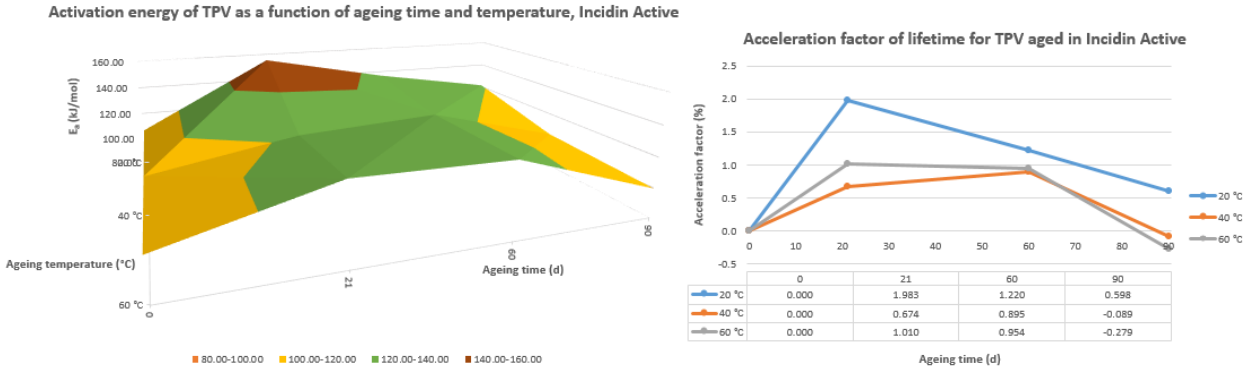

	0	21	60	90
20 °C	0.000	1.983	1.220	0.598
40 °C	0.000	0.674	0.895	-0.089
60 °C	0.000	1.010	0.954	-0.279

Figure 83: (l) Activation energy shown as a function of ageing time and temperature for TPV_A (r) Acceleration factor for end-of-life criterion

In the case of DISINF1 ageing, the effect of degradation on lifetime was less severe. Activation energy increased in the first 21-day period of the ageing but started to decline after 60 days. By the end of the 90-day ageing process, the TPV's lifetime has been shortened by 0.3% for TPV_A_60_90. The final activation energies were 121.15, 104.37 and 99.74 kJ/mol for 20, 40 and 60 °C aged samples. The corresponding acceleration factors were 0.60, -0.01 and -0.3%, respectively. This decline foreshadows that the material is going to continue degradation that will result in even lower activation energies regarding thermo-oxidation, and in turn even shorter expected lifetimes.

DISCUSSION

INHERENT PROBLEMS OF THE EXPERIMENT

When one decides to criticize their own work, a separation between individual mistakes and problems arising from the nature of the set of experiments can be made. The former category assumes that the author realizes these problems, and acknowledges the personal error or shortcomings of an experimental design. The latter is informative towards the reader that, even if all instructions are followed, some problems are inherent to the nature of the measurements or are imbedded deeply into the assumptions made during the execution.

The Arrhenius equation and the Ozawa method of determining lifetime fall under the consideration of the latter. Several of the disadvantages of both of these concepts were explained previously. First of all, the Arrhenius equation is a kinetic formula determining the activation energy of a single reaction. It shows what energy barrier needs to be tackled by two molecules colliding to form a product molecule. In a polymer, the reactions can happen almost anywhere in the chain, thus the activation energy would differ for each individual reaction. All atoms in the polymer experience different molecular environments, therefore the activation energy calculated is a mean of all reactions happening (Celina et al., 2005). Secondly, the Arrhenius equation cannot be extrapolated over phase transitions and the ceiling temperature (Wise et al., 1995). When the TPV samples are heated in the TGA, the TPV will melt and so will the physical behavior of the material change. Also, as said previously, the pre-exponential factor, A is temperature dependent, thus it cannot be neglected when calculating the acceleration factor. Heating the samples that hot also can give rise to competing reactions. These can result in two different activation energies of competing reactions.

The Ozawa method also makes several assumptions regarding the order of the reaction precisely that the initial degradation follows first-order kinetics (Ozawa, 1965). Another shortcoming of the different heating rates is that the temperatures read from the thermograms are approximated as the fast running tests do not give enough time for the sample to equilibrate at said temperature. This problem is further amplified by the fact that the method is integral in nature, and in turn all errors are cumulative (Eby, 1979).

The concept of ageing is already false as it does not represent real life situations. Immersing a specimen in disinfactants blocks the contact with air and does not include dynamic testing conditions (Brown, 2001). The samples in this case are tested for their chemical ageing much rather than tested for their active service life. For this, an experiment parallel to this one was set up that tried to assess the effect of exposure on the material. The conclusion of that experiment was that immersion has the most adverse effect on degradation and it was the least tedious way of establishing chemical contact.

WAYS TO IMPROVE EXPERIMENT IN THE FUTURE

How could one improve this experiment to account for the previously listed issues regarding lifetime estimation? Flynn and Dickens (Eby, 1979) describe different methods for determining the lifetime of polymers using TGA. It is explained that an automatic TGA protocol could be set up that measures weight loss, and equilibrates at temperatures associated with certain thermal conversions. This isothermal

method greatly increases the accuracy of a thermogram as it cancels out temperature-independent parameters and generates a direct correlation between rate, temperature of the isotherm and the activation energy.

Other way to improve the accuracy of the TGA method is to use more and slower heating (0.1, 0.5, 1, 2 °C/min) rates (Ozawa, 1965). The data could be collected for more heating rates and more conversion data (1-25% in steps of 1%). This would greatly increase the accuracy of the linear approximation and in turn would lead to more precise activation energies. Having lower conversion presets could be used to assess the lifetime of LSR samples too using the first 5% of thermal conversion as a reference.

Initially, a different method using mechanical failure criteria was intended to be used to draw an Arrhenius plot. The thermogravimetric analysis of the samples was a secondary plan. This estimation of the lifetime failed to show significant results due to the samples not reaching the criterion in the 90-day observation period. However, this method is considered to be important in correctly assessing lifetime. The TGA method sheds light on the thermo-oxidative degradation behavior of the material after ageing. As we saw with TPV_I, the samples' lifetime might be extended according to thermal experiments but can show significantly different mechanical characteristics. To correctly assess the lifetime of a plastic, this mechanical failure needs to be addressed too. However, mechanical degradation can often be mass transfer limited.

This mass transfer limitation brings me to my next point of discussing possible ways to improve the lifetime estimation. As it was shown in the case of many elastomers, mass transfer played an important role in how severe the degradation turned out to be. Often, a 21-day induction period was seen and in some cases the lack of this mass equilibrium resulted in non-conclusive degradation. As Brown (2001) explains, the thickness of the samples play an important role in said limitation. Thinner samples or longer exposure times would decrease the time required to reach an equilibrium meaning that the desired mechanical degradation criteria could be reached and valuable information could be extracted from the data.

Other ways to improve on this limitation would be creating a continuous ageing environment, one that carries out the liquid changes at an isotherm with a reflux condenser and one that regulates the concentration of the active species in the solution. This would greatly reduce the human error effect on the ageing. Often times, the reactions that occurred between the sample and the liquid had a rate determining step in the disassociation of the active component in the disinfectant, e.g. peracetic acid would react away in the few days between liquid changes, effecting the rate of degradation negatively.

One thing that helped understanding the severity of the results was COMPOUNDER2's (2017) fluid resistance datasheet. This aided the assessment of the results gained from mechanical data and served as a baseline for comparison. Similarly, the materials tested in this experiment could be aged in water as a control for other degradation pathways. The property changes of the water aged samples could be compared with aged samples' weight and volume loss and used as a guideline in understanding absorption and mass transfer limitations.

The other thing that often lead to incomprehensible data was the high standard deviations that arise as a result of compounding and thermal history of the samples. This could be avoided by increasing the number of samples for each sample set. Having more samples would have greatly influenced the

reliability of tensile data. General trends were still available for conclusion but the exact mechanical development of the materials after ageing remained unclear.

Compression set measurements were flawed because of the lack of 6 mm thick samples. Compression set is a simple experiment that was unfortunately inconclusive in this experiment. Having enough 6 mm samples, and a supply of PEEK compression disks would result in a more reliable data. Extending the 21-day exposure period would give more confident data about the behavior of e.g. seals in medical devices on the long-run.

The compounders are very secretive about the constitution of their products, which is understandable, but made estimating degradation characteristics and mechanics hard. It would be optimal, although not necessary that the correct composition of the elastomers at hand could be determined. Knowing the ratio of PP to EPDM to filler oil can be approximated using the TGA produced thermograms but is not known exactly. The case is direr for LSR where density of vinyl groups has a strong effect on degradation of the material. This compositional analysis could be done using low heating rate TGA in N_2 atmosphere, ^{1}H-NMR and FT-IR combined.

For future lifetime estimations, it is recommended that the material is tested for the specific application intended for the specimen. One problem with this experiment was that the samples were tested according to many of their properties. This generated a very hard to comprehend amount of data that served the purpose of understanding the approach to ageing and lifetime estimation of rubbers but gave little conclusive answers to how the materials degrade and what the results of these degradations regarding service life are.

CHECKING THE HYPOTHESES

TPV_I was indeed a diffusion dependent degradation, where the alcohol caused leaching of the filler oils. A 35% oil content was determined for 201-64. It seems that this leaching caused deplasticization and the effect of this is more severe in softer grades of TPV. Deplasticization resulted in decreased weight (-35%) and size, and increased hardness (from 71 to 85 Shore A). The material improved in its tensile properties (elongation increased by 250% and strength went from 6.2 to 16 MPa) and showed tensile whitening at large elongations. The compression of the samples resulted in complete recovery loss after 21 days at 60 °C. Reaction between the material and the liquid was very limited as confirmed by the IR measurements. The IR also confirmed that the filler oils have migrated to the surface which is in accordance to the mass transfer phenomena observed. TGA showed better thermal stability for the material after ageing but also justified the leaching claims. Although the resistance against thermo-oxidative degradation increased overtime, which in turn resulted in a (2-17%) longer expected lifetime, the mechanical data shows that the characteristics of the material changed drastically. This actually leads to a lower service time for application.

TPV_A showed severe yellowing as a sign of oxidation happening in the sample. The oxidation was confirmed by the IR spectra by newly formed peaks that can be linked to oxygen containing functional groups of carboxylic acid salts. The oxidation led to a modified chemical structure that made the material more susceptible to liquid absorption. This effect was present in the increased weight (+13%) and decreased hardness (from 71 to 65 Shore A). Tensile data was hard to interpret due to large standard deviations in the samples. Overall, elongation increased (+60%) but tensile strength decreased (from 6.2

to 5.3 MPa). Thermal resistance and expected lifetime were negatively influenced as the antioxidant mixture used in the material was fully reduced in the ageing process.

LSR_N was the hardest to access as during tests it showed huge variance, and unpredictable degradation trajectories. This can be credited for the reactive nature of the hypochlorite ions that disassociate in aqueous conditions to form other reactive species. LSR is also very unreactive which made for further unpredictabilities. LSR samples showed different haptics and a loss of transparency as visual signs of degradation without weight changes. To some extent oxidation and chain scission were accused of being the main degradation pathways. This was confirmed by IR measurements which show that the Si-C bonds remain unaffected during ageing while the Si-O-Si backbone was hydrolyzed in some cases. To further confirm this claim, molecular weight distribution measurements could be conducted.

LSR_C had severe visual degradation at elevated temperatures after long exposure times. The surface embrittlement and the change in transparency are all indicators of a clear degradation. The tensile, mass (-11%) and hardness (from 40 to 50 Shore A) data showed this evidently. The tensile properties were rapidly disappearing as crazing of the surface lead to rapid drop in stress-strain behavior of the LSR. This crazes were propagation sites for tearing. However, the nature of the degradation shows that it is far from only being a mass transfer controlled one. One theory would suggest that the smaller chain silicones that remain after the curing process and plasticize the elastomer were leached out of the material. IR shows new peak formation and a decrease in Si-O-Si related peaks which suggest that the degradation effect is only partially mass transfer related.

CONCLUSION

This experiment aimed to help Philips understand material testing and lifetime estimation for elastomers. As a result, loads of experiments were carried out to help streamline future material testing. Since there were so many measurements and the experiments differed for each chemical contact, it would be impossible to summarize all of these in one conclusion.

The test methods all showed different aspects of degradation. Weight and hardness were easy to test but they were efficient in detecting diffusion limited processes only. Tensile test proved to be useful as a qualitative method rather than a quantitative one, unless more specimens are tested to account for the large standard deviations of the compounding effect. Compression set in liquid media was tedious and showed little results due to the lack of inert compression disks and ISO compliant samples. However, compression set is a useful tool, and more tests are needed to confirm their usefulness in elastomer testing. IR spectrometry was useful for chemical degradation assessment but ultimately not much can be deducted from it that could be extrapolated over a longer exposure time.

The other method that was put to the test in this experiment was the TGA method of determining lifetime effects of chemical degradation. Here, an example was shown how it could be done and several suggestions were given on how this method could be improved on. It was also concluded that this method is only useful alongside other mechanical tests as both chemical and physical ageing of the materials affect the expected lifetime.

APPENDIX

List of additional documents handed:

- *S2706326_Thesis.docx*

  This document, i.e. the MSc thesis of Márton Péter Iritz.

- *S2706326_Thermal analysis.xlsx*

  All data concerning the TGA experiments, and calculations to estimate activation energy.

- *S2706326_Samples.xlsx*

All data concerning the mechanical tests. It includes a detailed schedule for the duration of the experiment, raw data, calculations regarding change of properties, order list for chemicals used in the experiment. It also contains the data for the exposure methods test.

- *S2706326_Elastomers for medical devices.docx*

  A preliminary study of all elastomers with a conclusive decision on why LSR and TPV are tested.

- *S2706326_Tensile test results.xlsx*

Raw data concerning tensile tests. It also includes images of the broken tensile bars and the stress-strain curves of the samples.

- *S2706326_Presentation.pptx*

  The slides used for the final presentation on the last day at Philips.

- *S2706326_Results.zip*

All raw data collected in a zipped file. It includes TGA thermograms and protocols, IR spectra, literature used, pictures of tensile bars and other images used during the making of the thesis.

- *Lab journal "Márton Iritz – THESIS RuG/PHILIPS"*

  Contains material safety, weight and hardness raw data, experimental, observations, scheduling.

SOURCES

Introduction

Accini, S. (2012, May 14). Top ten disinfectants to control HAIs.

Aubert Y. Coran; Balbhadra Das; Raman P. Patel (1978). *United States Patent No. US 4,130,535.*

Bhowmick, A. and Stephens, H. (2001). Handbook of elastomers. New York: Marcel Dekker.

Bhowmick, A. and Stephens, H. (2001). Handbook of elastomers. New York: Marcel Dekker.

Bhowmick, A., Baranwal, K., Mukhopadhyay, R. and Das Gupta, S. (2014). Reverse engineering of rubber products. Boca Raton: Taylor & Francis.

CES Selector 2018 datasheets.

CES Selector 2018 datasheets.

CES Selector 2018 datasheets.

CES Selector 2018 datasheets.

CES Selector and MSDS – Valuable tools for material comparison

Sperling, L. H. (2005). *Introduction to Physical Polymer Science*, Chapter 9: Crosslinked Polymers and Rubber Elasticity. pp.427-505.

Dettenkofer, M., & Block, C. (2005). Hospital disinfection: Efficacy and safety issues. Current Opinion in Infectious Diseases, 18(4), 320-325. doi:10.1097/01.qco.0000172701.75278.60

Drobny, J. (2014). Handbook of thermoplastic elastomers. Oxford, UK: William Andrew Publishing.

Drobny, J. (2014). Handbook of thermoplastic elastomers. Oxford, UK: William Andrew Publishing.

[redacted]

Hurley, P. (1981). History of Natural Rubber. Journal of Macromolecular Science: Part A - Chemistry, 15(7), pp.1279-1287.

Klevens, R., Edwards, J., Richards, C., Horan, T., Gaynes, R., Pollock, D. and Cardo, D. (2007). Estimating Health Care-Associated Infections and Deaths in U.S. Hospitals, 2002. Public Health Reports, 122(2), pp.160-166.

Maki, D., Alvarado, C. and Ringer, M. (1991). Prospective randomised trial of povidone-iodine, alcohol, and chlorhexidine for prevention of infection associated with central venous and arterial catheters. The Lancet, 338(8763), pp.339-343.

Medical Device Directive 93/42 European Economic Commission (MDD 93/42 EEC)

Nash, L. (1979). Entropy and rubbery elasticity. Journal of Chemical Education, 56(6), p.363.

Naskar, Kinsuk & Noordermeer, Jacques. (2005). Thermoplastic elastomers by dynamic vulcanization. Progress in Rubber, Plastics and Recycling Technology. 21. 1-26.

NHS Southern Health. (December 2017) Decontamination of Medical Devices (Infection Prevention and Control Policy: Appendix 12) SH CP 100

OxyChem (2014). Sodium Hypochlorite Handbook. (pdf)

Pubchem. (2019). *Isopropyl alcohol*. Available at: https://pubchem.ncbi.nlm.nih.gov/compound/isopropanol#section=Experimental-Properties.

Pubchem.ncbi.nlm.nih.gov. (2005). *Sodium percarbonate*. [online] Available at: https://pubchem.ncbi.nlm.nih.gov/compound/Sodium_percarbonate#section=Top

Sabet Abdou-Sabet, Akron; Michael A. Fath, Wadsworth (1982). *United States Patent No. US 4,311,628.*

Sandin, S., Karlsson, R. and Cornell, A. (2015). Catalyzed and Uncatalyzed Decomposition of Hypochlorite in Dilute Solutions. *Industrial & Engineering Chemistry Research*, 54(15), pp.3767-3774.

Sastri, V. (2014). Plastics in Medical Devices. Norwich, New York: William Andrew.

Statista – Rubber dossier (2018). Available at: https://www.statista.com/study/40624/rubber-statista-dossier/

TPE Magazine (2017). ”A history of resounding success” - Santoprene celebrates 40th anniversary. 2017(3); p. 154-158.

Whelan, A. (2013). Polymer technology dictionary. Springer.

Whelan, A. (2013). Polymer technology dictionary. Springer.

Theory

Ammala, A., Hill, A., Meakin, P., Pas, S. and Turney, T. (2002). *Journal of Nanoparticle Research*, 4(1/2), pp.167-174.

Arrhenius, S. (1889). Über die Dissociationswärme und den Einfluss der Temperatur auf den Dissociationsgrad der Elektrolyte. *Zeitschrift für Physikalische Chemie*, 4U(1).

Assink, R., Gillen, K. and Sanderson, B. (2002). Monitoring the degradation of a thermally aged EPDM terpolymer by 1 H NMR relaxation measurements of solvent swelled samples. *Polymer*, 43(4), pp.1349-1355.

Brown, R. (2001). *Practical guide to the assessment of the useful life of rubbers*. Shawbury, Shrewsbury, Shropshire: Rapra Technology.

Celina, M., Gillen, K. and Assink, R. (2005). Accelerated ageing and lifetime prediction: Review of non-Arrhenius behaviour due to two competing processes. *Polymer Degradation and Stability*, 90(3), pp.395-404.

Connors, K. (1990). *Chemical kinetics*. New York, N.Y.: VCH.

Crompton, T. (2010). *Thermo-oxidative degradation of polymers*. Shrewsbury: ISmithers.

Cui, T., Lin, C., Chien, C., Chao, Y. and Van Zee, J. (2010). Service Life Prediction of Liquid Silicone Rubber Seal in PEM Fuel Cells. *ASME 2010 8th International Fuel Cell Science, Engineering and Technology Conference: Volume 2*.

Doyle, C. (1962). Estimating isothermal life from thermogravimetric data. *Journal of Applied Polymer Science*, 6(24), pp.639-642.

Flynn, J. H.; Wall, L. A. (1966). A quick, direct method for determination of activation energy from thermogravimetric data. *Polymer Letters,* vol. 4, pp.323-328.

Kwon, Y., Jun, S. and Song, J. (2015). Lifetime Analysis of Rubber Gasket Composed of Methyl Vinyl Silicone Rubber with Low-Temperature Resistance. *Mathematical Problems in Engineering*, 2015, pp.1-9.

Mahomed, A., Hukins, D. and Kukureka, S. (2015). Effect of accelerated ageing on the viscoelastic properties of a medical grade silicone. *Bio-Medical Materials and Engineering*, 25(4), pp.415-423.

Mandal, D., Bhunia, H., Bajpai, P. and Bhalla, V. (2017). Thermal degradation kinetics and estimation of lifetime of radiation grafted polypropylene films. *Radiation Physics and Chemistry*, 136, pp.1-8.

Moghadam, M., Morshedian, J., Ehsani, M., Bahrami, M. and Saddadi, H. (2013). Lifetime prediction of HV silicone rubber insulators based on mechanical tests after thermal ageing. *IEEE Transactions on Dielectrics and Electrical Insulation*, 20(3), pp.711-716.

Ozawa, T. (1965). A New Method of Analyzing Thermogravimetric Data. *Bulletin of the Chemical Society of Japan*, 38(11), pp.1881-1886.

Saboo, Nikhil & Kumar, Praveen. (2018). Equivalent Slope Method for Construction of Master Curves. *46*.

Wise, J., Gillen, K. and Clough, R. (1995). An ultrasensitive technique for testing the Arrhenius extrapolation assumption for thermally aged elastomers. *Polymer Degradation and Stability*, 49(3), pp.403-418.

Yazdan Mehr, M., van Driel, W., De Buyl, F. and Zhang, K. (2018). Study on the Degradation of Optical Silicone Exposed to Harsh Environments. *Materials*, 11(8), p.1305.

Experimental

Brown, R. (2001). *Practical guide to the assessment of the useful life of rubbers*. Shawbury, Shrewsbury, Shropshire: Rapra Technology.

Crompton, T. (2010). *Thermo-oxidative degradation of polymers*. Shrewsbury: ISmithers.

Gabbott, P. (2010). *Principles and applications of thermal analysis*. Oxford: Blackwell Pub.

International Standard (2003). *ISO 868* – Determination of indentation hardness by means of a durometer (Shore hardness). 3rd edition.

International Standard (2011). *ISO 37* Rubber, vulcanized or thermoplastic – Determination of tensile stress-strain properties. 5th edition.

International Standard (2014). *ISO 815-1* Rubber, vulcanized or thermoplastic – Determination of compression set – Part 1: At ambient or elevated temperatures. 2nd edition.

Results

Aubert Y. Coran; Balbhadra Das; Raman P. Patel (1978). *United States Patent No. US 4,130,535.*

[redacted]

[redacted]

Gao, Y., Wang, J., Liang, X., Yan, Z., Liu, Y. and Cai, Y. (2014). Investigation on permeation properties of liquids into HTV silicone rubber materials. *IEEE Transactions on Dielectrics and Electrical Insulation*, 21(6), pp.2428-2437.

Krimm, S., Liang, C. and Sutherland, G. (1956). Infrared Spectra of High Polymers. II. Polyethylene. *The Journal of Chemical Physics*, 25(3), pp.549-562.

Launer, P.J. (2013) Infrared analysis of organosilicon compounds: Spectra-structure correlations. *Silicon Compounds: Silanes and Silicones,* Gelest, Inc.

Le Huy, Mai & Evrard, G. (1998). Methodologies for lifetime predictions of rubber using Arrhenius and WLF models. *Angewandte Makromolekulare Chemie - ANGEW MAKROMOL CHEM.* 261-262. 135-142.

Lisa.chem.ut.ee. (2015). *Castor oil – Database of ATR-FT-IR spectra of various materials*. [online] Available at: http://lisa.chem.ut.ee/IR_spectra/paint/binders/castor-oil/ [Accessed 17 Feb. 2019].

N. Roeges, A guide to the complete interpretation of Infrared Spectra of Organic Structures, Wiley, 1994, pp. 1 – 340.

Price, G., Keen, F. and Clifton, A. (1996). Sonochemically-Assisted Modification of Polyethylene Surfaces. *Macromolecules*, 29(17), pp.5664-5670.

Pubchem.ncbi.nlm.nih.gov. (2019). *Ethanol*.

Pubchem.ncbi.nlm.nih.gov. (2019). *Isopropanol*.

Wacker Chemie AG (NA). Solid and Liquid Silicone Rubber – Material and Processing Guidelines.

Wen, X., Yuan, X., Lan, L., Hao, L., Wang, Y., Li, S., Lu, H. and Bao, Z. (2017). RTV Silicone Rubber Degradation Induced by Temperature Cycling. *Energies*, 10(7), p.1054.

Discussion

Brown, R. (2001). *Practical guide to the assessment of the useful life of rubbers*. Shawbury, Shrewsbury, Shropshire: Rapra Technology.

Celina, M., Gillen, K. and Assink, R. (2005). Accelerated ageing and lifetime prediction: Review of non-Arrhenius behaviour due to two competing processes. *Polymer Degradation and Stability*, 90(3), pp.395-404.

Eby, R. (1979). *Durability of macromolecular materials*. Washington, DC, pp.97-115.

Ozawa, T. (1965). A New Method of Analyzing Thermogravimetric Data. *Bulletin of the Chemical Society of Japan*, 38(11), pp.1881-1886.

Wise, J., Gillen, K. and Clough, R. (1995). An ultrasensitive technique for testing the Arrhenius extrapolation assumption for thermally aged elastomers. *Polymer Degradation and Stability*, 49(3), pp.403-418.